# 2016 Summer Neuroimaging Course

| | Day | Date | Bldg & Rm | Time | Topic | Lecturer |
|---|---|---|---|---|---|---|
| | | | | | | |
| 1 | Friday | 6/2/17 | 40, Rm 1201/1203 | 2:00 PM | Introduction to Course & A history of fMRI and Neuroimaging | Peter Bandettini |
| 2 | Monday | 6/5/17 | 49, Rm 1A51/1A59 | 2:00 PM | fMRI Limits, Paradigms, and Processing | Peter Bandettini |
| 3 | Wednesday | 6/7/17 | 49, Rm 1A51/1A59 | 2:00 PM | fMRI methods and applications at high field and high resolution | Renzo Huber |
| 4 | Friday | 6/9/17 | 49, Rm 1A51/1A59 | 2:00 PM | fMRI and MRI at the NIH | Sean Marrett |
| 5 | Monday | 6/12/17 | 49, Rm 1A51/1A59 | 2:00 PM | Basics of MRI and how to identify artifacts | Vinai Roopchansingh |
| 6 | Wednesday | 6/14/17 | 49, Rm 1A51/1A59 | 2:00 PM | Advanced MRI and fMRI Acquisition Methods | Andy Debyshire |
| 7 | Friday | 6/16/17 | 49, Rm 1A51/1A59 | 2:00 PM | Minimizing noise during fMRI acquisition | Dan Handwerker |
| 8 | Monday | 6/19/17 | 49, Rm 1A51/1A59 | 2:00 PM | What's neuronal and what's not in fMRI | Dan Handwerker |
| 9 | Wednesday | 6/21/17 | 49, Rm 1A51/1A59 | 2:00 PM | Magnetoencephalography (MEG) | Richard Coppola |
| 10 | Friday | 6/23/17 | 49, Rm 1A51/1A59 | 2:00 PM | Approaches to functional activity mapping during natural viewing | Brian Russ |
| | Monday | 6/26/17 | | 2:00 PM | No Lecture | |
| 11 | Wednesday | 6/28/17 | 49, Rm 1A51/1A59 | 2:00 PM | Studying CNS diseases with advanced MRI | Pascal Sati |
| 12 | Friday | 6/30/17 | 49, Rm 1A51/1A59 | 2:00 PM | Human Spectroscopy Introduction and Glutamate Spectroscopy at 7T | Li An |
| 13 | Monday | 7/3/17 | TBA | 2:00 PM | AFNI plus SUMA: analyzing your data | Bob Cox |
| 14 | Wednesday | 7/5/17 | 49, Rm 1A51/1A59 | 2:00 PM | The AFNI - based Functional and Anatomical Connectivity Platform | Paul Taylor |
| 15 | Friday | 7/7/17 | 49, Rm 1A51/1A59 | 2:00 PM | fMRI Data Sharing | Adam Thomas |
| 16 | Monday | 7/10/17 | 49, Rm 1A51/1A59 | 2:00 PM | T1 Contrast, MPRAGE and MT | Peter van Gelderen |
| 17 | Wednesday | 7/12/17 | TBA | 2:00 PM | Resting State fMRI | Catie Chang |
| 18 | Friday | 7/14/17 | 40, Rm 1201/1203 | 2:00 PM | Reliability vs Validity in Resting State fMRI | Steve Gotts |
| 19 | Monday | 7/17/17 | 49, Rm 1A51/1A59 | 2:00 PM | MRI Brain Segmentation Algorithms | Dzung Pham |
| 20 | Wednesday | 7/19/17 | 40, Rm 1201/1203 | 2:00 PM | Positron Emission Tomography (PET) | Bob Innis |
| 21 | Friday | 7/21/17 | 49, Rm 1A51/1A59 | 2:00 PM | Perfusion Imaging | Lalith Talagala |
| 22 | Monday | 7/24/17 | 40, Rm 1201/1203 | 2:00 PM | Neuromodulation methods | Bruce Luber |
| 23 | Wednesday | 7/26/17 | 49, Rm 1A51/1A59 | 11:00 AM | EEG/fMRI and Pharmacologic fMRI | Jen Evans |
| 24 | Friday | 7/28/17 | 40, Rm 1201/1203 | 2:00 PM | EEG/fMRI and the study of Language | Peter Molfese |
| 25 | Monday | 7/31/17 | 40, Rm 1201/1203 | 2:00 PM | EEG/fMRI and Neurofeedback | Silvina Horovitz |
| 26 | Tuesday | 8/1/17 | TBA | 2:00 PM | Quantitative MRI | Govind Bhagavatheeshwaran |
| 27 | Wednesday | 8/2/17 | 40, Rm 1201/1203 | 11:00 AM | Neuromodulation applications | Sarah Hollingsworth Lisanby |
| 28 | Friday | 8/4/17 | 40, Rm 1201/1203 | 2:00 PM | The physics of neuromodulation | Zhi Deng and Tom Radman |
| 29 | Monday | 8/7/17 | 40, Rm 1201/1203 | 2:00 PM | Machine Learning and fMRI | Javier Gonzalez-Castillo |
| 30 | Wednesday | 8/9/17 | 40, Rm 1201/1203 | 2:00 PM | Multi-echo EPI for task-based and resting-state fMRI | Javier Gonzalez-Castillo |
| 31 | Friday | 8/11/17 | 49, Rm 1A51/1A59 | 2:00 PM | Dynamic Resting State fMRI | Javier Gonzalez-Castillo |
| 32 | Monday | 8/14/17 | 40, Rm 1201/1203 | 2:00 PM | Depression and Multimodal Neuroimaging | Allison Nugent |
| 33 | Tuesday | 8/15/17 | TBA | 2:00 PM | Statistics of fMRI | Gang Chen |
| 34 | Wednesday | 8/16/17 | 49, Rm 1A51/1A59 | 2:00 PM | Multivariate pattern analysis and brain decoding | Martin Hebart |
| 35 | Friday | 8/18/17 | 49, Rm 1A51/1A59 | 2:00 PM | Imaging Changes in Brain Anatomy | Cibu Thomas |
| 36 | Monday | 8/21/17 | 40, Rm 1201/1203 | 2:00 PM | Anatomical and Functional Neuroimaging in Animal Models | Afonso Silva |
| 37 | Wednesday | 8/23/17 | 40, Rm 1201/1203 | 2:00 PM | Genetics and Neuroimaging: How to analyze imaging data and SNPs | Yin Yao |
| 38 | Friday | 8/25/17 | 40, Rm 1201/1203 | 2:00 PM | Imaging Stroke and Traumatic Brain Injury | Lawrence Latour |
| 39 | Monday | 8/28/17 | 40, Rm 1201/1203 | 2:00 PM | Diffusion MRI | Joelle Sarlls |
| 40 | Wednesday | 8/30/17 | 40, Rm 1201/1203 | 2:00 PM | What you can and cannot do with diffusion MRI | Carlo Pierpaoli |
| 41 | Friday | 9/1/17 | 40, Rm 1201/1203 | 2:00 PM | The future of fMRI & Course Conclusion | Peter Bandettini |

# A Brief History of Neuroimaging & fMRI


**Peter A. Bandettini, Ph.D.**

**Section on Functional Imaging Methods**

**Laboratory of Brain and Cognition**

http://fim.nimh.nih.gov

**&**

**Functional MRI Facility**

http://fmrif.nimh.nih.gov

## Brief History of Brain Imaging

1. **Lesion-based Mapping.**
2. **Anatomic Imaging.**
3. **Hemodynamic and Metabolic Imaging.**
4. **Electrophysiologic Imaging**
5. **Functional MRI**

## Brief History of Brain Imaging

1. **Lesion-based Mapping.**
2. **Anatomic Imaging.**
3. **Hemodynamic and Metabolic Imaging.**
4. **Electrophysiologic Imaging**
5. **Functional MRI**

# 1848


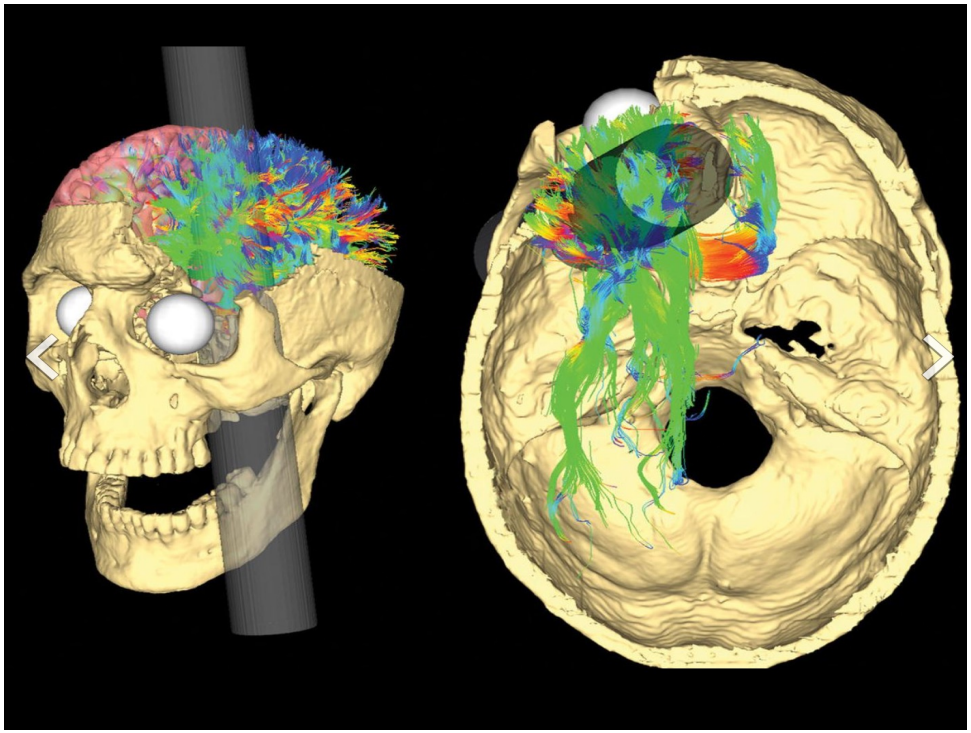

# 1861 Paul Broca:

## His patient, Leborgne, could only produce "tan."

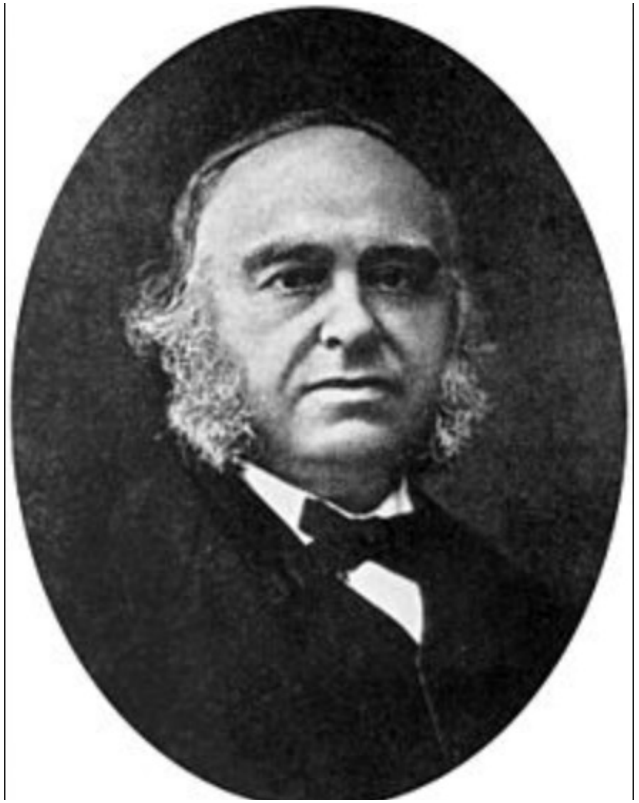

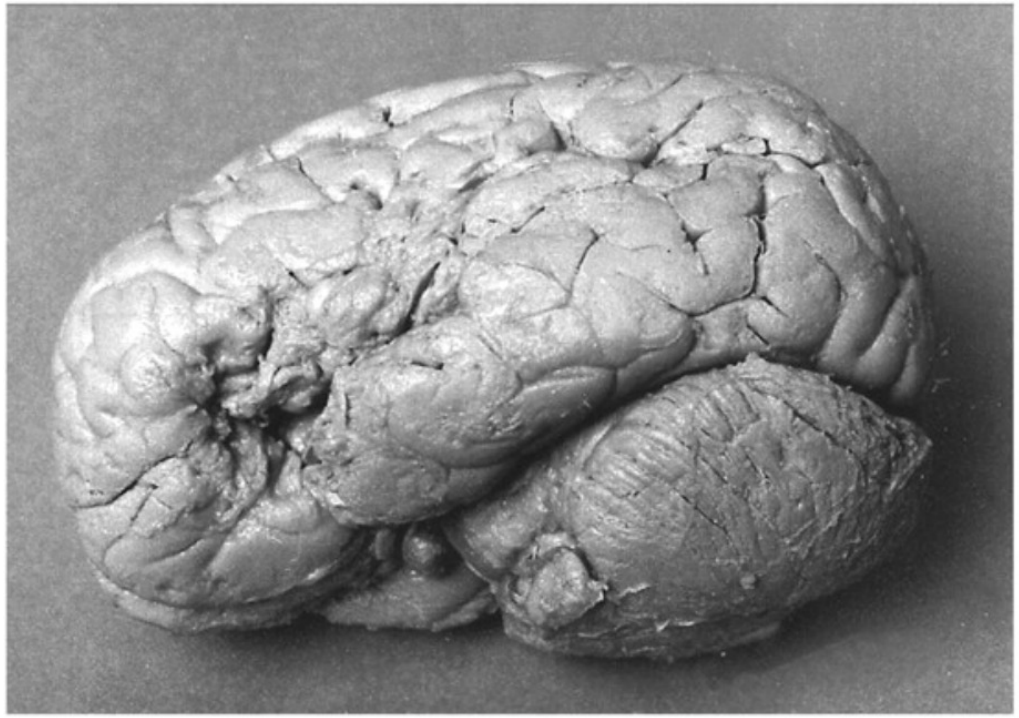

# 1874: Carl Wernicke

**His patients could not understand or produce meaningful speech but could articulate words.**


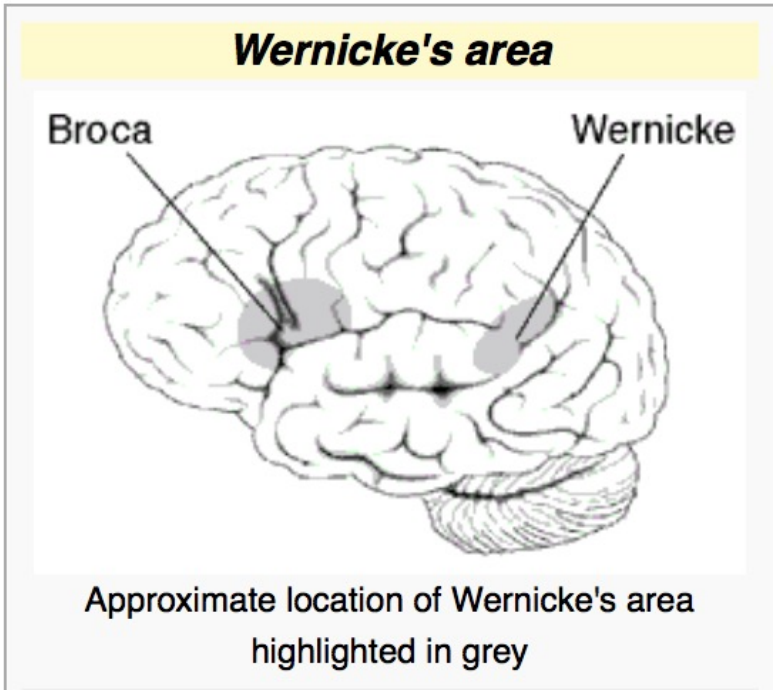

## Brief History of Brain Imaging

1. **Lesion-based Mapping.**
2. **Anatomic Imaging.**
3. **Hemodynamic and Metabolic Imaging.**
4. **Electrophysiologic Imaging**
5. **Functional MRI**

# 1895: Roentgen discovers x-rays and their utility

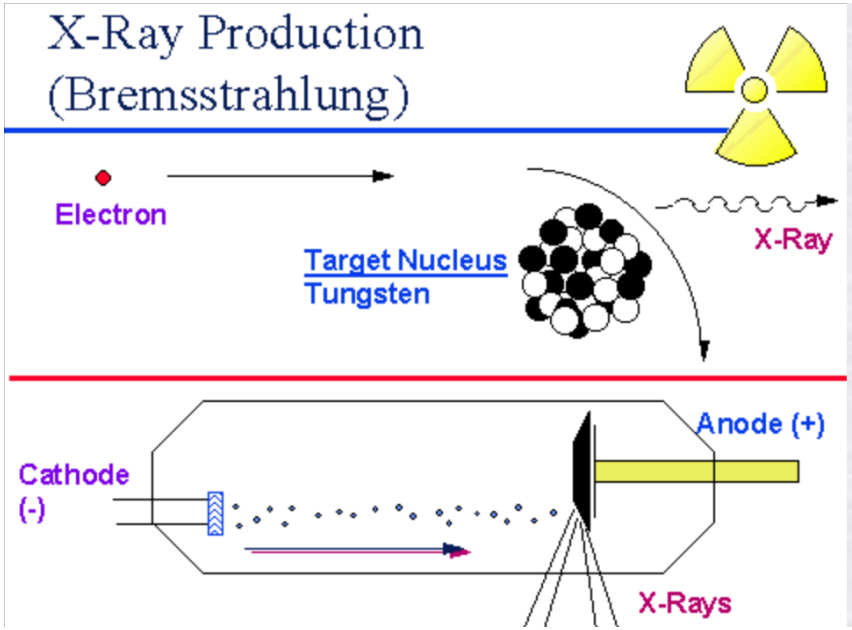


## Crooke's tube

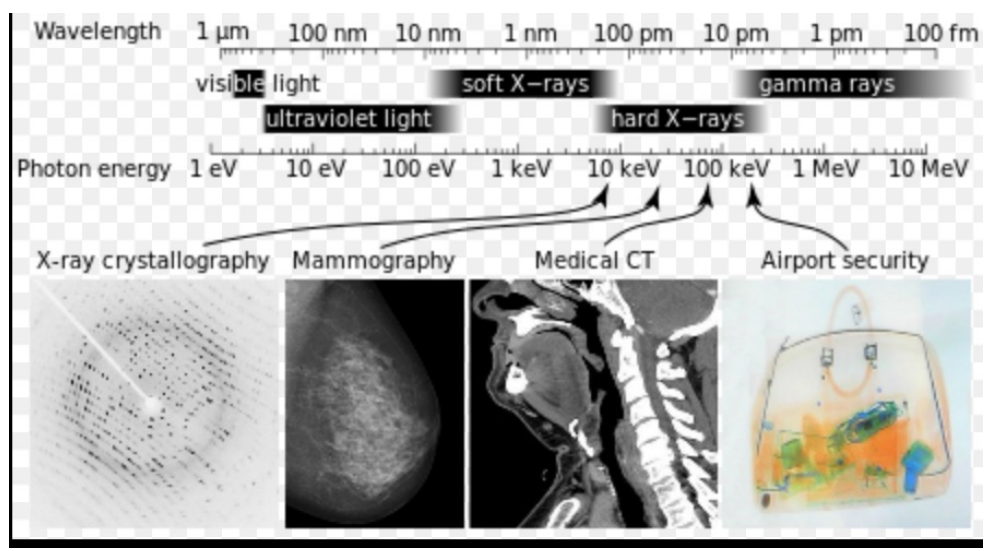

# Early 1900's: Pneumoencephalography

**CSF drained from the brain to enhance contrast in x-rays**

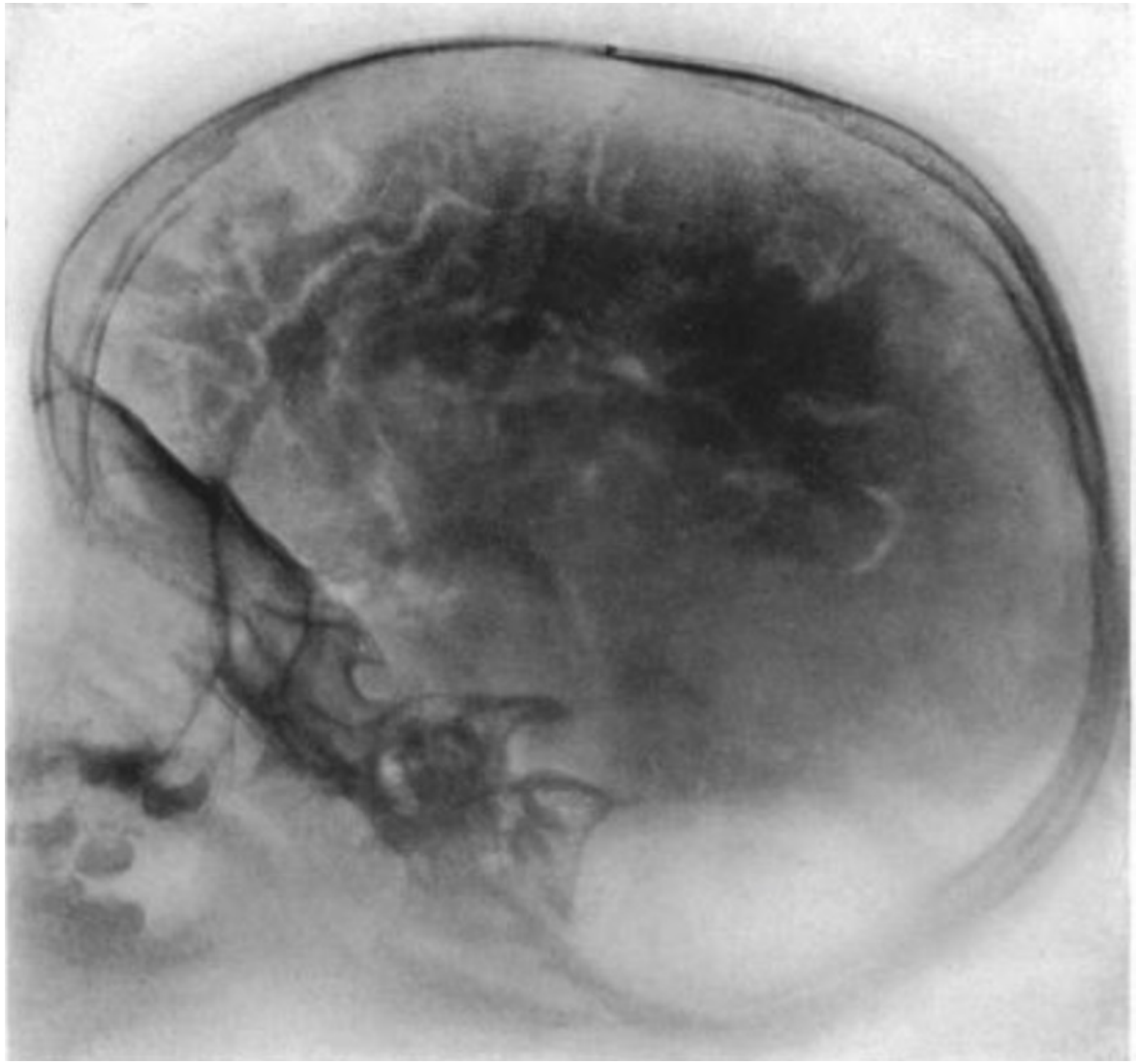

# 1927: Antonio Egas Moniz – first Arteriogram

***... also invented the lobotomy***

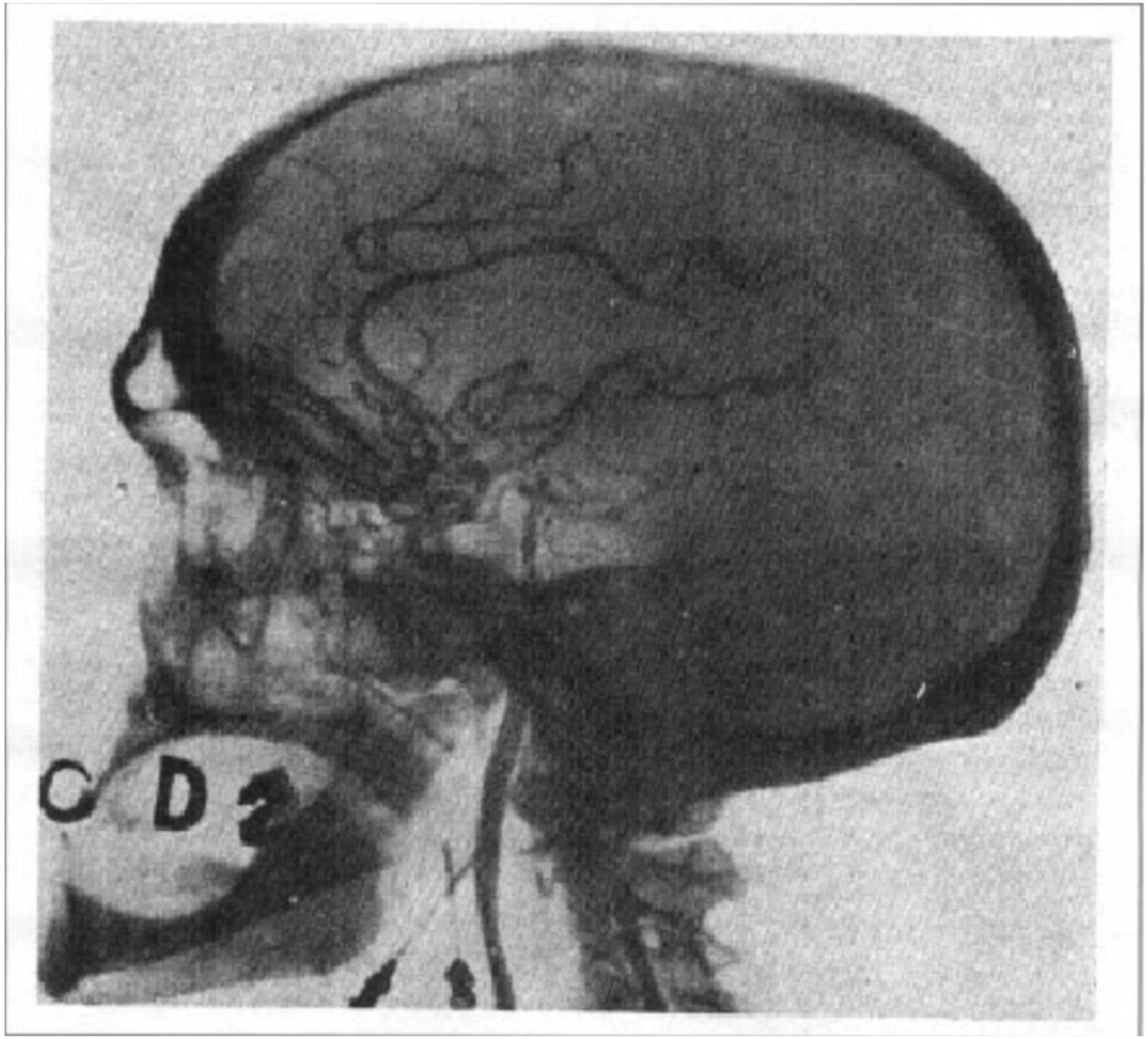


**strontium and lithium bromide contrast agent**

**1960, William Oldendorf patented an electronically based device that could capture image slices continuously through a solid object**

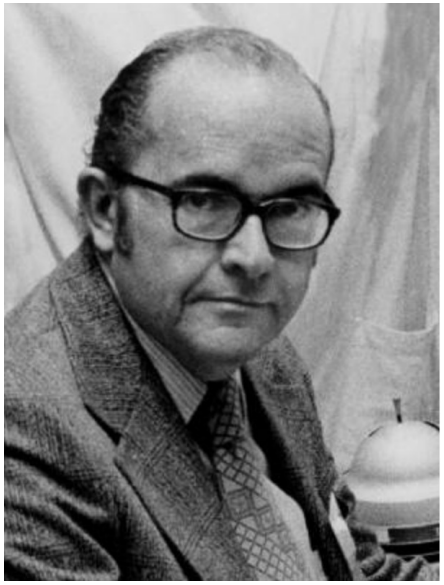

**1971: Hounsfield implemented the first CT scanner**

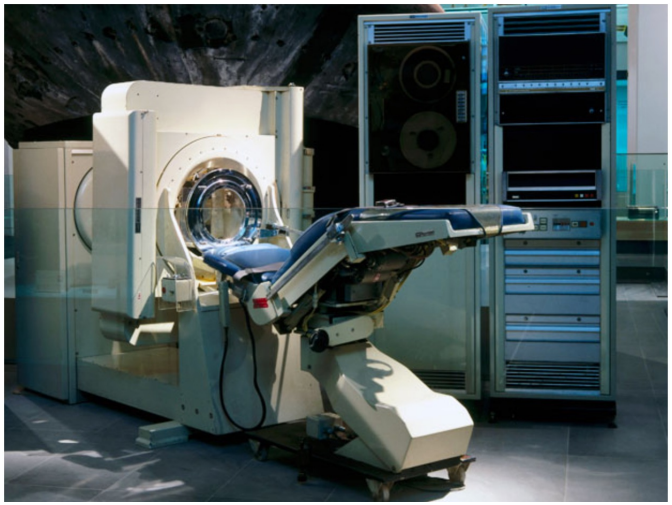

*Godfrey Hounsfield received the 1979 Nobel Prize in Medicine for his work in the development of computer assisted tomography (CAT) scanning.*

# MRI: Magnetic Resonance Imaging

Sir Peter Mansfield and Paul Lauterbur, Winners of the Nobel Prize for Medicine, 2003

## Lauterbur's Contribution: Projectional NMR Tomography

***Paul Lauterbur*** (1909-2007), a chemist working at the State University of New York at Stony Brook, published the first true MR image in *Nature* in March, 1973. His experimental setup involved two 1-mm-diameter tubes filled with water placed in an 1.4T magnet. Applying magnetic field gradients rotated successively by 45°, he was able to obtain four different 1-dimensional projections of the NMR signal. These data were then mathematically "back-projected" to form a 2-dimensional tomographic image. Because the result depended on the combined effects of two magnetic fields, Lauterbur named his technique "***zeugmatography***" after the Greek word, *zeugma*, meaning "that which is used for joining." Shortly thereafter, Lauterbur produced crude images of his first living subject: a tiny clam.

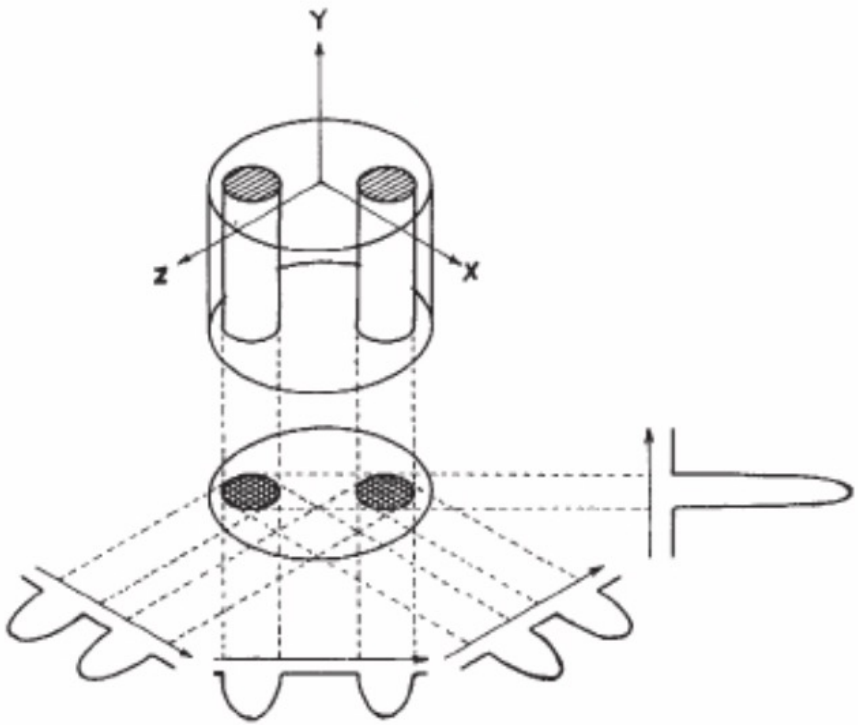


**Fig. 1** Relationship between a three-dimensional object, its two-dimensional projection along the Y-axis, and four one-dimensional projections at 45° intervals in the XZ-plane. The arrows indicate the gradient directions.

**Fig. 2** Proton nuclear magnetic resonance zeugmatogram of the object described in the text, using four relative orientations of object and gradients as diagrammed in Fig. 1.

## Mansfield's Contribution: Use of a field gradient for slice selection

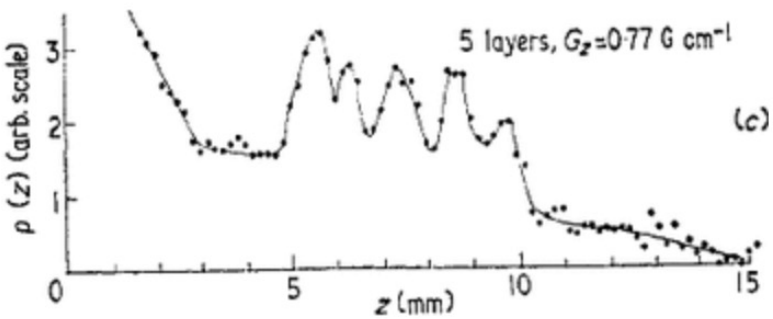


From Mansfield (1973). Five peaks corresponding to five stacked blocks of solid camphor.

Also in 1973, ***Peter Mansfield*** (b. 1933), a physicist working at the University of Nottingham, demonstrated how a linear field gradient could be used to localize the NMR signal on a slice-by-slice basis. Mansfield's experimental setup involved stacking multiple 1-mm-thick sheets of solid camphor into the bore of an NMR spectrometer. Applying a magnetic field gradient perpendicular to the sheets, Mansfield measured the transient NMR signal response to an applied RF-pulse. Interference peaks similar to those seen in x-ray diffraction were observed, which when inverse Fourier transformed revealed discrete layers of the camphor sample.

Later in the decade, Mansfield and his collaborator, Andrew Maudsley, further refined this method into a line-scan technique, producing the first image of a human body part, a finger, in 1977.

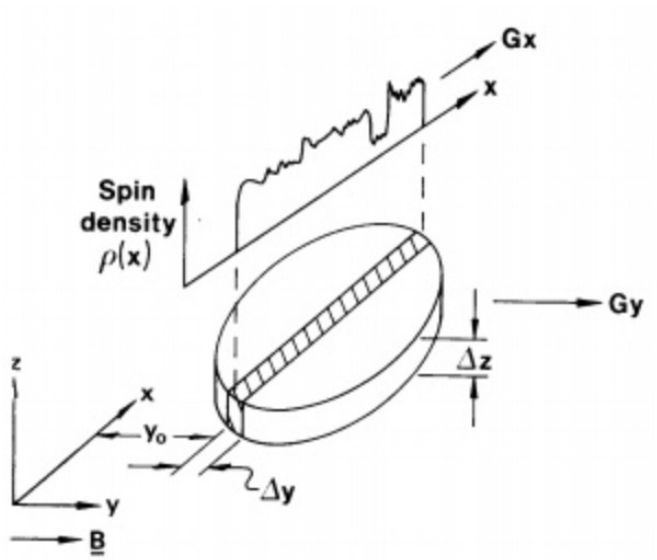


Line-scan technique, selectively irradiating a narrow strip with an isolated slice of magnetization.

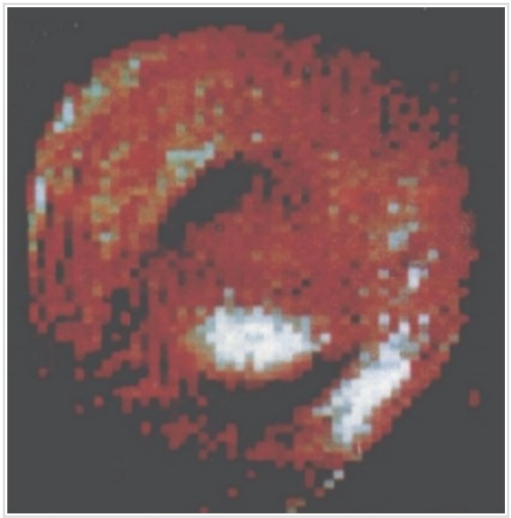

Image of human finger from Mansfield and Maudsley (1977) using line-scan technique obtained at 0.35T in 23 minutes. The white oval is marrow within the phalanx and the dark bands are tendons.

## Damadian's Contribution: Vision of a human-sized scanner to detect disease

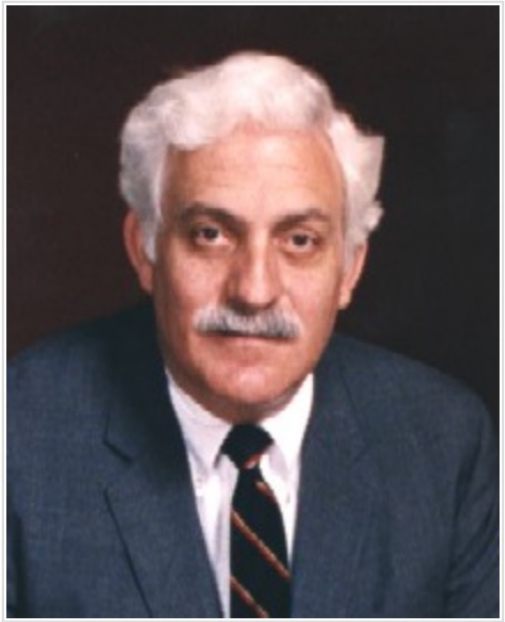

Raymond V. Damadian

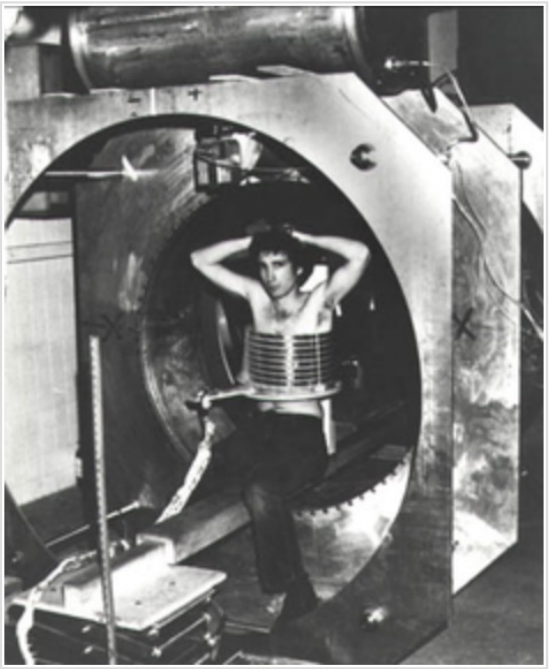

Assistant Larry Minkoff in Indomitable

While Lauterbur and Mansfield were basic scientists, ***Raymond V. Damadian*** (b. 1936) was a physician, an Associate Professor of Medicine at the State University of New York - Brooklyn (Downstate). He looked at NMR from a different and original perspective — as a phenomenon that might be used to probe the body and diagnose human disease. In one of his landmark early papers (*Science*, 1971) Damadian demonstrated that cancer cells had longer T1 and T2 values than normal cells. In 1972 he filed a US patent application for an apparatus and method to detect cancer in tissue. Although the details of exactly how this 'apparatus" would produce images were not included in the application, Damadian and his team set out to build such a device which was named "***Indomitable***." By mid-summer, 1977, the first whole-body MR images were being produced, including the famous one shown below of his assistant's chest.

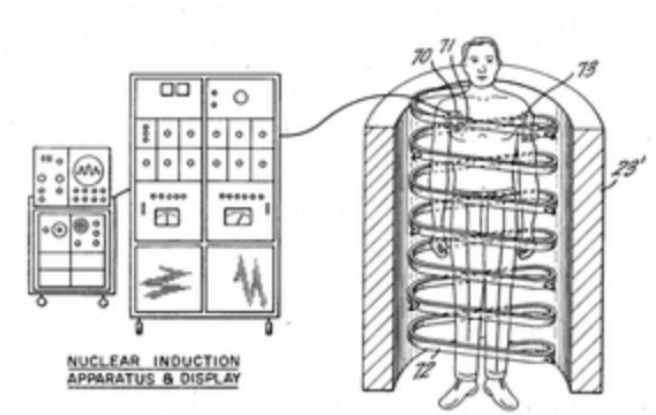


Damadian's 1972 patent application

Damadian used a "sensitive point" method for spatial localization of the NMR signal. This was based on a saddle-shaped magnetic field where only a small volume at the center matched the resonance frequency of the RF pulse. The patient's body was physically moved in a rectangular pattern until signals from all pixels were obtained.

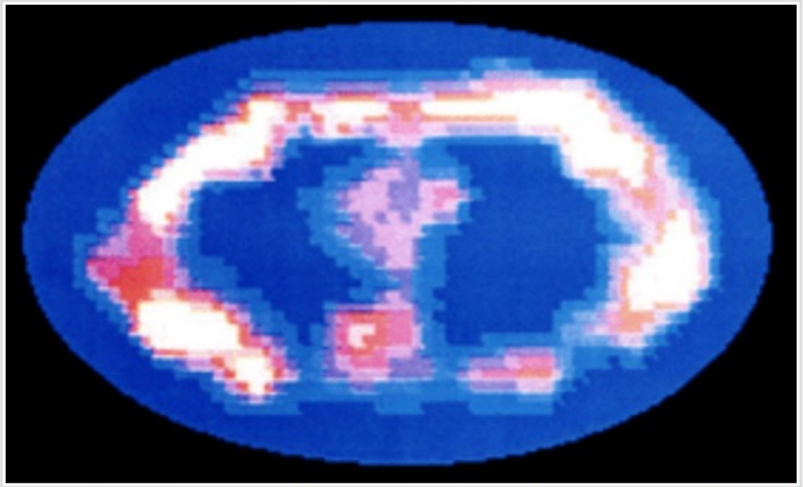

First whole body image (Minkoff's chest), obtained July, 1977. It required nearly 5 hours to produce.

Damadian called his imaging method "field-focused NMR" or FONAR. This became the name of his company, the first to manufacture clinical MR scanners commercially. It was soon recognized that the field-focused method was far too slow and clumsy for routine clinical imaging, and so it was abandoned in favor of the methods of Lauterbur and Mansfield in subsequent versions of the scanner.

When the 2003 Nobel Prizes for Medicine were announced, Damadian considered it a personal injustice that he was excluded. He placed full-page ads in several large world newspapers urging the Nobel committee to change its mind. The decision stood.

| V·T·E | Medical imaging (ICD-9-CM V3 87–88, ICD-10-PCS B, CPT 70010–79999) | | | [hide] |
|---|---|---|---|---|
| X-ray/ Radiography | 2D | Medical: | Pneumoencephalography · Dental radiography · Sialography · Myelography · CXR (Bronchography) · AXR · KUB · DXA/DXR · Upper gastrointestinal series/Small-bowel follow-through/Lower gastrointestinal series · Cholangiography/Cholecystography · Mammography · Pyelogram · Cystography · Arthrogram · Hysterosalpingography · Skeletal survey · Angiography (Angiocardiography · Aortography) · Venography · Lymphogram | |
| | | Industrial: | Radiographic testing | |
| | 3D / XCT | Medical: | CT pulmonary angiogram · Computed tomography of the heart · Computed tomography of the abdomen and pelvis (Virtual colonoscopy) · CT angiography · Computed tomography of the head · Quantitative computed tomography · Spiral computed tomography · High resolution CT · Whole body imaging (Full-body CT scan) · X-ray microtomography · Electron beam tomography | |
| | | Industrial: | Industrial computed tomography | |
| | Other | Fluoroscopy · X-ray motion analysis | | |
| MRI | MRI of the brain · MR neurography · Cardiac MRI/Cardiac MRI perfusion · MR angiography · MR cholangiopancreatography · Breast MRI · Functional MRI · Diffusion MRI · Synthetic MRI | | | |
| Ultrasound | Echocardiography · Doppler echocardiography (TTE · TEE) · Intravascular · Gynecologic · Obstetric · Echoencephalography · Transcranial Doppler · Abdominal ultrasonography · Transrectal · Breast ultrasound · Transscrotal ultrasound · Carotid ultrasonography · Contrast-enhanced · 3D ultrasound · Endoscopic ultrasound · Emergency ultrasound (FAST · Pre-hospital ultrasound) · Duplex | | | |
| Radionuclide | 2D / scintigraphy | Cholescintigraphy · Scintimammography · Ventilation/perfusion scan · Radionuclide ventriculography · Radionuclide angiography · Radioisotope renography · Sestamibi parathyroid scintigraphy · Radioactive iodine uptake test · Bone scintigraphy · Immunoscintigraphy · Dacryoscintigraphy | | |
| | | Full body: | Octreotide scan · Gallium 67 scan · Indium-111 WBC scan | |
| | 3D / ECT | SPECT (gamma ray: Myocardial perfusion imaging) | | |
| | | PET (positron): | Brain PET · Cardiac PET · PET mammography · PET-CT | |
| Optical laser | Optical tomography (Optical coherence tomography) · Confocal microscopy · Endomicroscopy | | | |
| Thermography | non-contact thermography · contact thermography · dynamic angiothermography | | | |

Categories: Radiology | Medical imaging | Inverse problems | Multidimensional signal processing | Signal processing | Tomography

## Brief History of Brain Imaging

1. **Lesion-based Mapping.**
2. **Anatomic Imaging.**
3. **Hemodynamic and Metabolic Imaging.**
4. **Electrophysiologic Imaging**
5. **Functional MRI**

# 1880's: Angelo Mosso's balance

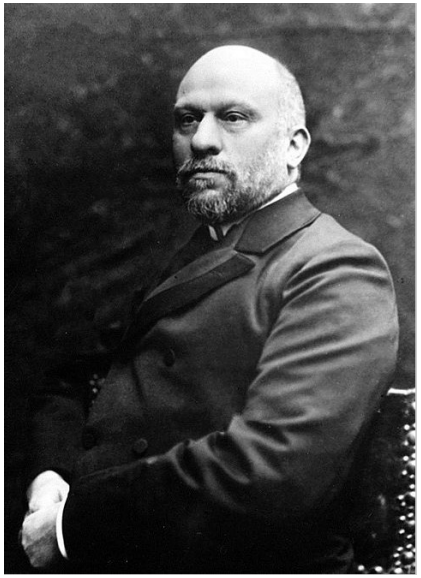

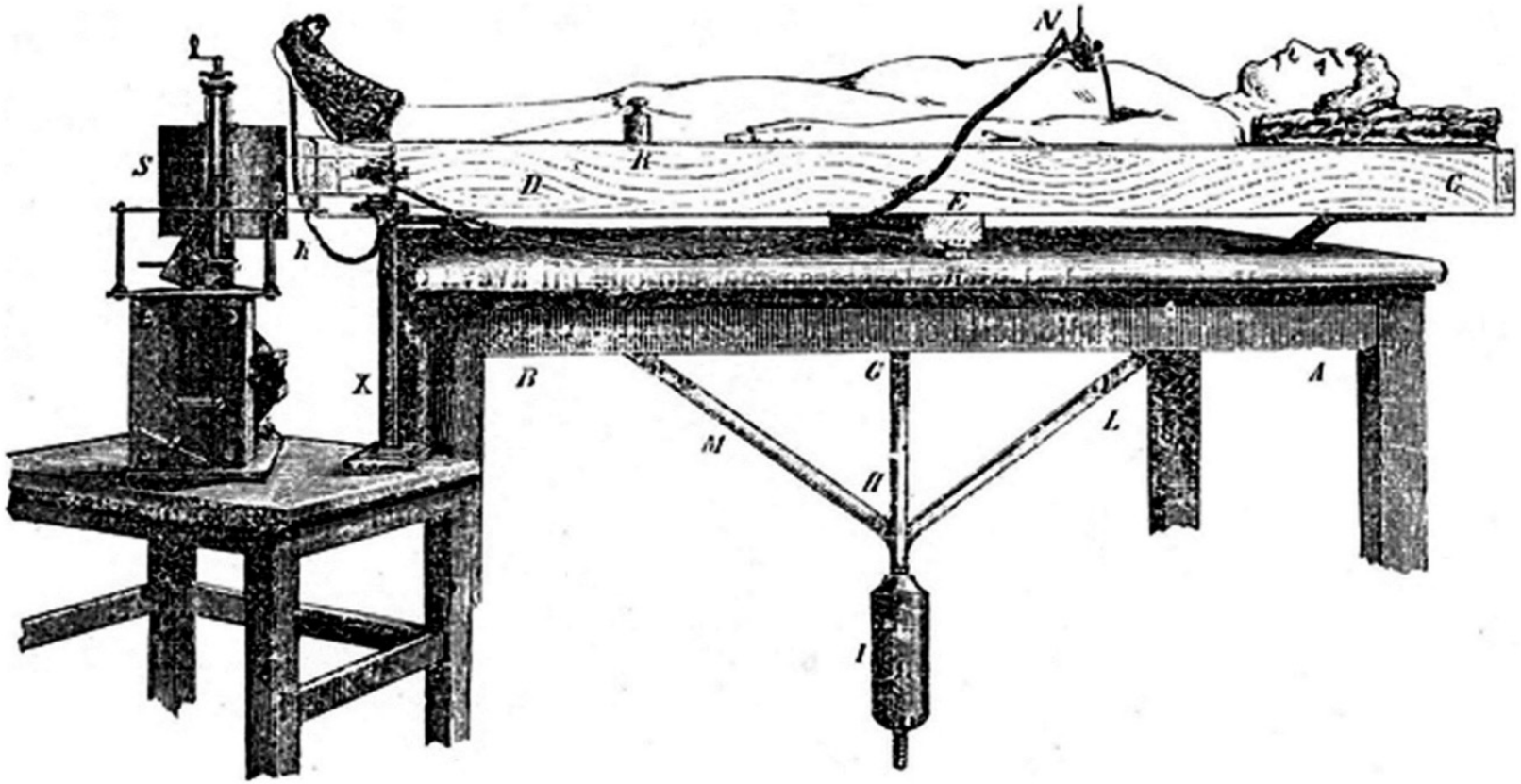

# “On the Regulation of the Blood-Supply of the Brain”

**C. S. Roy and C. S. Sherrington,** J Physiol. 1890 Jan; 11(1-2): [85]-108, 158-7-158-17.

***…measured cerebral pressure and brain position***

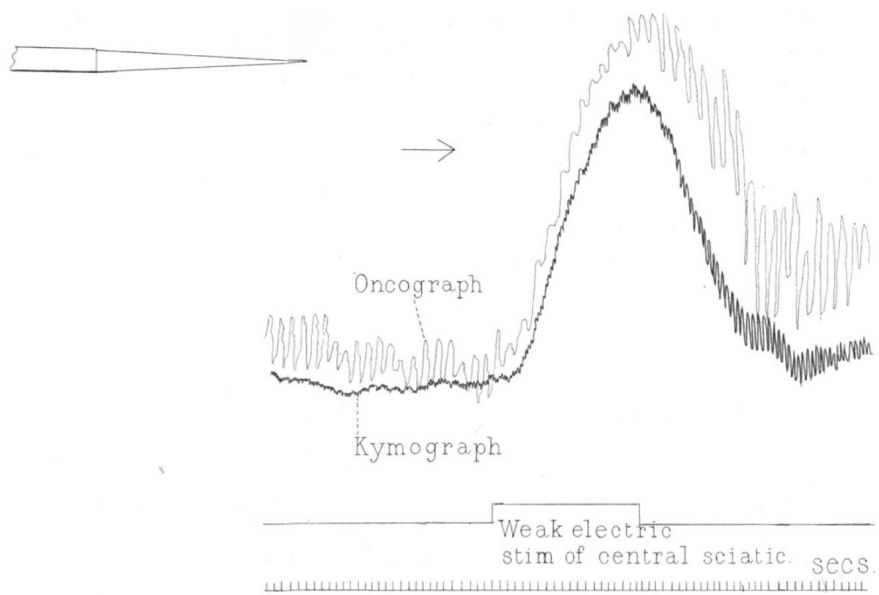

# 1960's to 70's: Xenon inhalation – radiation detection at the surface of brain

Niels A. Lassen, David H. Ingvar, Erik Skinhøj, "Brain Function and Blood Flow", Scientific American, 239(4):50-59, 1978 October

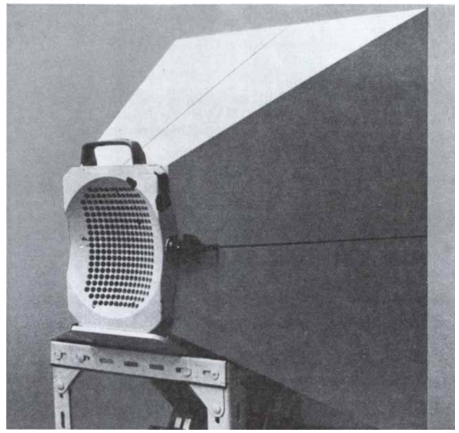

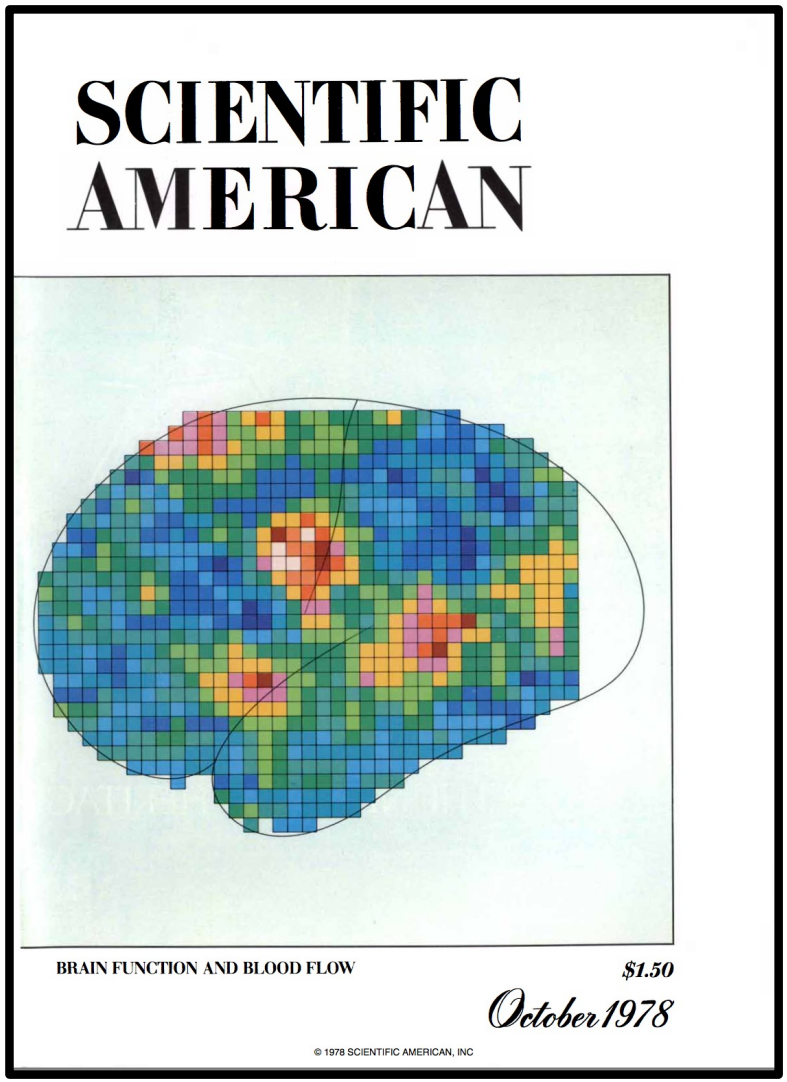


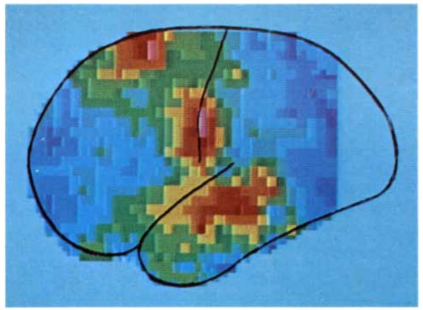

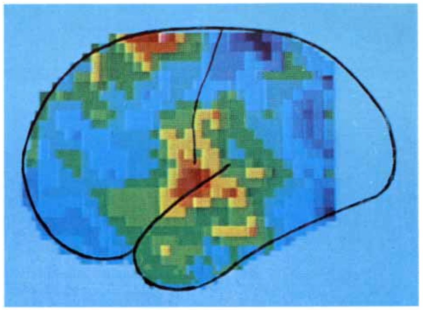

**SPEAKING** activates three centers in each hemisphere: the mouth-tongue-larynx area of the somatosensory and motor cortex, the supplementary motor area and the auditory cortex. Differences in activity between the two hemispheres can be seen in these averaged images from nine different subjects: in the right hemisphere (*right*) the mouth-tongue-larynx area is less distinct and coalesces with auditory cortex.

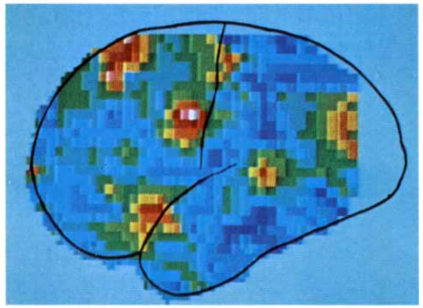

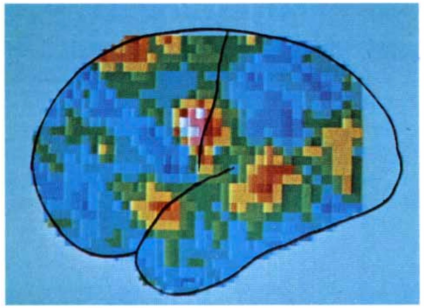

**READING SILENTLY AND READING ALOUD** involve different patterns of activity in the cortex. Reading silently (*left*) activates four areas: the visual association area, the frontal eye field, the supplementary motor area and Broca's speech center in the lower part of the frontal lobe. Reading aloud (*right*) activates two more centers: the mouth area and the auditory cortex. The left hemisphere is shown in both cases, but similar results have been obtained from the right hemisphere. Adding the primary visual cortex, which is not reached by the radioactive isotope, the act of reading aloud calls for simultaneous activity in seven discrete cortical centers in each hemisphere.

# 1973: Michael Ter-Pogossian, Edward Hoffman, and Micahale Phelps - First Human PET scanner

## *Coincidence Detection*

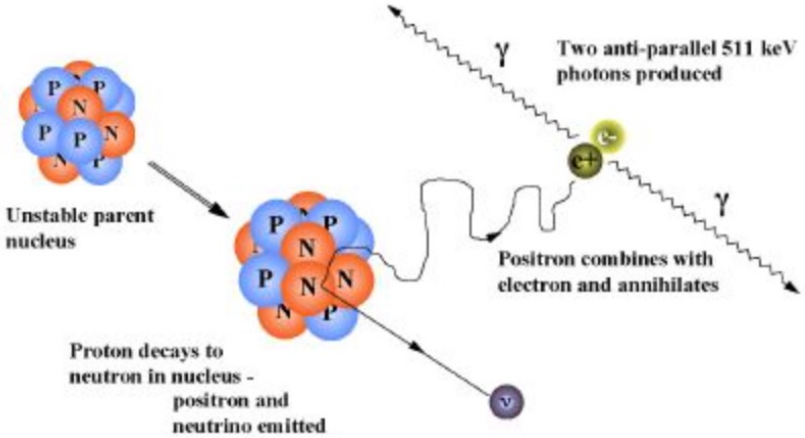


**Figure 1. Positron emission and annihilation.**

| Isotope | half-life (min) | Maximum positron energy (MeV) | Positron range in water (FWHM in mm) | Production method |
|---|---|---|---|---|
| $^{11}C$ | 20.3 | 0.96 | 1.1 | cyclotron |
| $^{13}N$ | 9.97 | 1.19 | 1.4 | cyclotron |
| $^{15}O$ | 2.03 | 1.70 | 1.5 | cyclotron |
| $^{18}F$ | 109.8 | 0.64 | 1.0 | cyclotron |
| $^{68}Ga$ | 67.8 | 1.89 | 1.7 | generator |
| $^{82}Rb$ | 1.26 | 3.15 | 1.7 | generator |

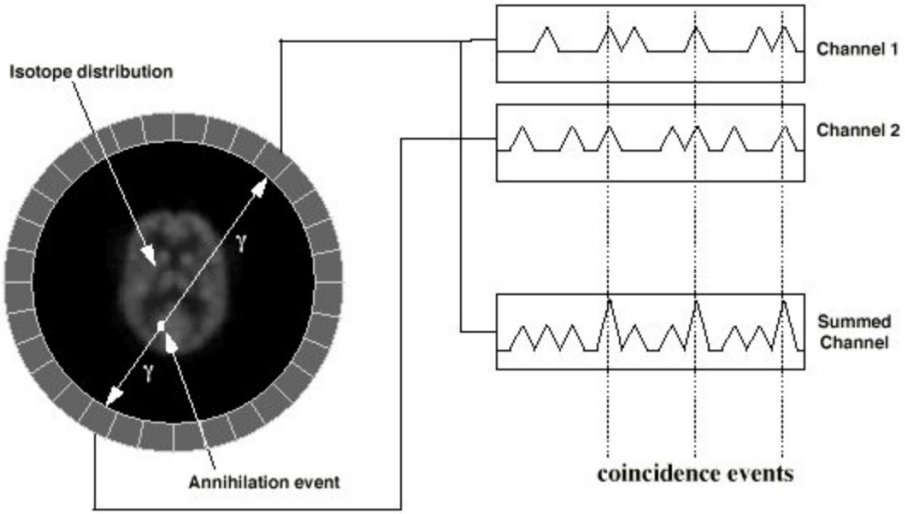


**Figure 2. Coincidence detection in a PET camera.**

# 1973: Michael Ter-Pogossian, Edward Hoffman, and Micahale Phelps - First Human PET scanner

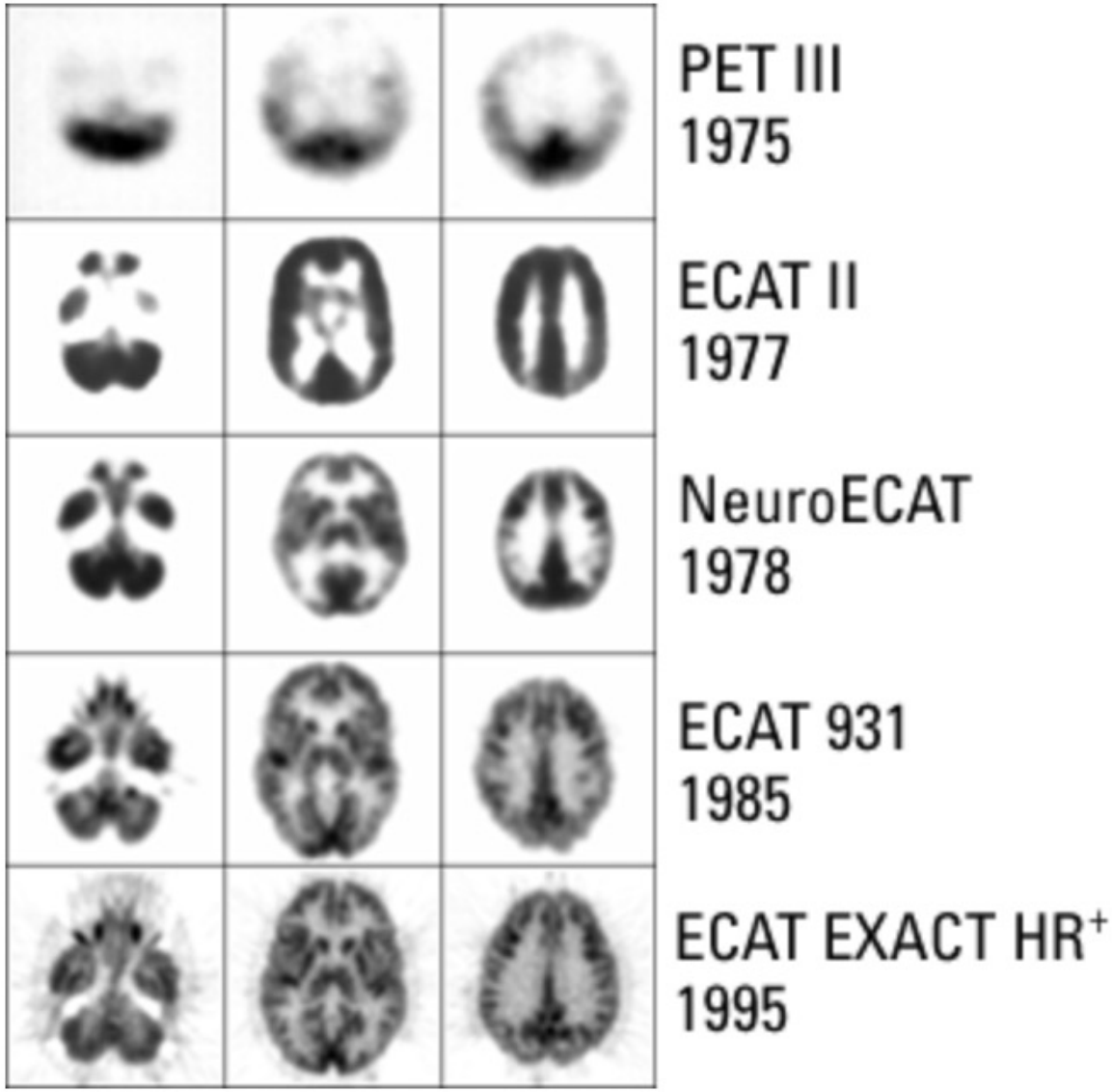

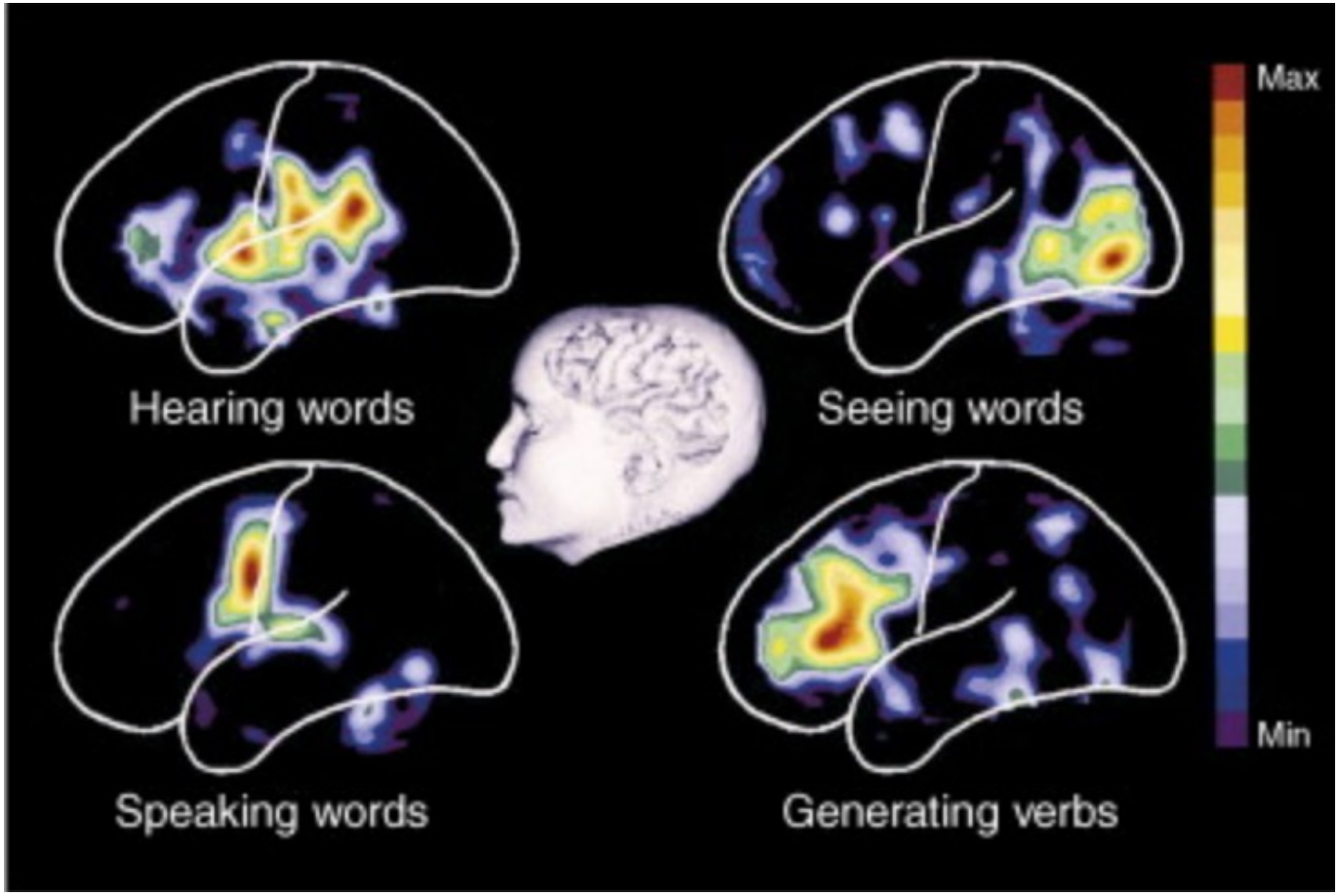


**Positron emission tomographic studies of the cortical anatomy of single-word processing. Petersen, S.E. et al. Nature. 1988; 331: 585–589**

## Brief History of Brain Imaging

1. **Lesion-based Mapping.**
2. **Anatomic Imaging.**
3. **Hemodynamic and Metabolic Imaging.**
4. **Electrophysiologic Imaging**
5. **Functional MRI**

## From the electrical nature of brain signals …

**1875**: R.C. measured currents inbetween the cortical surface and the skull, in dogs and monkeys

*Richard Caton*
*1842 - 1926*

**1924**: H.B. first EEG in humans, description of alpha and beta waves

Alpha actiity ~ 200 $\mu$V

*Hans Berger*
*1873 - 1941*

http://www.slideshare.net/nikhilprerana/meg-final

## About 50 years later …

***Brian-David Josephson***

**1968**: first (noisy) measure of a magnetic brain signal *[Cohen, Science 68]*

**1970**: James Zimmerman invents the
'*Superconducting quantum interference device*' (SQUID)

**1972**: first (1 sensor) MEG recording based on SQUID

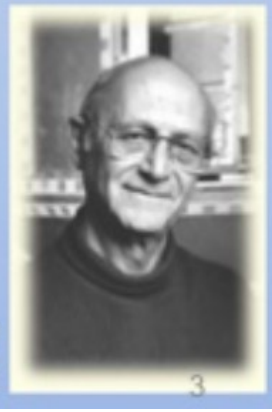

***David Cohen***



http://www.slideshare.net/nikhilprerana/meg-final

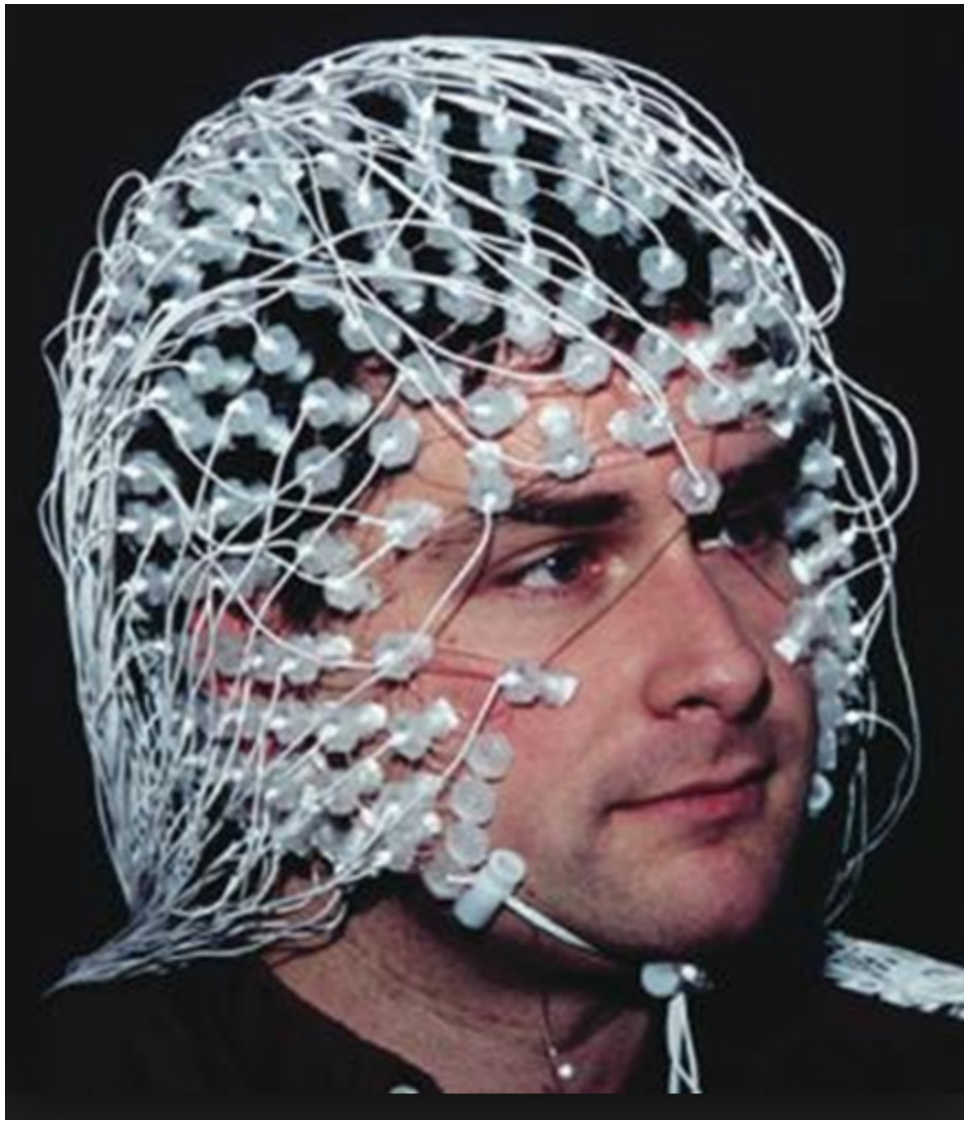

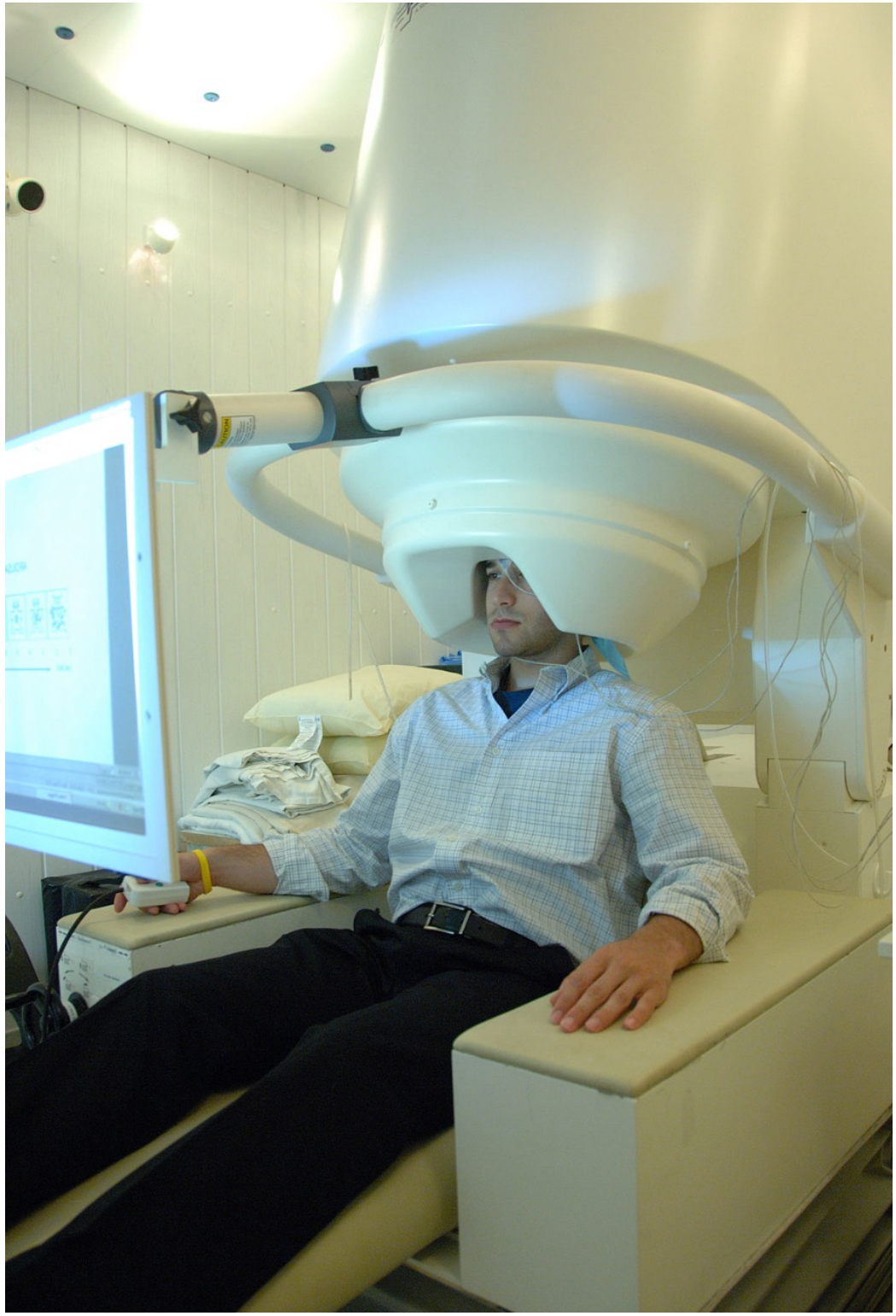

## Brief History of Brain Imaging

1. **Lesion-based Mapping.**
2. **Anatomic Imaging.**
3. **Hemodynamic and Metabolic Imaging.**
4. **Electrophysiologic Imaging**
5. **Functional MRI**

ISSN 1053-8119
Volume 62, Issue 2, August 15, 2012

ELSEVIER

# NeuroImage

*Editor-in-Chief*
**Peter Bandettini**


*Special Issue*
**20 Years of fMRI: The Science and the Stories**

Available online at www.sciencedirect.com
SciVerse ScienceDirect


SPM CENTRAL
FSL
AFNI
SCIENCE

| | | | | | | | | | | |
|---|---|---|---|---|---|---|---|---|---|---|
| Peter Jezzard | Alan Koretsky | Fahmeed Hyder | Robert Savoy | David Norris | Steve Engel | Klaas Enno Stephan | John Baptiste Poline | Andrew Blamire | Kamil Ugurbil, Seiji Ogawa, Ravi Menon, Seong-Gi Kim | Mark Woolrich |
| David McGonigle | Tom Liu | Ken Kwong, Van Wedeen, Jack Belliveau, Bruce Rosen | Joe Mandeville | SPM | Dan Handwerker | Franz Schmitt, Mark Cohen | Eleanor Maguire | Christian Beckmann | Jim Haxby | Denis LeBihan |
| Jack and Amelie Belliveau | fMRI course cartoon from Robert Savoy | Alan Evans | Bruce Jenkins | Jia-Hong Gao | Ed Vul | Fa-Hsuan Lin | Tom Nichols | Multivariate Analysis Display from Niko Kriegeskorte | Peter van Gelderen | Rick Hoge |
| Jeff Duyn | David Feinberg | Hanzhang Lu | Mark Jenkenson | Randy McIntosh | Bruce Rosen | Afonso Silva | Bharat Biswal | Alard Roebroeck | Keith Thulborn | First MGH Functional Images |
| Rainer Goebel | Orientation Column fMRI data from Noam Harel | Steve Petersen, Joseph Dubis | Tom Talavage | Vince Clark | Gary Glover | Russ Poldrack | Seiji Ogawa | Eric Wong | Deb Hall | Krish Singh |
| Mark Lowe | Kamil Ugurbil | Uri Hasson | Susan Courtney | Elia Formisano | Peter Bandettini | Ed Bullmore | Network Connectivity Depictions from Steve Smith | Robert Weisskoff | Martin Lauritzen | Geoff Aguirre |
| FSL | Jurgen Reichenbach | James Hyde | Vascular Tree Depiction from Ravi Menon | Bruce Fischl | Scott Huettel | Bob Cox | Karla Miller | Ken Kwong | Nikos Logothetis | Keith Worsley |
| Ravi Menon | Robert Turner | Helmut Laufs | Kang Cheng | Xiaoping Hu | Andrzej Jesmanowicz | Rick Buxton | Olaf Sporns | AFNI | Larry Wald | Karl Friston |
| Stefan Posse | Brain Connectivity Display from Olaf Sporns | Peter van Zijl | John Ashburner | Rafi Malach | Jeff Binder | Heidi Johansen-Berg | Ziad Saad | Marcus Raichle, Avi Snyder | Niko Kriegeskorte, Marieke Mur | First fMRI results from Jack Belliveau (with gadolinium) |
| Geoff Boynton | Jurgen Hennig | Dave Rumelhart, Gary Glover, Brian Wandell | Seong-Gi Kim | Arno Villringer | Randy and Benjamin Buckner | First MCW Functional Image | Allen Song | Peter Bandettini, Eric Wong | Andreas Meyer-Lindenberg | Bruce Pike |
| Nikolaus Weiskopf | Steve Smith | Peter Fox | Gunnar Kreuger | Resting State Networks from Avi Snyder | Cathy Price | Rasmus Birn | Mark Haacke | Noam Harel | First U. Minn. Fuctional Images and Time Course | David Van Essen |

| Section | Paper Number | Paper Title | Author |
|---|---|---|---|
| **Pre-fMRI** | 1 | The science and the stories: fMRI over the past 20 years | Peter Bandettini |
| | 2 | My starting point: the discovery of an NMR method for measuring blood oxygenation using the transverse relaxation time of blood water | Keith Thulborn |
| | 3 | The coupling controversy | Peter Fox |
| | 4 | Early development of arterial spin labeling to measure regional brain blood flow by MRI | Alan Korestky |
| | 5 | Finding the BOLD effect in brain images | Seiji Ogawa |
| **The first BOLD Brain Activation Results** | 6 | Record of a single fMRI experiment in May of 1991 | Ken Kwong |
| | 7 | Development of functional Imaging in the human brain (fMRI); the university of Minnesota experience | Kamil Ugurbil |
| | 8 | Sewer pipe, epoxy, wire, and finger tapping: the start of fMRI at the Medical College of Wisconsin | Peter Bandettini |
| | 9 | The NIH experience in first advancing fMRI | Robert Turner |
| | 10 | The Yale Experience in first advancing fMRI | Andrew Blamire |
| **Developments in Pulse Sequences, Imaging Methods, and Hardware for fMRI** | 11 | How the challenges of auditory fMRI led to general advancements for the field | Tom Talavage |
| | 12 | Correction of geometric distortion in fMRI data | Peter Jezzard |
| | 13 | Echo Planar Imaging before and after fMRI: a personal history | Mark Cohen & Franz Schmitt |
| | 14 | Local Head Gradient Coils: wondow(s) of opportunity | Eric Wong |
| | 15 | Multi-echo acquisition | Stefan Posse |
| | 16 | Perfusion MRI Imaging: evolution from initial developments to functional studies | Seong-Gi Kim |
| | 17 | The PRESTO technique for fMRI | Peter van Gelderen |
| | 18 | Real Time fMRI and its application to neurofeedback | Nikolaus Weiskopf |
| | 19 | Functional spectroscopy to no-gradient fMRI | Jurgen Hennig |
| | 20 | Ultrafast Inverse imaging techniques for fMRI | Fa-Hsuan Lin |
| | 21 | Spiral Imaging in fMRI | Gary Glover |
| | 22 | fMRI using steady-state free precession (SSFP) sequences | Karla Miller |
| | 23 | The rapid development of high speed, resolution, and precision in fMRI | David Feinberg & Essa Yacoub |
| | 24 | The road to functional imaging at ultrahigh fields | Kamil Ugurbil |
| | 25 | A review of the development of vascular space occupancy (VASO) fMRI | Hanzhang Lu |
| **The emergence of processing and display packages** | 26 | AFNI: what a long strange trips its been | Bob Cox |
| | 27 | Brain Voyager - past, present, and future | Rainer Goebel |
| | 28 | Cortical Cartography and Caret software | David van Essen |
| | 29 | FIASCO, STIMULATE, VoxBo, MEDx, Early fMRI Software: Where are they now? | Geoff Aguirre |
| | 30 | SUMA | Ziad Saad |
| | 31 | Free Surfer | Bruce Fischl |
| | 32 | FSL | Mark Jenkinson |
| | 33 | SPM: a history | John Ashburner |
| **Development of Processing Methods for fMRI** | 34 | Bayesian Inference in fMRI | Mark Woolrich |

| | | | |
|---|---|---|---|
| | 35 | Multiple testing corrections, nonparametric methods, and Random Field Theory | Tom Nichols |
| | 36 | A review and synthesis of the first 20 years of PET and fMRI studies of spoken language and reading | Cathy Price |
| | 37 | Cross-correlation: an fMRI signal-processing strategy | Jim Hyde & Andrzej Jesmanowicz |
| | 38 | Multivariate patterns analysis of fMRI: the early beginnings | Jim Haxby |
| | 39 | A short history of causal modeling of fMRI data | Klaas Enno Stephan & Alard Roebroeck |
| | 40 | The role of physiologic noise in resting-state functional connectivity | Rasmus Birn |
| | 41 | General Linear Model and fMRI: does love last forever? | Jean-Babtiste Poline |
| | 42 | From simple graphs to the connectome: networks in neuroimaging | Olaf Sporns |
| | 43 | Tracing the route to path analysis in neuroimaging | Randy McIntosh |
| | 44 | Modeling with independent components | Christian Beckmann |
| | 45 | A brief history of resting state: the Washington university perspective | Avi Snyder & Marcus Raichle |
| | 46 | Brain templates and atlases | Alan Evans |
| **Methodological Developments, Issues, and Mechanisms** | 47 | The role of susceptibility weighted imaging in functional MRI | Mark Haacke & Yongquan Ye |
| | 48 | Calibrated fMRI | Rick Hoge |
| | 49 | Resting state fMRI: a personal history | Bharat Biswal |
| | 50 | Voodoo and circularity errors | Ed Vul |
| | 51 | Diffusion modulation of the fMRI signal | Alan Song |
| | 52 | Dynamic Models of BOLD contrast | Rick Buxton |
| | 53 | Intracortical Recordings and fMRI: An attempt to study operational modules and networks simultaneously. | Nikos Logothetis |
| | 54 | The Great Brain versus Vein Debate | Ravi Menon |
| | 55 | Linear systems analysis of the fMRI signal | Geoff Boynton |
| | 56 | Quantitative fMRI and oxidative neuroenergetics | Fahmeed Hyder & Douglas Rothman |
| | 57 | The meaning of fMRI signals | Arno Villringer |
| | 58 | IRON fMRI measurements of CBV and implications for BOLD signal | Joe Mandeville |
| | 59 | Using manganese-enhanced MRI to understand BOLD | Afonso Silva |
| | 60 | The characterization of dynamic susceptibility effects | Robert Weisskoff |
| | 61 | The continuing challenge of understanding and modeling hemodynamic variation in fMRI | Dan Handwerker |
| | 62 | Ultra-high resolution fMRI at ultra-high field | Noam Harel |
| | 63 | Revealing Ocular Dominance Columns using high resolution functional MRI | Kang Cheng |
| | 64 | Inflow effects on functional MRI | Jia Hong Gao |
| | 65 | Neuronal inhibition and excitation, and the dichotomic control of brain hemodynamic and oxygen responses | Martin Lauritzen |
| | 66 | The history and role of long duration stimulation in fMRI | Gunnar Krueger |
| | 67 | A personalized history of EEG-fMRI integration | Helmut Laufs |
| | 68 | Mental Chronometry with MRI | Ravi Menon |
| | 69 | Pharmacologic Magnetic Resonance Imaging (phMRI): Imaging Drug Action in the Brain. | Bruce Jenkins |
| | 70 | Task induced deactivation and the "resting" state | Jeff Binder |

| | | | |
|---|---|---|---|
| | 71 | The BOLD post-stimulus undershoot, one of the most debated issues in fMRI | Peter van Zijl |
| | 72 | The story of the initial dip in fMRI | Xiaoping Hu |
| | 73 | Spin-echo fMRI: the poor relation? | David Norris |
| | 74 | Test-retest reliability in fMRI: or How I learned to stop worrying and love the variability | David McGonigle |
| | 75 | Which "neural activity" do you mean? fMRI, MEG, oscillations and neurotransmitters | Chris Singh |
| | 76 | Diffusion, Confusion and functional MRI | Denis LeBihan |
| | 77 | The serendipitous discovery of the brain's default network | Randy Buckner |
| **New Paradigm Designs** | 78 | The emergence of doing "nothing" as a viable paradigm design. | Mark Lowe |
| | 79 | Event-related fMRI in Cognition | Scott Huettel |
| | 80 | The development of event-related fMRI designs | Tom Liu |
| | 81 | Targeting the functional properties of cortical neurons using fMR-adaptation | Rafi Malach |
| | 82 | Studying the freely-behaving brain with fMRI | Elanor Maguire |
| | 83 | The mixed blocked and event-related design | Joseph Dubis & Steven Petersen |
| | 84 | Development of orthogonal task designs in fMRI studies of higher cognition: the NIMH experience | Susan Courtney |
| | 85 | A history of randomized task designs in fMRI | Vince Clark |
| | 86 | The development and use of phase encoded functional MRI designs | Steve Engel |
| **Education** | 87 | The Evolution and current challenges in the teaching of functional MRI and functional brain imaging | Bob Savoy |

| | | | |
|---|---|---|---|
| **The Future** | 88 | Is there a path beyond BOLD? Molecular Imaging of Brain Function | Alan Koretsky |
| | 89 | The future of fMRI in Cognitive Neuroscience | Russ Poldrack |
| | 90 | The future of acquisition speed, coverage, sensitivity, and resolution | Larry Wald |
| | 91 | The history of the future of the Bayesian Brain | Karl Friston |
| | 92 | Quantitative functional MRI: concepts, issues, and future challenges | Bruce Pike |
| | 93 | The future of ultra-high field MRI and fMRI for study of the human brain | Jeff Duyn |
| | 94 | Seeing patterns through the hemodynamic veil - the future of pattern-information fMRI | Niko Kriegeskorte & Elia Formisano |
| | 95 | The future of fMRI connectivity | Steve Smith |
| | 96 | The future of fMRI in clinical medicine | Ed Bullmore |
| | 97 | Future trends in Neuroimaging: neuronaprocesses as expressed within real-life social contexts | Uri Hasson |
| | 98 | The future of fMRI with perfusion imaging | Geoff Aguirre |
| | 99 | The future of fMRI and genetics research | Andreas Meyer-Lindenberg |
| | 100 | The future of functionally related structural change assessment | Heidi Johansen-Berg |
| | 101 | The future of the human connectome | David van Essen & Kamil Ugurbil |
| | 102 | The future of susceptibility contrast for assessment of anatomy and function | Jurgen Reichenbach |
| | 103 | fMRI at 20: Has it changed the world? | Bruce Rosen |

# Functional Magnetic Resonance Imaging in Medicine and Physiology

Chrit T. W. Moonen, Peter C. M. van Zijl, Joseph A. Frank, Denis Le Bihan, Edwin D. Becker

**(1990) *Science*, 250, 53-61.**

**metabolic imaging (NAA)**

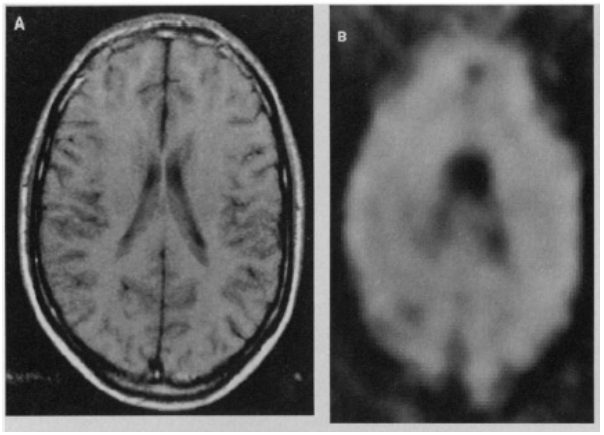


**angiography**

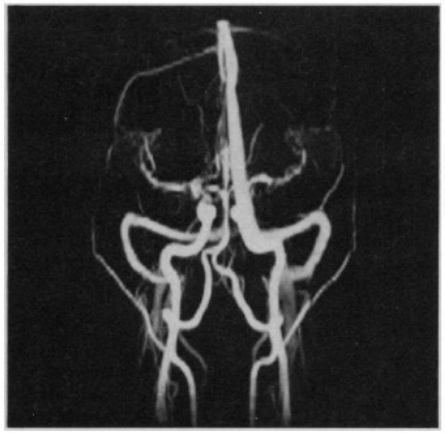

**Diffusion**

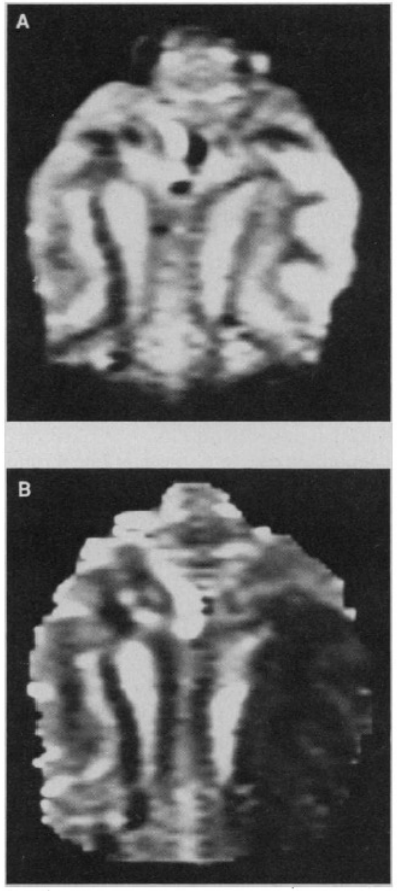


**magnetization transfer**

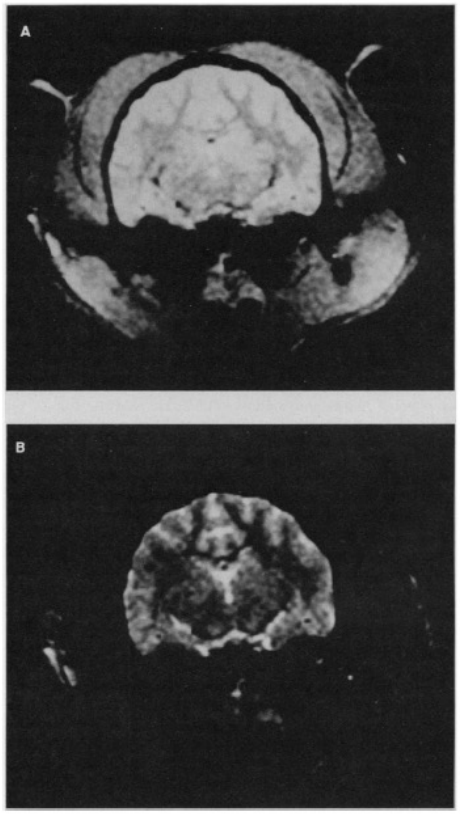


**Gadolinium perfusion**

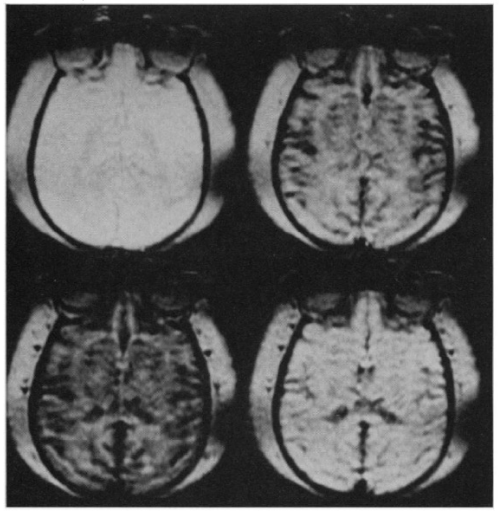

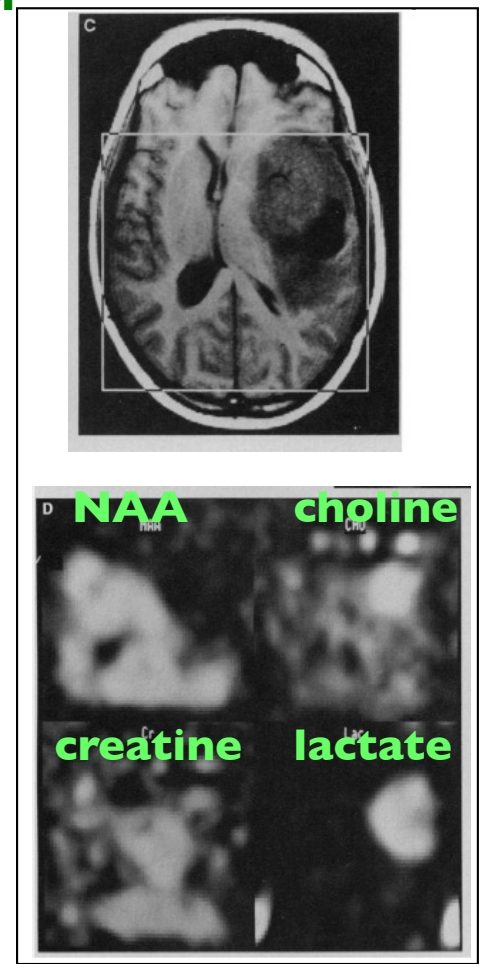

## *How it all came together…*

## Five Key Factors For The Emergence of Functional MRI

1. **Magnetic properties of red blood cells**
2. **Activation related hemodynamic changes**
3. **Spatial scale of brain activation**
4. **Echo Planar Imaging**
5. **Prevalence of MRI scanners**

# Five Key Factors For The Emergence of Functional MRI

1. Magnetic properties of red blood cells
2. Activation related hemodynamic changes
3. Spatial scale of brain activation
4. Echo Planar Imaging
5. Prevalence of MRI scanners

# Magnetic Properties of Blood

L. Pauling, C. D. Coryell, *Proc.Natl.Acad. Sci. USA 22, 210-216*, **1936**.

K.R. Thulborn, J. C. Waterton, et al., *Biochim. Biophys. Acta. 714: 265-270*, **1982**.

S. Ogawa, T. M. Lee, A. R. Kay, D. W. Tank, *Proc. Natl. Acad. Sci. USA 87, 9868-9872*, **1990**.

Turner, R., Lebihan, D., Moonen, C. T. W., Despres, D. & Frank, J. *Magnetic Resonance in Medicine,* 22, 159-166, **1991.**

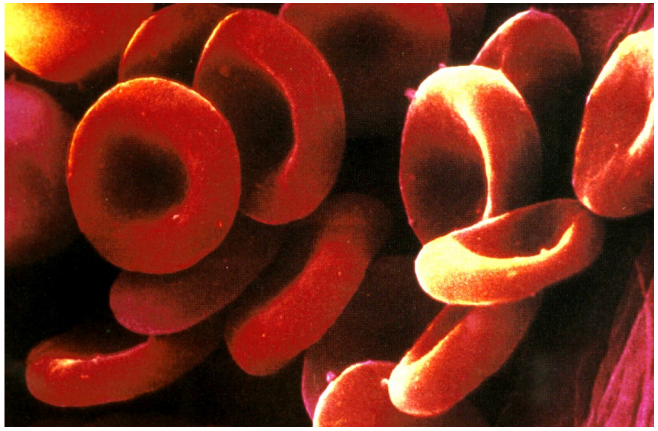

red blood cells

oxygenated

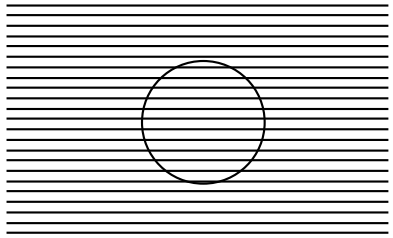

deoxygenated

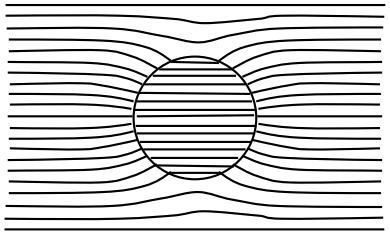

BOLD contrast investigation started in 1936…or even 1845.



# THE MAGNETIC PROPERTIES AND STRUCTURE OF HEMOGLOBIN, OXYHEMOGLOBIN AND CARBONMONOXYHEMOGLOBIN

BY LINUS PAULING AND CHARLES D. CORYELL

GATES CHEMICAL LABORATORY, CALIFORNIA INSTITUTE OF TECHNOLOGY

Communicated March 19, 1936

Over ninety years ago, on November 8, 1845, Michael Faraday investigated the magnetic properties of dried blood and made a note "Must try recent fluid blood." If he had determined the magnetic susceptibilities of arterial and venous blood, he would have found them to differ by a large amount (as much as twenty per cent for completely oxygenated and completely deoxygenated blood); this discovery without doubt would have excited much interest and would have influenced appreciably the course of research on blood and hemoglobin.[1]

Continuing our investigations of the magnetic properties and structure of hemoglobin and related substances,[2] we have found oxyhemoglobin and carbonmonoxyhemoglobin to contain no unpaired electrons, and ferrohemoglobin (hemoglobin itself) to contain four unpaired electrons per heme. The description of our experiments and the interpretation and discussion of the results are given below.

*Biochimica et Biophysica Acta*, 714 (1982) 265–270
Elsevier Biomedical Press



BBA 20122

# OXYGENATION DEPENDENCE OF THE TRANSVERSE RELAXATION TIME OF WATER PROTONS IN WHOLE BLOOD AT HIGH FIELD

KEITH R. THULBORN, JOHN C. WATERTON *, PAUL M. MATTHEWS and GEORGE K. RADDA

*Department of Biochemistry, University of Oxford, South Parks Road, Oxford OX1 3QU (U.K.)*

(Received August 4th, 1981)

*Key words: Oxygenation dependence; Transverse relaxation time; Water proton; High field NMR; (Whole blood)*

**At high and medium magnetic field, the transverse NMR relaxation rate ($T_2^{-1}$) of water protons in blood is determined predominantly by the oxygenation state of haemoglobin. $T_2^{-1}$ depends quadratically on the field strength and on the proportion of haemoglobin that is deoxygenated. Deoxygenation increases the volume magnetic susceptibility within the erythrocytes and thus creates local field gradients around these cells.From volume susceptibility measurements and the dependence of $T_2^{-1}$ on the pulse rate in the Carr-Purcell-Meiboom-Gill experiment, we show that the increase in $T_2^{-1}$ with increasing blood deoxygenation arises from diffusion of water through these field gradients.**

Oxygenation Changes T2

*Biochimica et Biophysica Acta*, 714 (1982) 265–270
Elsevier Biomedical Press

BBA 20122

# OXYGENATION DEPENDENCE OF THE TRANSVERSE RELAXATION TIME OF WATER PROTONS IN WHOLE BLOOD AT HIGH FIELD

KEITH R. THULBORN, JOHN C. WATERTON *, PAUL M. MATTHEWS and GEORGE K. RADDA

*Department of Biochemistry, University of Oxford, South Parks Road, Oxford OX1 3QU (U.K.)*

(Received August 4th, 1981)

**R2 effect is due to bulk susceptibility and not dipole-dipole interaction**

**Blood R2 proportional to Oxygenation**

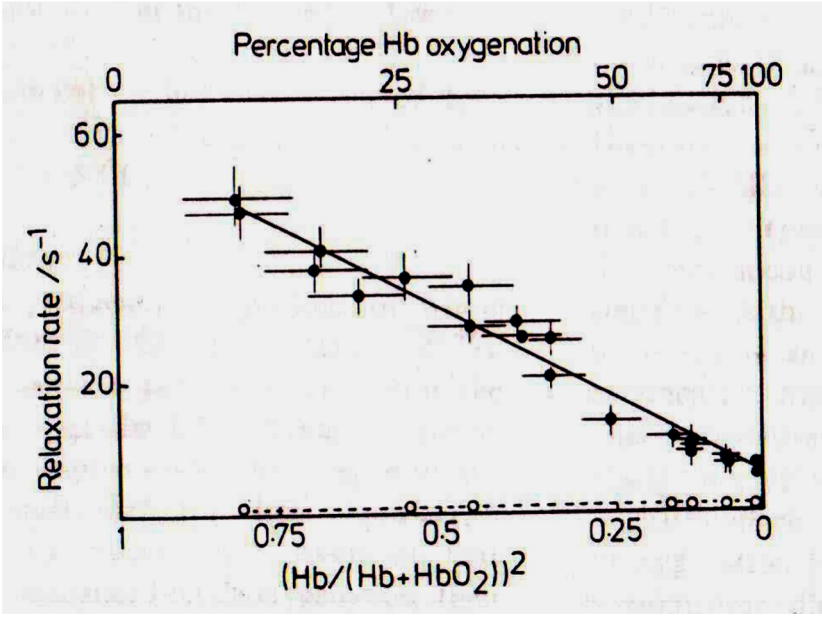


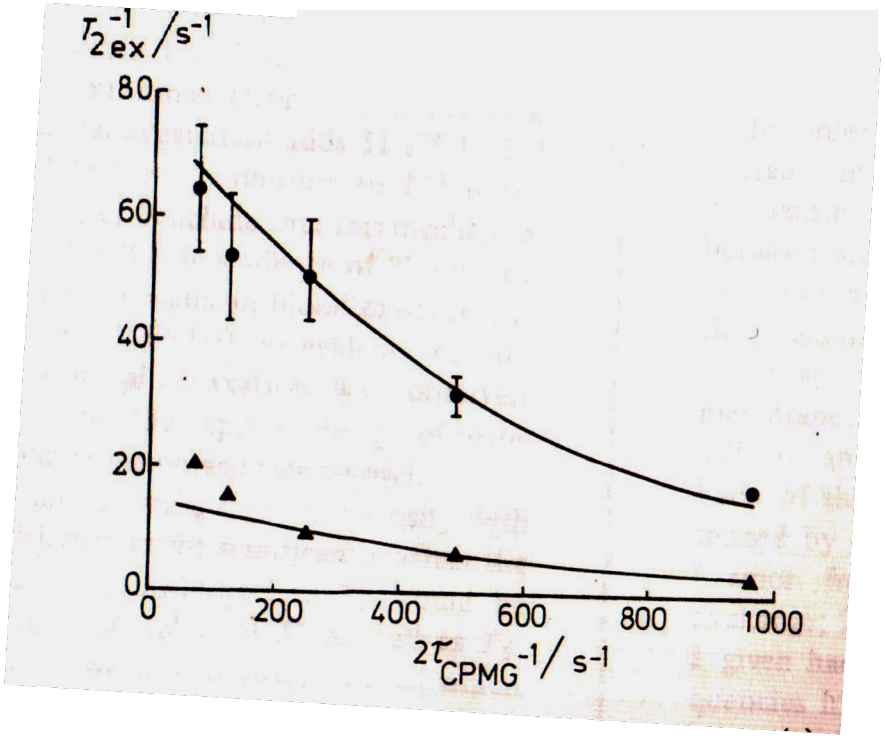

...Six years later...

# Oxygenation-Sensitive Contrast in Magnetic Resonance Image of Rodent Brain at High Magnetic Fields

SEIJI OGAWA, TSO-MING LEE, ASHA S. NAYAK,* AND PAUL GLYNN

*AT&T Bell Laboratories, Murray Hill, New Jersey 07974*

Received November 30, 1988; accepted June 20, 1989

At high magnetic fields (7 and 8.4 T), water proton magnetic resonance images of brains of live mice and rats under pentobarbital anesthetization have been measured by a gradient echo pulse sequence with a spatial resolution of 65 × 65-μm pixel size and 700-μm slice thickness. The contrast in these images depicts anatomical details of the brain by numerous dark lines of various sizes. These lines are absent in the image taken by the usual spin echo sequence. They represent the blood vessels in the image slice and appear when the deoxyhemoglobin content in the red cells increases. This contrast is most pronounced in an anoxy brain but not present in a brain with diamagnetic oxy or carbon monoxide hemoglobin. The local field induced by the magnetic susceptibility change in the blood due to the paramagnetic deoxyhemoglobin causes the intra voxel dephasing of the water signals of the blood and the surrounding tissue. This oxygenation-dependent contrast is appreciable in high field images with high spatial resolution.

## in vivo

## in vitro

**100% $O_2$**

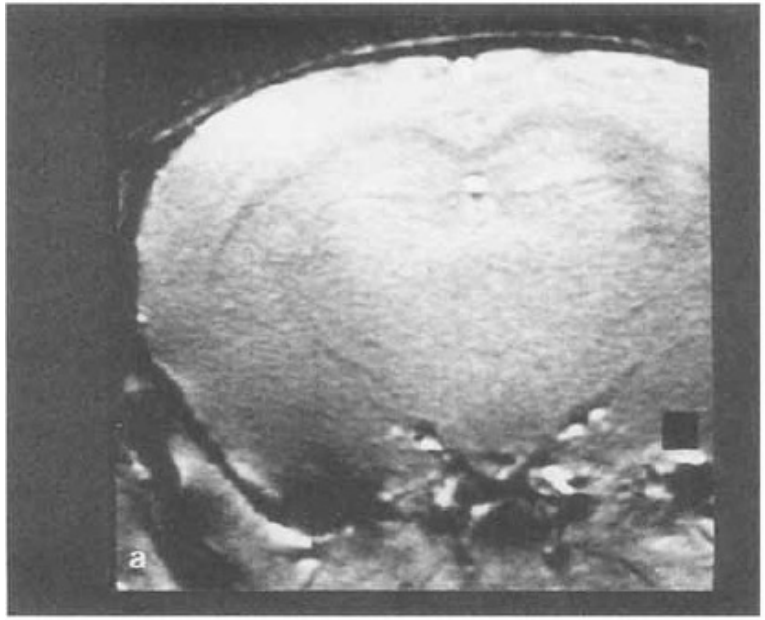


**20% $O_2$**

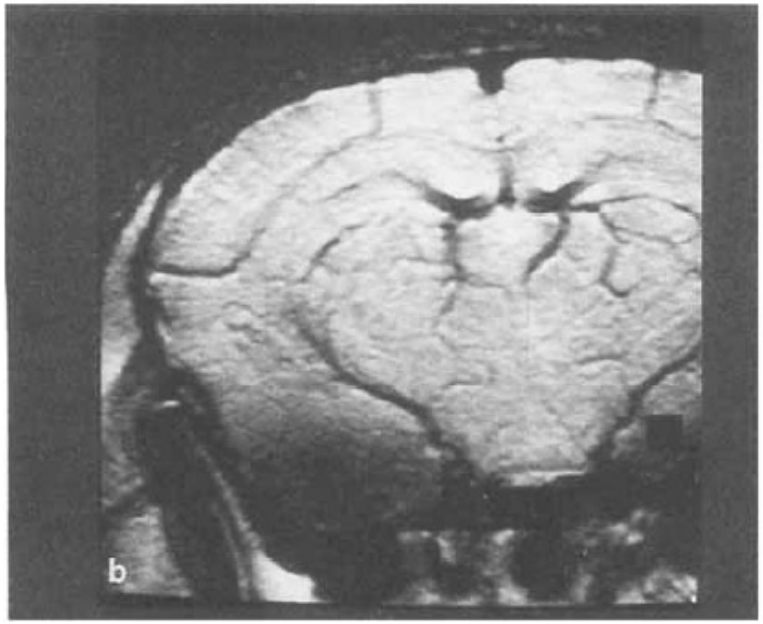


**100% oxygenated blood**

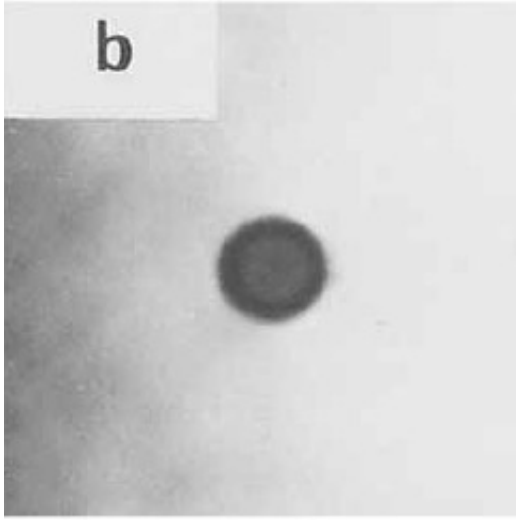


**0% oxygenated blood**

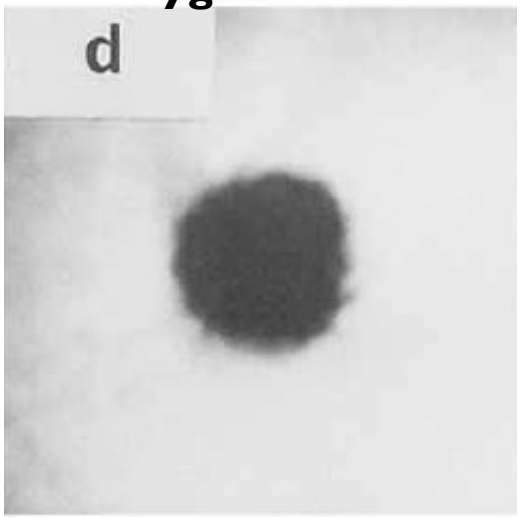


S. Ogawa, T.-M. Lee, A. S. Nayak, P. Glynn, Magn. Reson. Med, 14, 68-78 (1990)

Susceptibility-Induced Field Distortion in the Vicinity of a Microvessel $\perp$ to $B_O$.

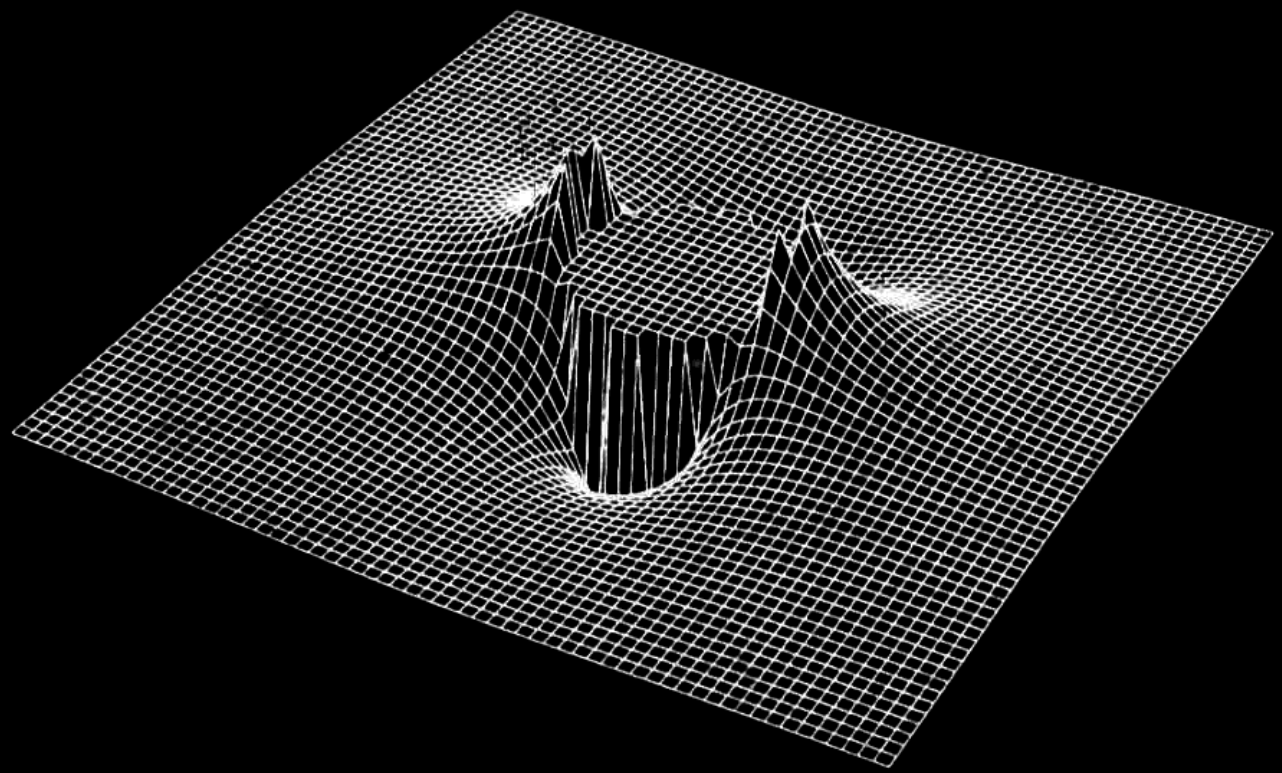

MAGNETIC RESONANCE IN MEDICINE **22,** 159–166 (1991)

# Echo-Planar Time Course MRI of Cat Brain Oxygenation Changes

ROBERT TURNER,*,† DENIS LE BIHAN,‡ CHRIT T. W. MOONEN,§
DARYL DESPRES,§ AND JOSEPH FRANK‡

** Laboratory of Cardiac Energetics, ‡ Diagnostic Radiology Department, and § In Vivo NMR Research Center, National Institutes of Health, Bethesda, Maryland 20892*

Received June 25, 1991; revised August 7, 1991

When deoxygenated, blood behaves as an effective susceptibility contrast agent. Changes in brain oxygenation can be monitored using gradient-echo echo-planar imaging. With this technique, difference images also demonstrate that blood oxygenation is increased during periods of recovery from respiratory challenge. 

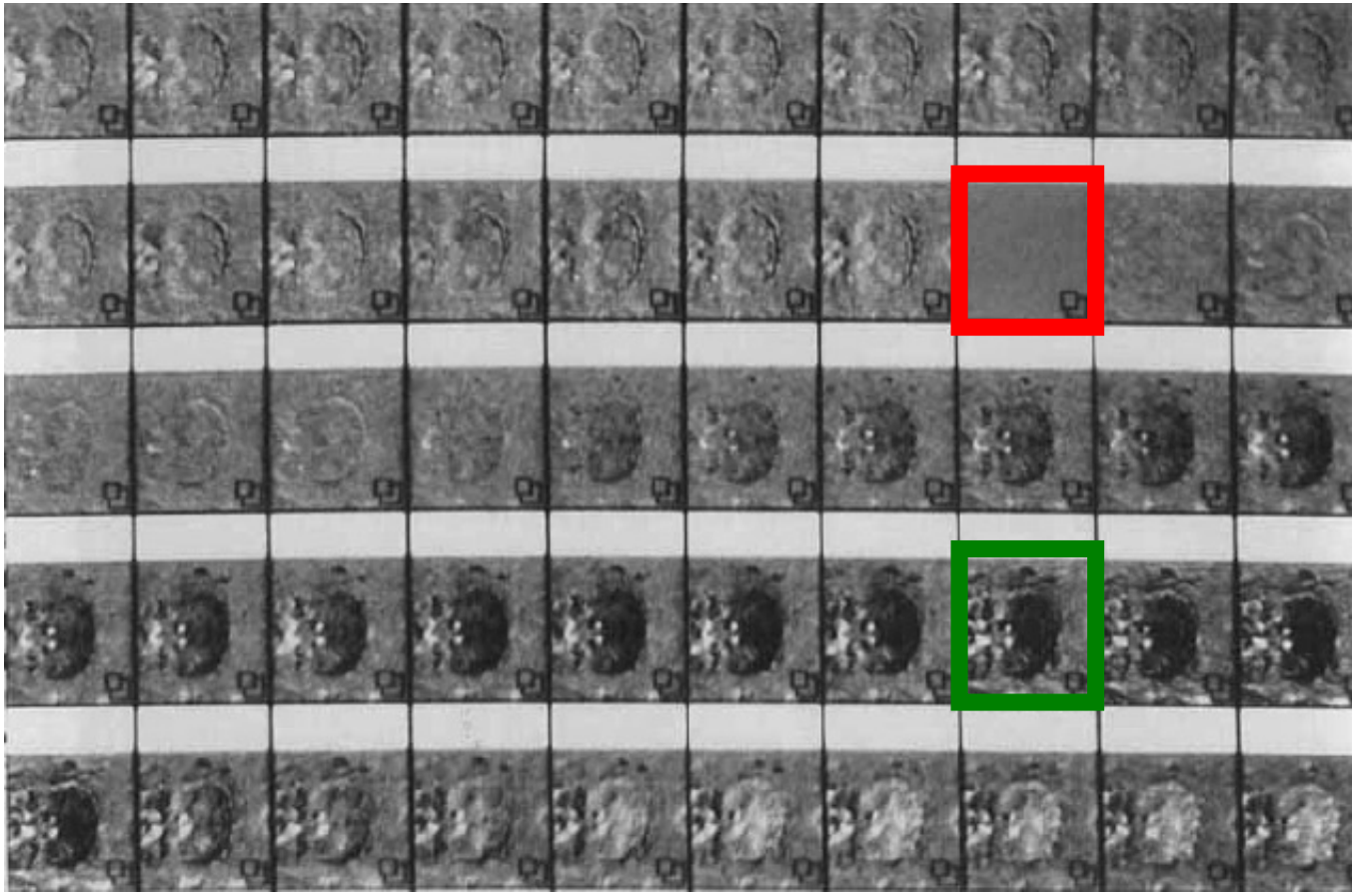

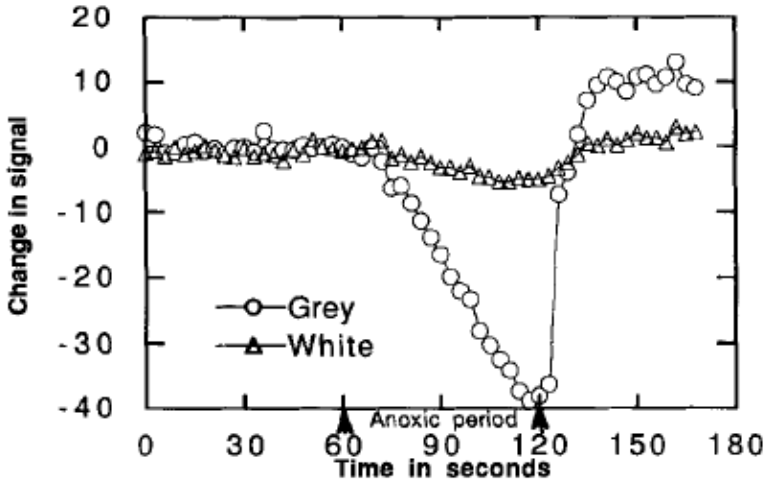


**R. Turner, D. LeBihan, C.T.W. Moonen, D. Despres, J. Frank, Magn. Reson. Med, 22, 159-166 (1991)**

## Ogawa predicted fMRI but got the sign wrong…

**"...we expect this oxygenation-sensitive contrast could be used to monitor regional oxygen usages in the brain. When some region in a brain is much more active than other regions, the active region could show darker lines in the image because of the increased level of deoxyhemoglobin resulting from higher oxygen consumption."**

**"Therefore, in addition to the anatomy of the brain, one aspect of its physiology can be studied by the MRI of water"**

Oxygenation-Sensitive Contrast in Magnetic Resonance Image of Rodent Brain at High Magnetic Fields, Seiji Ogawa, Tso-Ming Lee, Asha S. Nayak, and Paul Glynn. **Magnetic Resonance in Medicine 14, 68-78 (1990).**

# Five Key Factors For The Emergence of Functional MRI

1. Magnetic properties of red blood cells
2. Activation related hemodynamic changes
3. Spatial scale of brain activation
4. Echo Planar Imaging
5. Prevalence of MRI scanners

# The First Functional MRI Results (MGH)

Susceptibility Contrast agent bolus injection and time series collection of T2 - weighted images

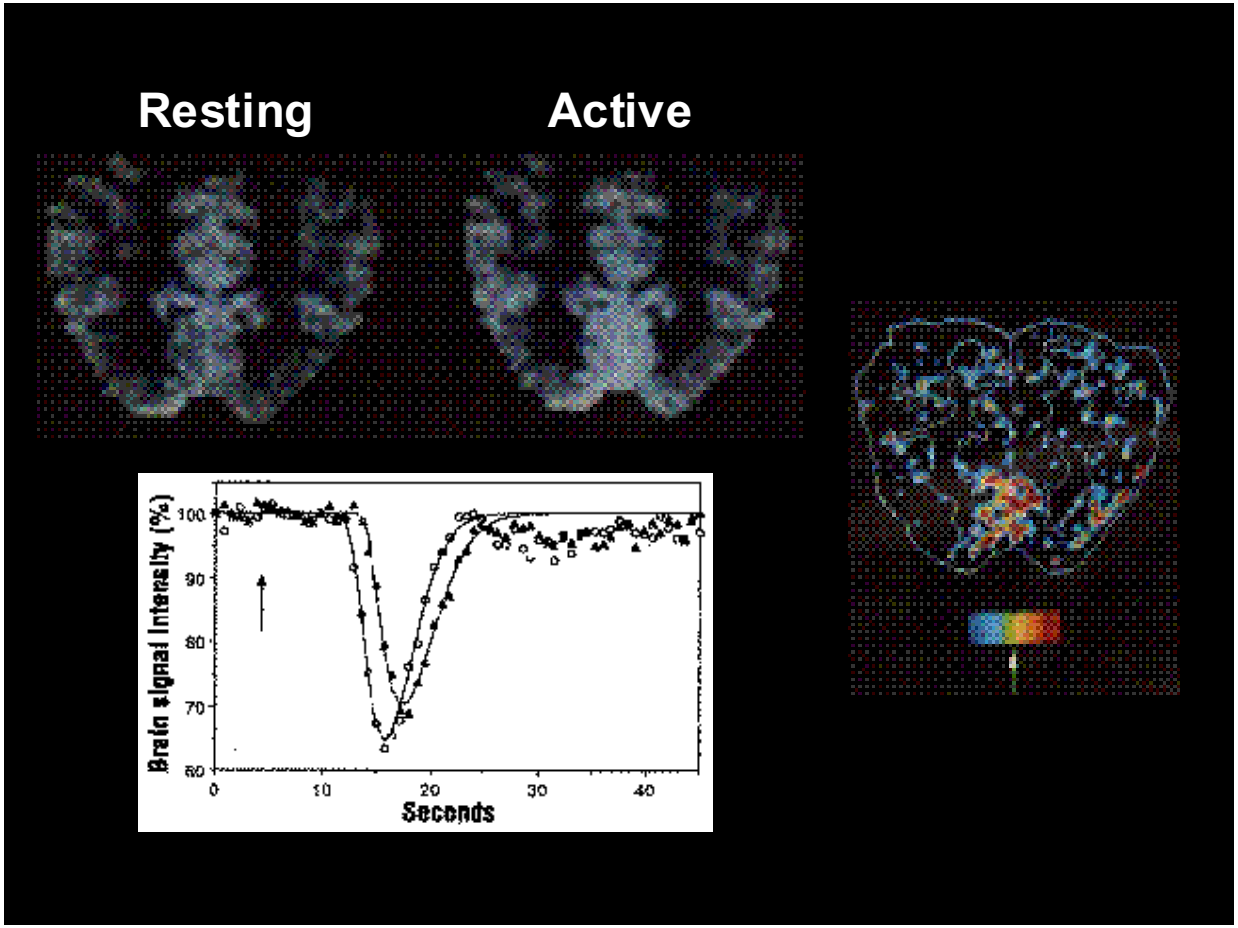

# The First Functional MRI Results (MGH)

Susceptibility Contrast agent bolus injection and time series collection of T2 - weighted images

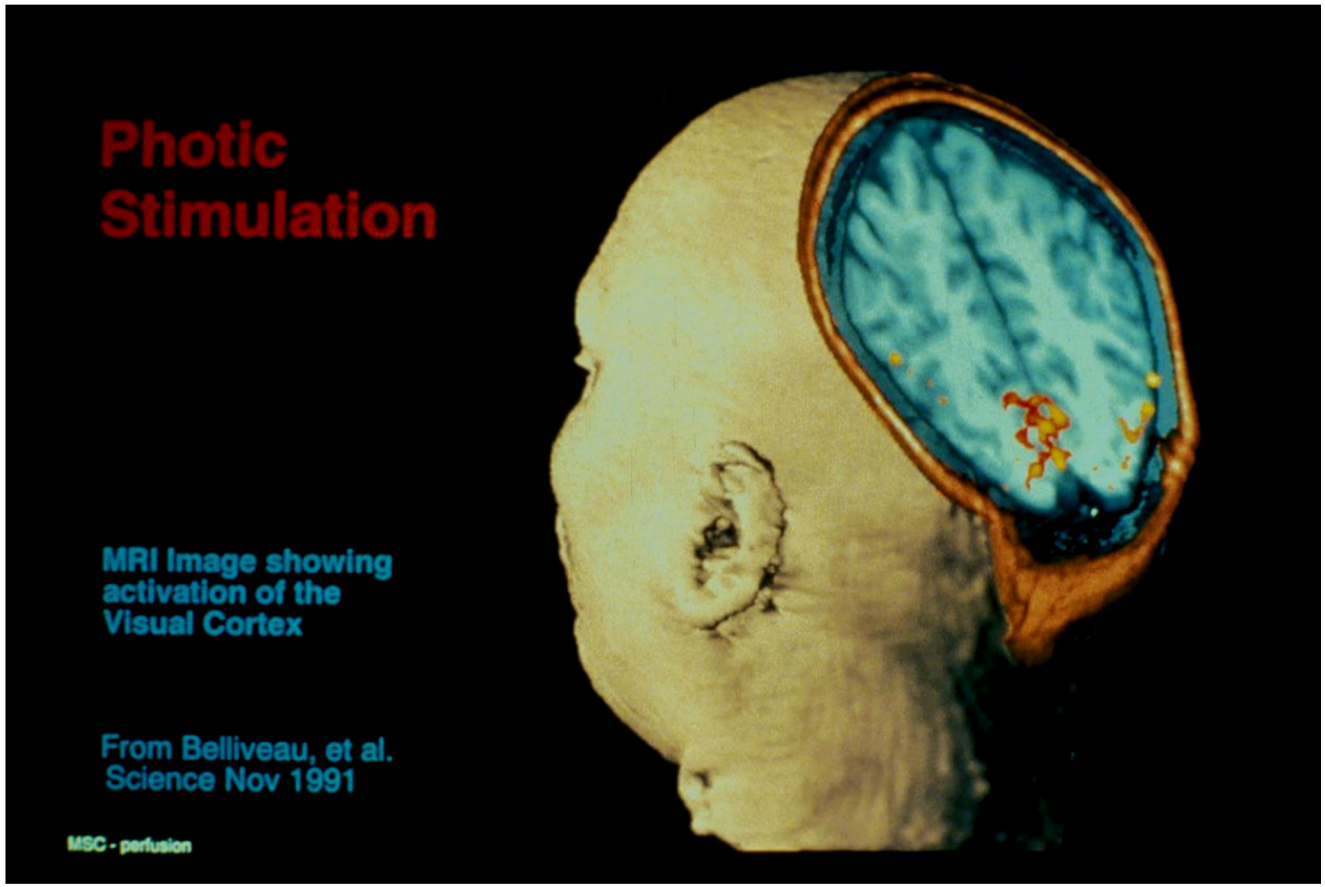

# The MGH Gang

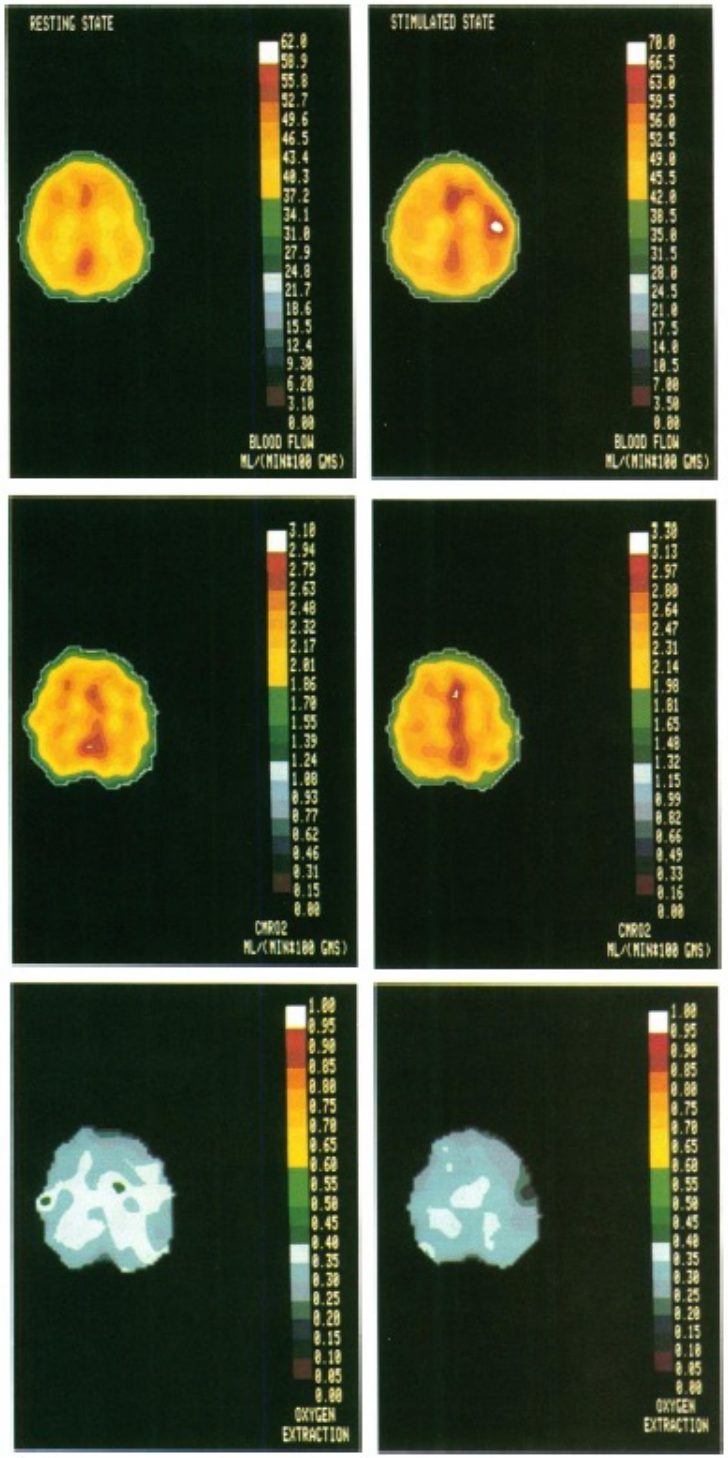


*Proc. Natl. Acad. Sci. USA*
Vol. 83, pp. 1140–1144, February 1986
Neurobiology

# Focal physiological uncoupling of cerebral blood flow and oxidative metabolism during somatosensory stimulation in human subjects

**(positron emission tomography)**

PETER T. FOX*†‡ AND MARCUS E. RAICHLE*†

*Department of Neurology and Neurological Surgery (Neurology), †Department of Radiology (Radiation Sciences), and The McDonnell Center for Studies of Higher Brain Function, Washington University School of Medicine, St. Louis, MO 63110

*Communicated by Oliver H. Lowry, October 7, 1985*

FIG. 1. Physiological uncoupling of brain blood flow and metabolism. (*Left*) Resting-state measurements. (*Right*) Stimulated-state measurements (unilateral vibrotactile stimulation of the fingers). All images are from a single subject's scanning session and pass through the same brain plane. Color scales are linear with the maxima set at a fixed multiple (1.6) of the global average, to facilitate visual comparisons (16). During specific somatosensory stimulation a marked focal increase in CBF (29% of mean, nine subjects, three trials per subject) was produced in the contralateral sensorimotor cortex. The observed increase in the $CMRO_2$ was much smaller (5% of mean, nine subjects, three trials per subject) and failed to attain significance. This physiological uncoupling of CBF and $CMRO_2$ flow produced a highly significant decrease in the local OEF (−19% of mean), indicating that tissue $PO_2$ (and probably pH) rose during stimulation. Note that, although the data were analyzed as contralateral/ipsilateral ratios (see text and Tables 1–4), the disparity between blood flow and metabolism was evident from the raw data and was not dependent on a particular strategy of analysis.

**Cerebral Tissue Activation**

↓

**Local Vasodilatation**

↓

**Increase in Cerebral Blood Flow and Volume** → **Oxygen Delivery Exceeds Metabolic Need**

↓

**Increase in Capillary and Venous Blood Oxygenation**

↓

**Decrease in Deoxy-hemoglobin**

***Deoxy-hemoglobin: paramagnetic***
***Oxy-hemoglobin: diamagnetic***

↓

**Decrease in susceptibility-related intravoxel dephasing** → **Increase in T2 and T2***

↓

**Local Signal Increase in T2 and T2* - weighted sequences**

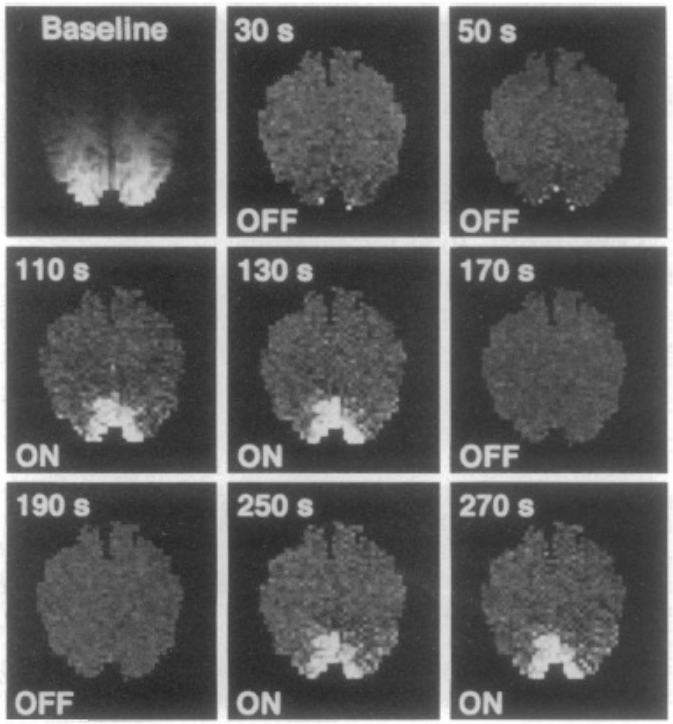


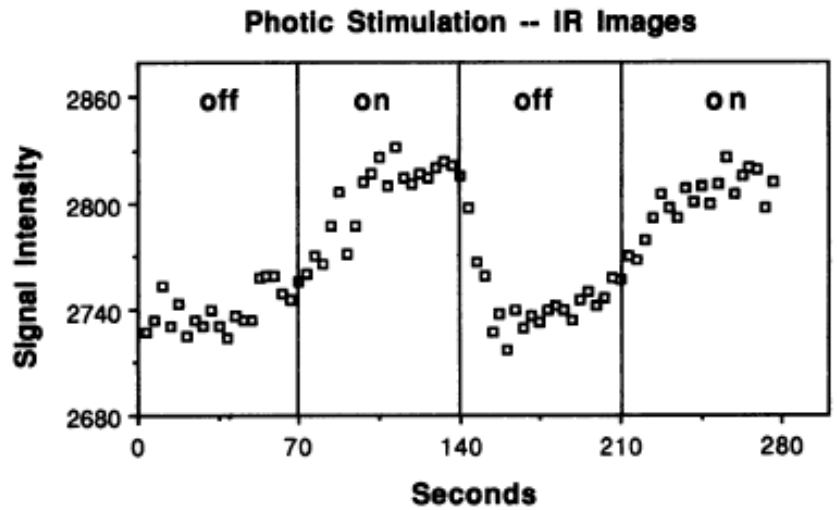


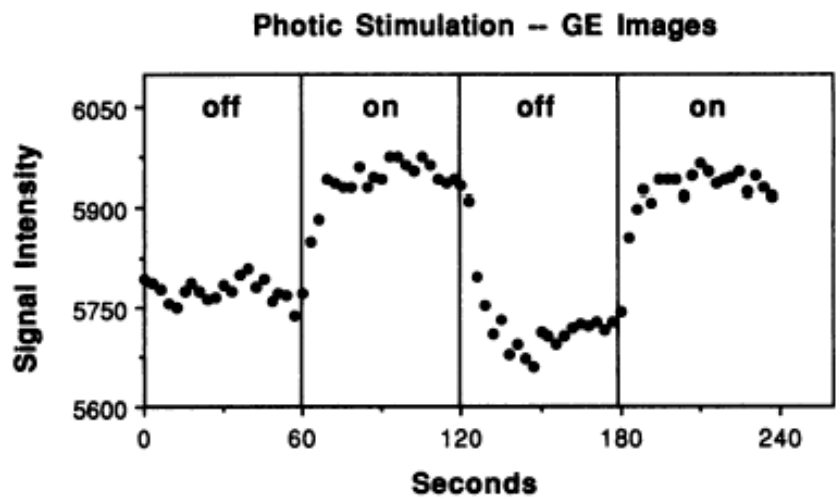


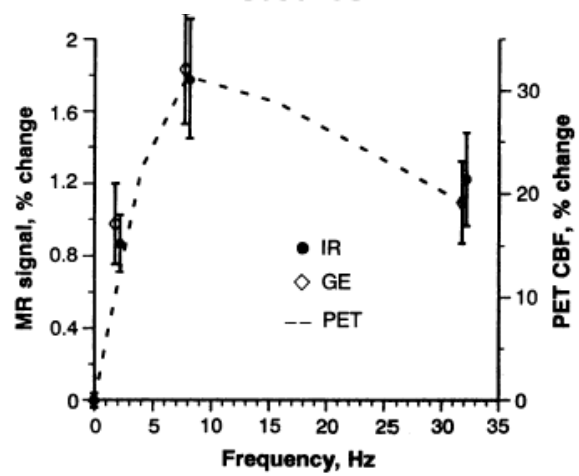


K. K. Kwong, et al, (1992) "Dynamic magnetic resonance imaging of human brain activity during primary sensory stimulation." Proc. Natl. Acad. Sci. USA. 89, 5675-5679.

photo stc. 5 in GP

~~GP~~
IR

GE 3.5
70 sec shim

disdaq = 2 | 30 pre | 40 post

2.5

IR
disdaq 3.0 TR
= 2

TI = 1.05 s.

40 pre 40 post

SG

80

20 | 30 | 20

90 sec

40 | 80 | 40

20 20 20

10 cm. slice cardiac.

removing spikes

irstim. pre 2 3 5-8 13 14 16 18 19 25-29 (16 together)

irstim. pos 34-38 40-47 49-65 67-80 (44 together)

Avg them (with scaling x512)

Set mirstim.avg (save them)

10 cm. slice cardiac

TR = 2.5 s TE = 45

GE TA = 10 9

RA = 350

7106

MAY 9, 91

Michelle

30 TR 40 on

GE-stim. dat

gestim.pre 3-30 (28)

gestim.pos 33-70 (38) 30 (30 ovr) (2.3 s)

~~gest~~ gepre.avg

gepos.avg.

7106

gestim.avg

gestim.sub 28 / 7 ovr

| | RA | TA |
|---|---|---|
| IR | 370 | 10 2 |

TR = 3 s TI = 1100 ms TE = 42

40 → 40

30 50

IR Image 66

jump up.

irstim. p

irstim

irstim.

irstim.avg

irstim.s

irstim.s

irstim.sub (45 → including ...)

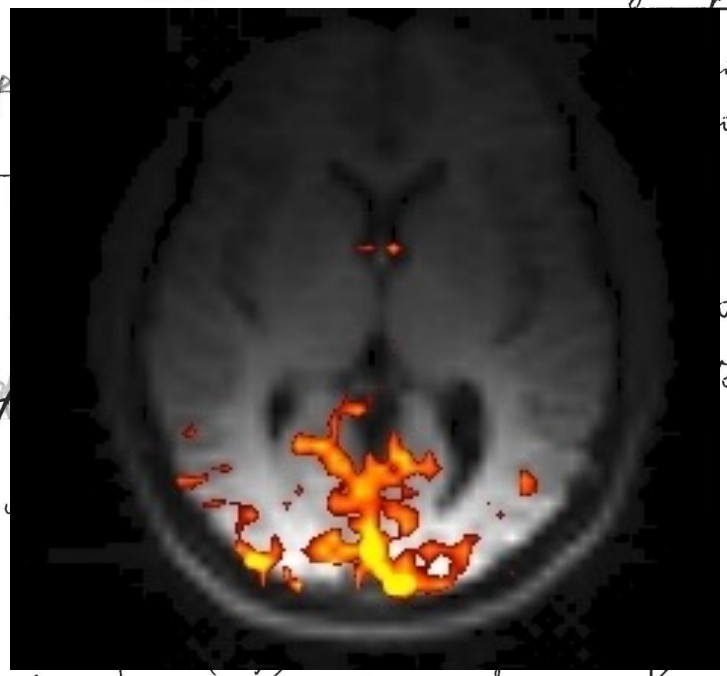

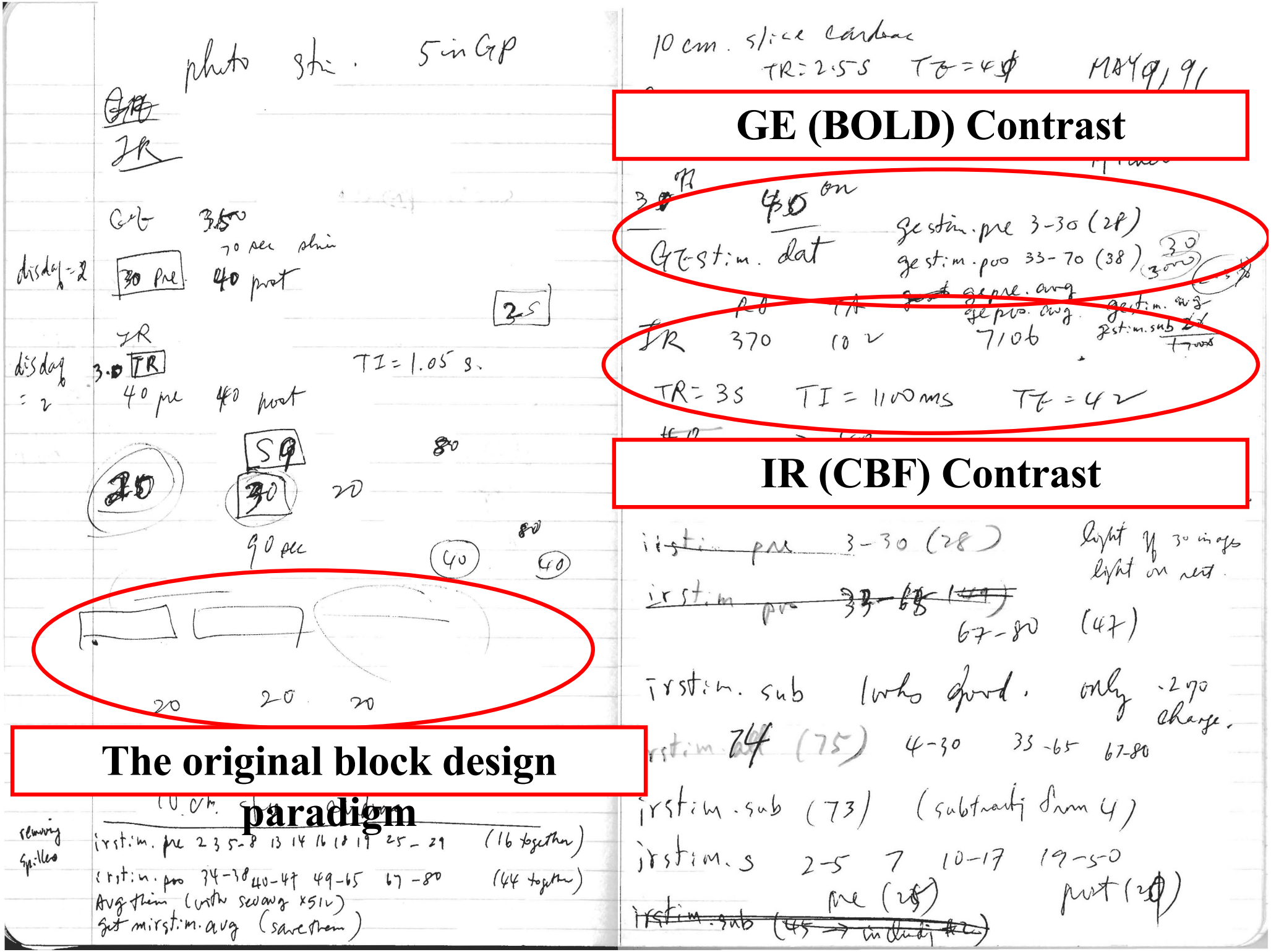
GE (BOLD) Contrast
IR (CBF) Contrast
The original block design paradigm

Multi-shot results at 4T, U. Minnesota.

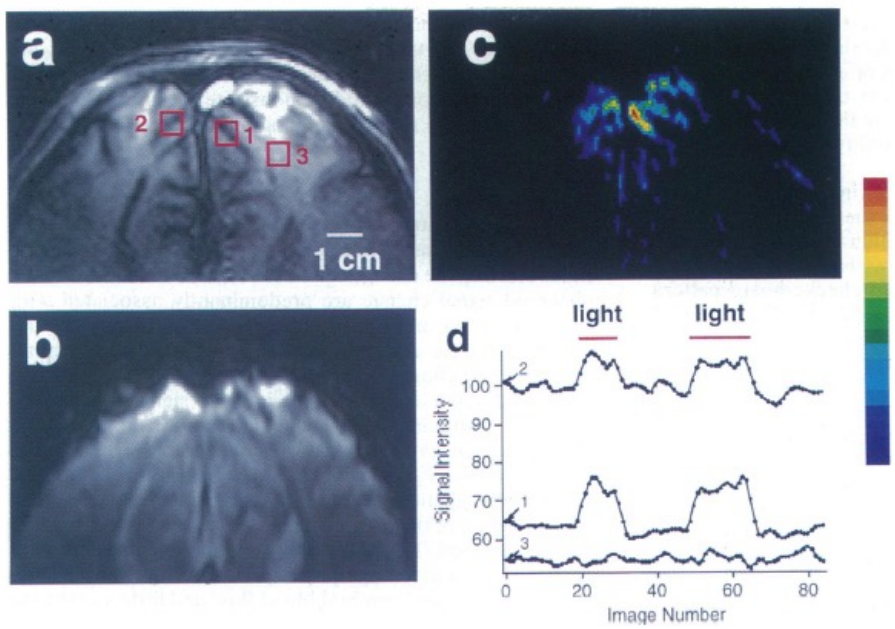


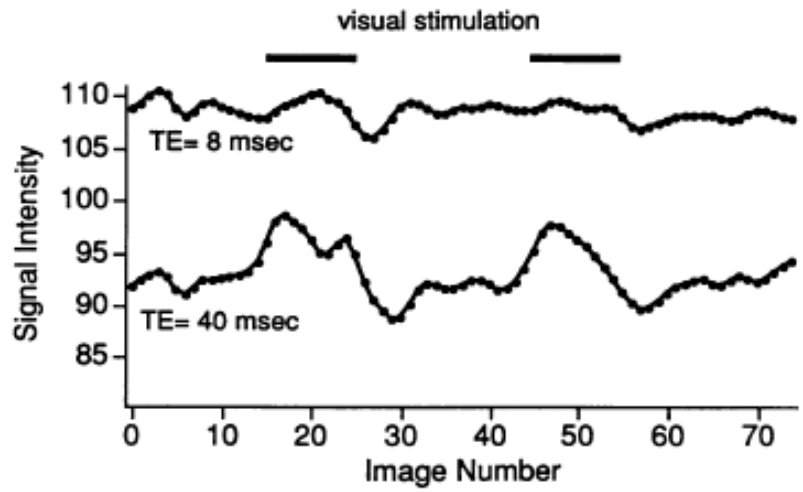


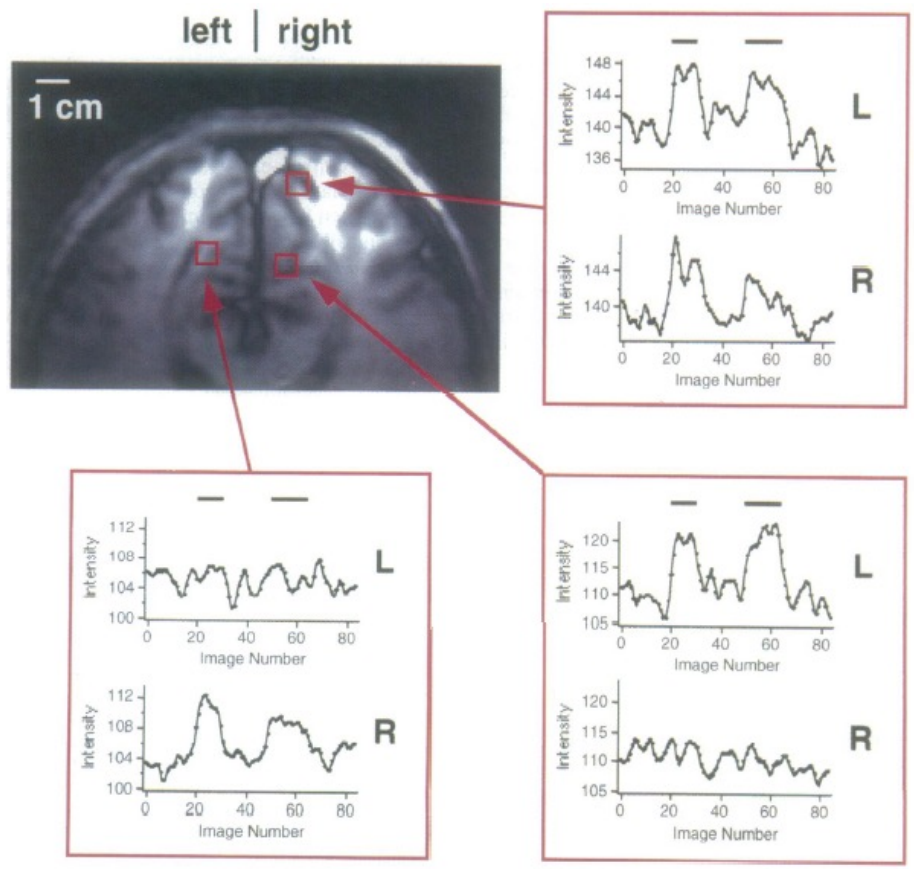


S. Ogawa, et al., (1992) "Intrinsic signal changes accompanying sensory stimulation: functional brain mapping with magnetic resonance imaging." Proc. Natl. Acad. Sci. USA. 89, 5951-5955.

Single Shot Echo Planar Imaging (EPI)

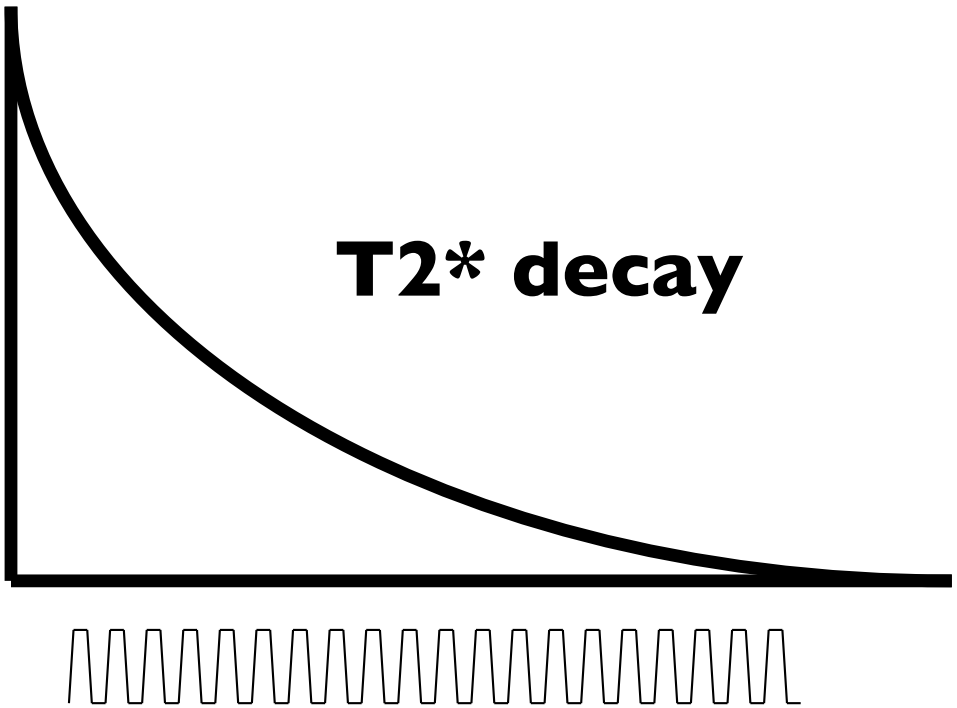


**EPI Readout Window**

**≈ 20 to 40 ms**

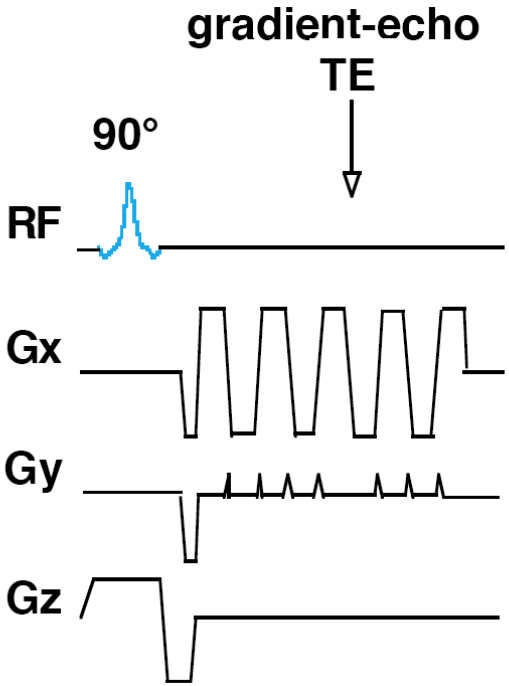


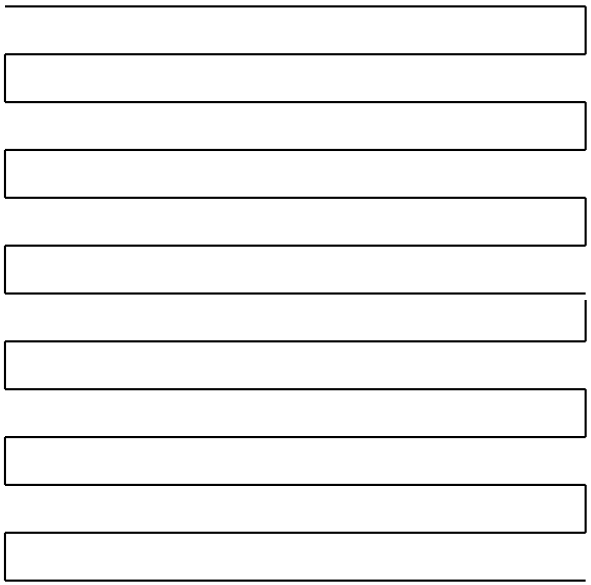

## First Fast Imaging Approaches

1. **MGH: ANMR retrofitted resonant gradient system with EPI**

2. **Minnesota: Standard gradients with Multi-shot with navigator echoes**

3. **MCW: local low-inductance gradient coil with EPI**

What preceded the results from the Medical College of Wisconsin…

MAGNETIC RESONANCE IN MEDICINE **21**, 39–48 (1991)

# Coil Optimization for MRI by Conjugate Gradient Descent

ERIC C. WONG,* A. JESMANOWICZ, AND JAMES S. HYDE

*Biophysics Section, Department of Radiology, Medical College of Wisconsin, Milwaukee, Wisconsin 53226*

Received April 30, 1990; revised June 29, 1990

# Local head gradient coils: Window(s) of opportunity

Eric C. Wong

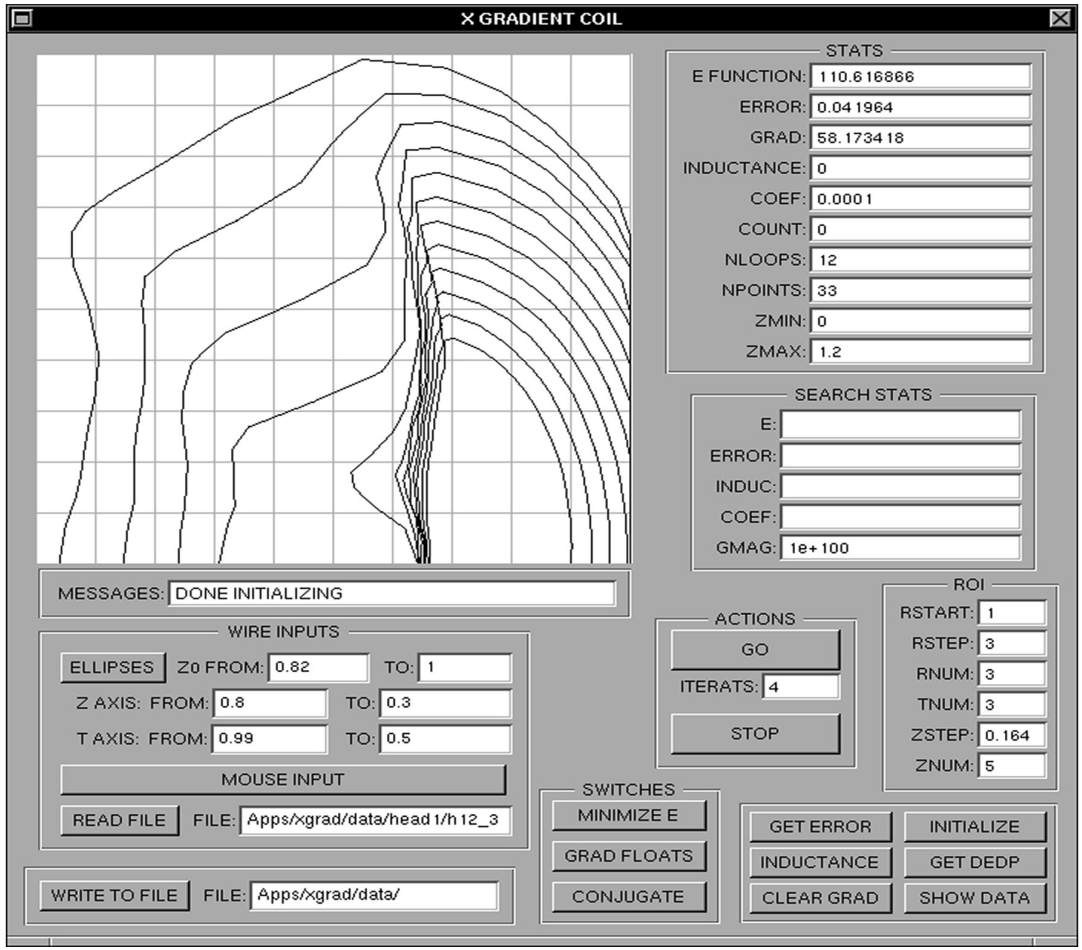


Fig. 1 GUI for gradient descent gradient coil design tool. The design shown is one octant of the X gradient coil designed and built in August 1991. The program was written in Objective C and ran on a NeXT Cube computer.

NeuroImage, Volume 62, Issue 2, 2012, 660 - 664

http://dx.doi.org/10.1016/j.neuroimage.2012.01.025

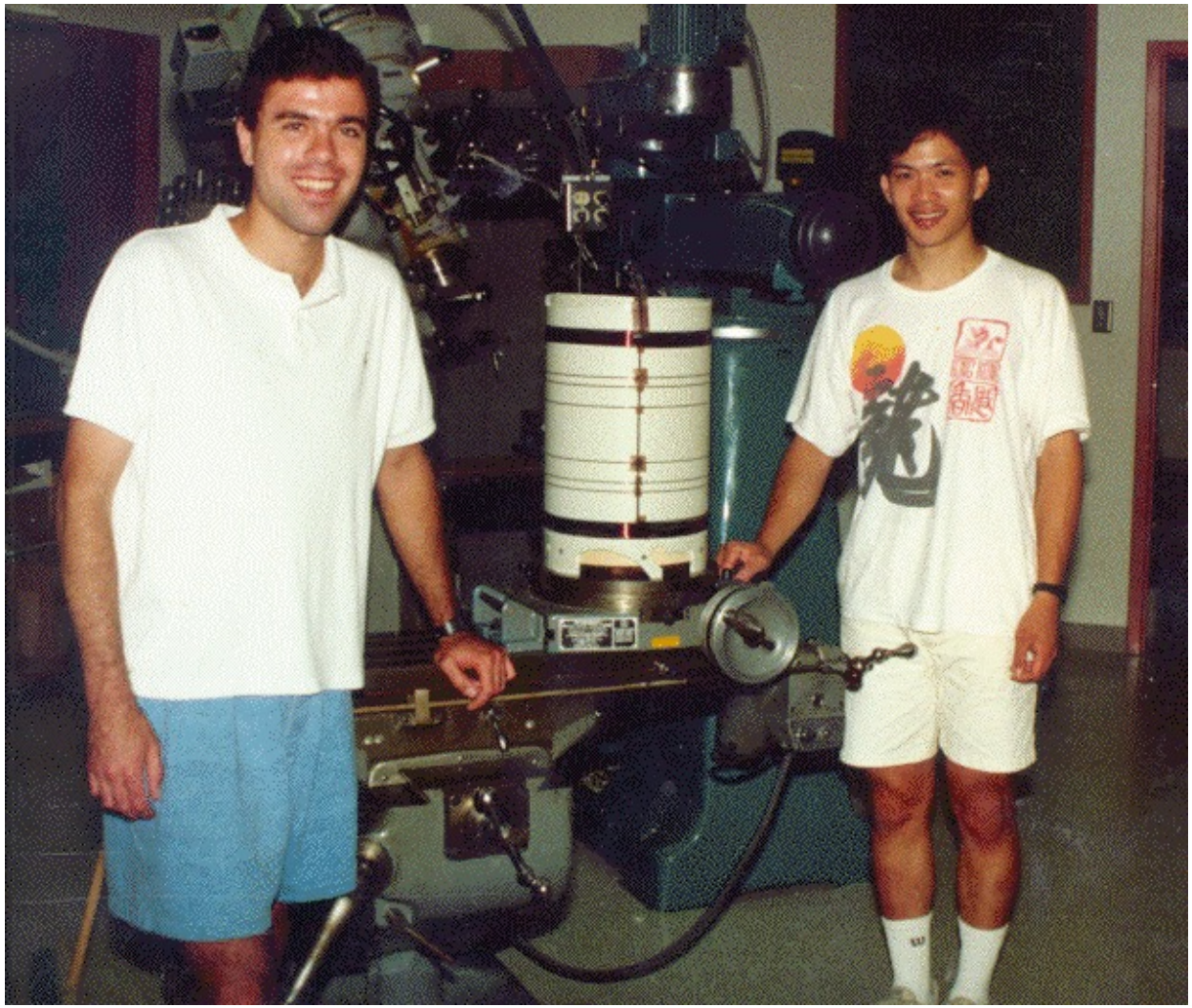

**August, 1991**

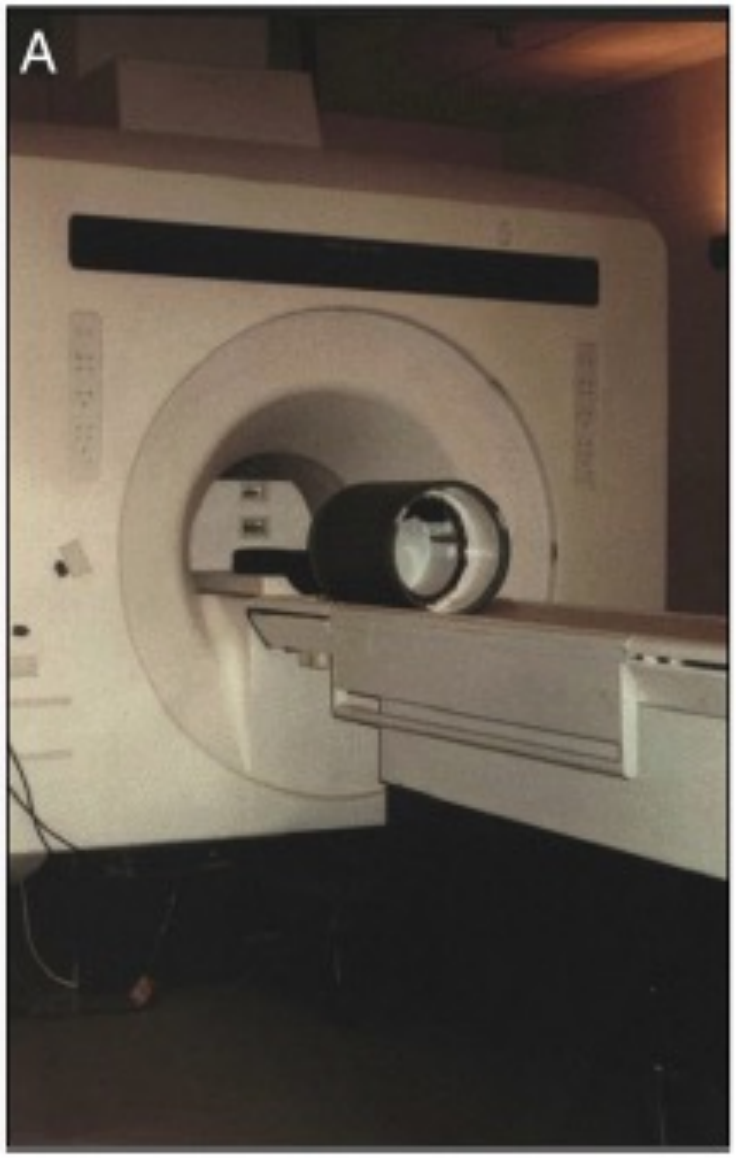
A


1991-1992
B

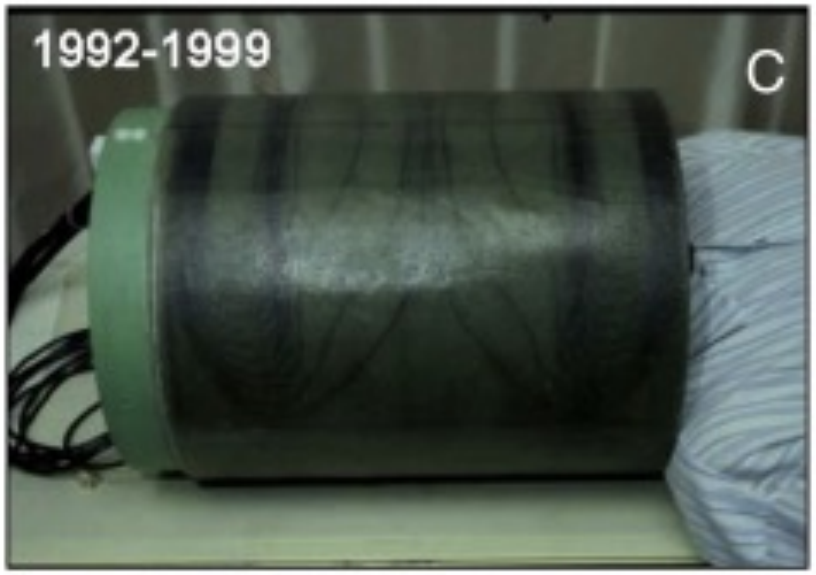
1992-1999
C

Initially could only do one slice…

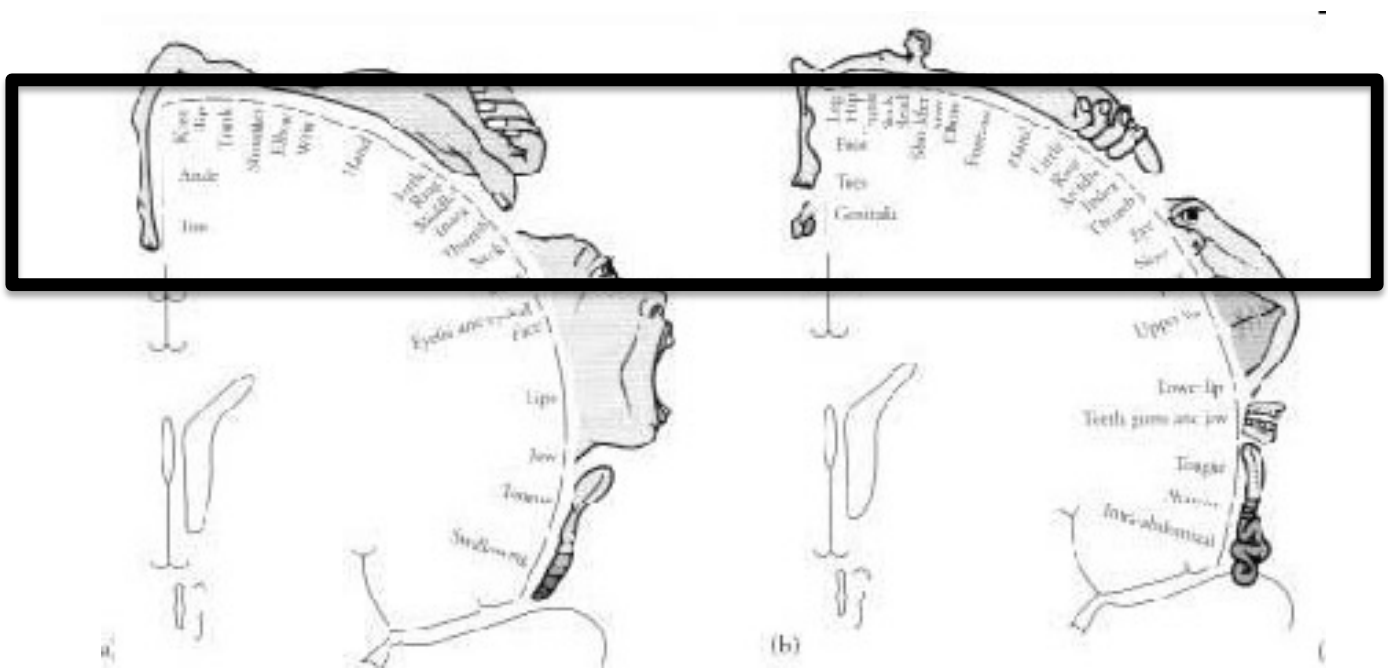


**2.5 cm !**

**TR = 2 sec**
**TE = 50 ms**
**One slice**
**In plane 3.75 x 3.75**

## One little known fact…

**We didn't even need a gradient coil:**

**EPI at 5mm x 5mm x 5mm was quite possible using 100 amp gradient amplifiers and the whole body gradient coils…**

**Every scanner in the world in 1991 could have performed EPI-based fMRI at perfectly reasonable resolution.**

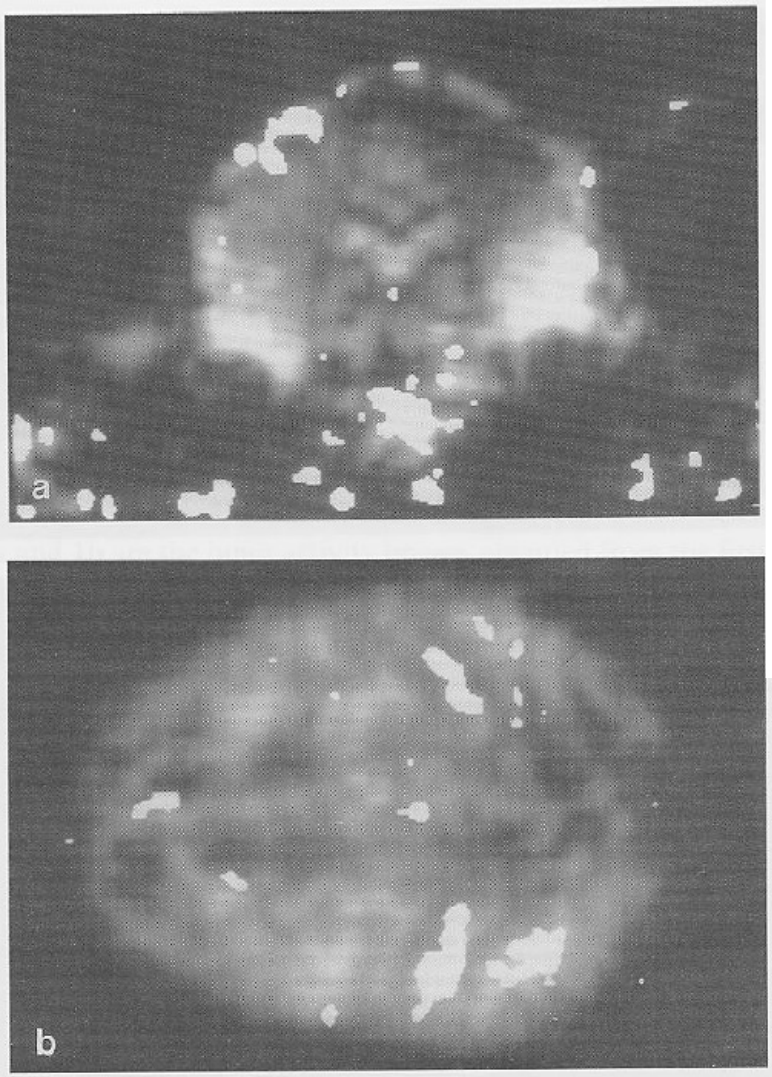


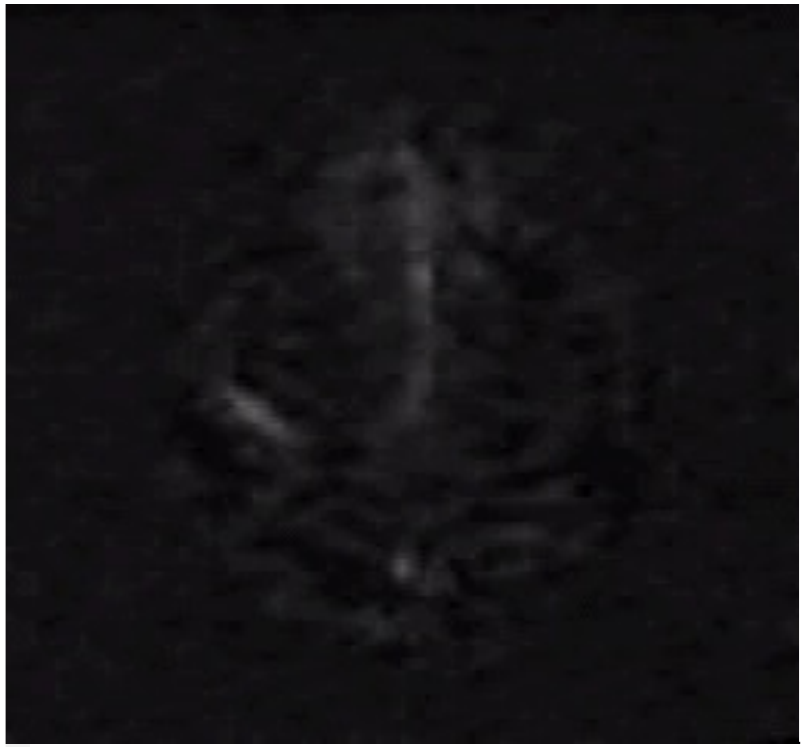

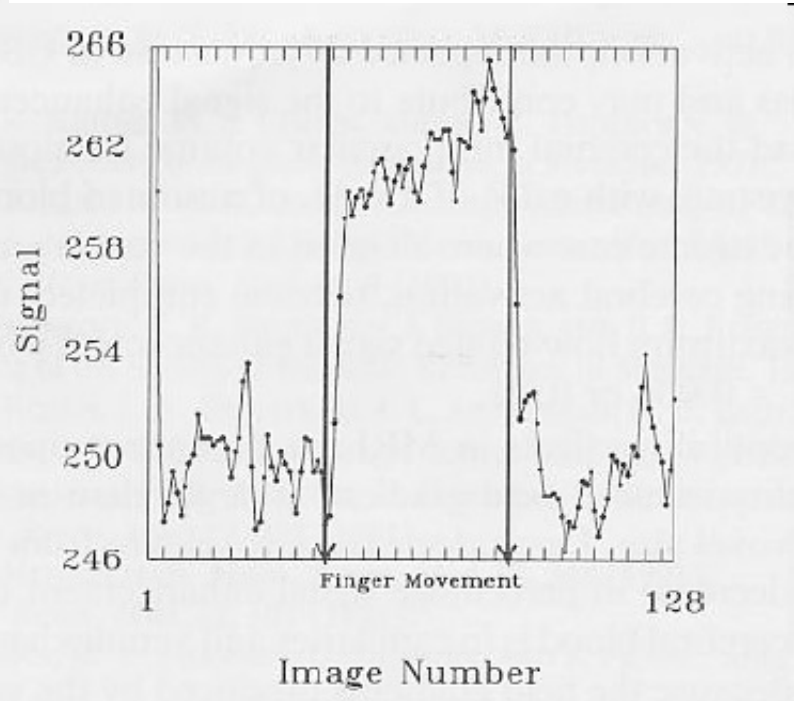


**P. A. Bandettini, et al., (1992)**
"Time course EPI of human brain function during task activation."
**Magn. Reson. Med 25, 390-397.**

9-16-91 Results from dH61 (sig ↑ upon stim?!!)

Experiment 1: Rest until G3 then move right fingers

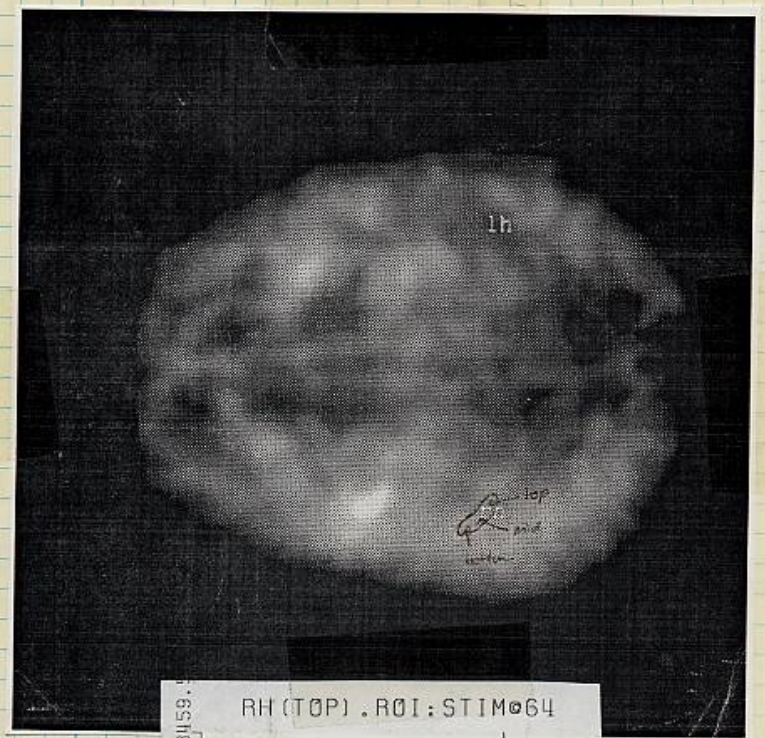


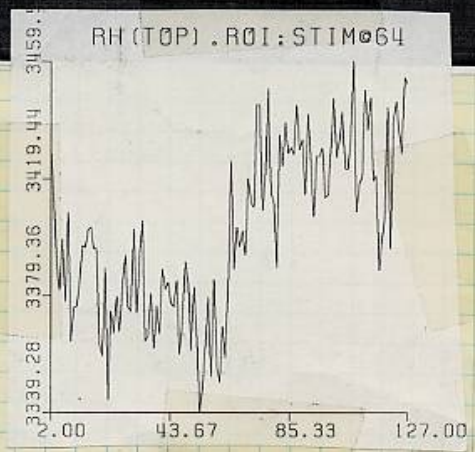




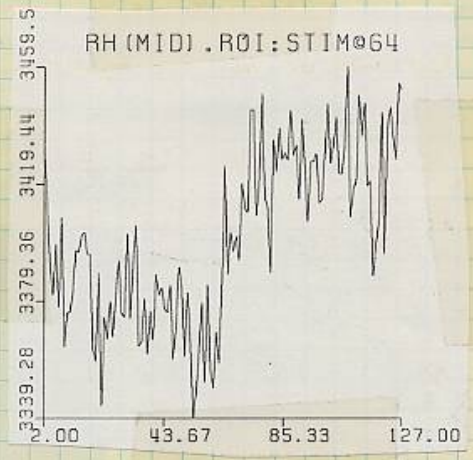


ROI's from p17

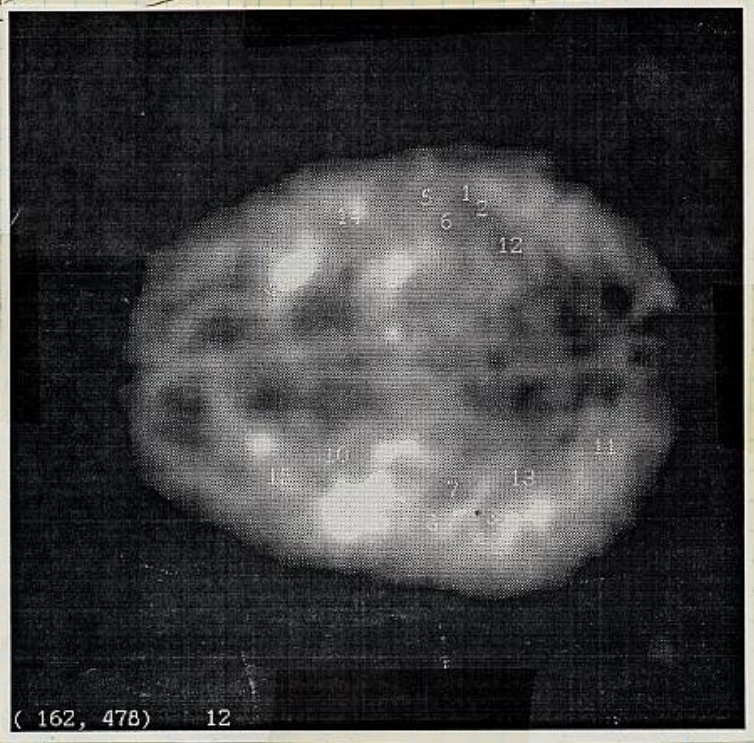

9-16-91

Finally, ~~a~~ difference image in which

the average of the first 64 images (no movement) is subtracted from the last 64 images (movement) of right hand.

Right-Hand Movement

Axial

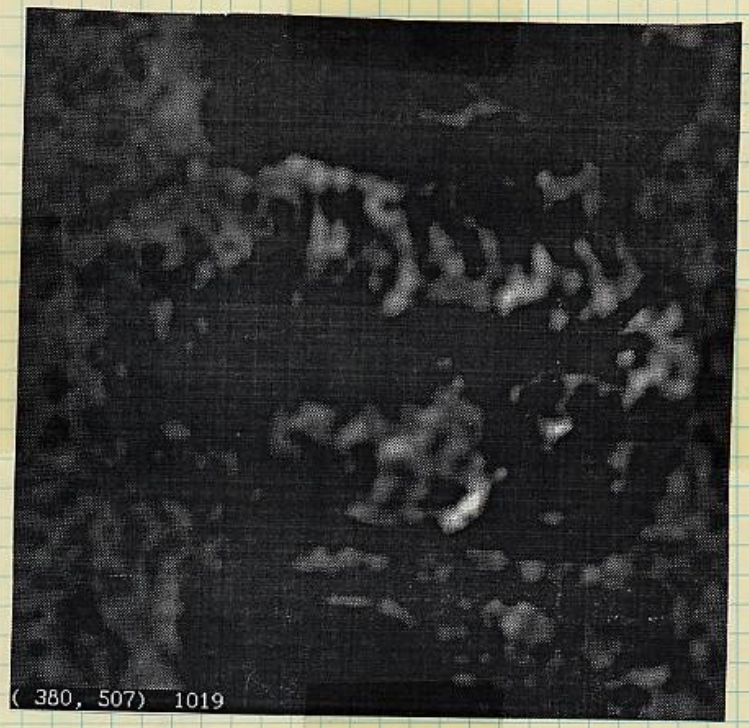


Resolution.

20 cm / 64

.3125 cm

= 3.125 mm

15/20 15/2

Brightest ~~spot~~ area is an indicator of largest signal increase when the ~~area~~ right hand was stimulated (fingers moved) → exactly corresponds to region of motor cortex and sensory and supplementary motor cortex as well that is associated with right hand movement.



9-16-91

Results from experiment #2

Experiment #2 consisted of moving the left hand and then stopping the movement after 86 images.

LH ROI from p16

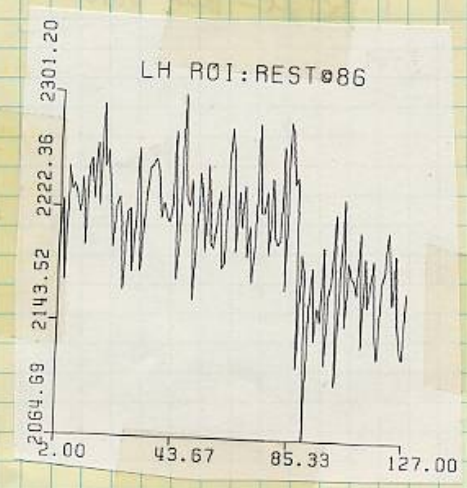


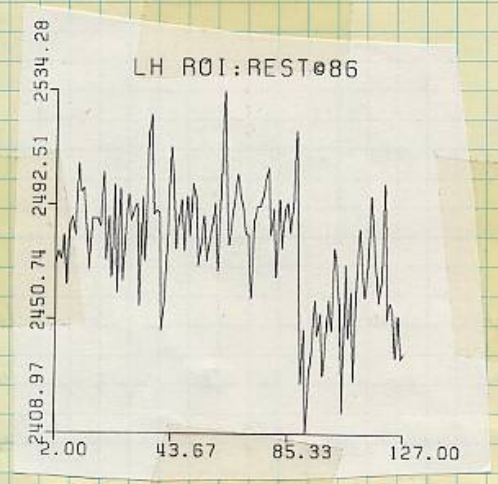

**Trying to figure out the basic mechanism.**

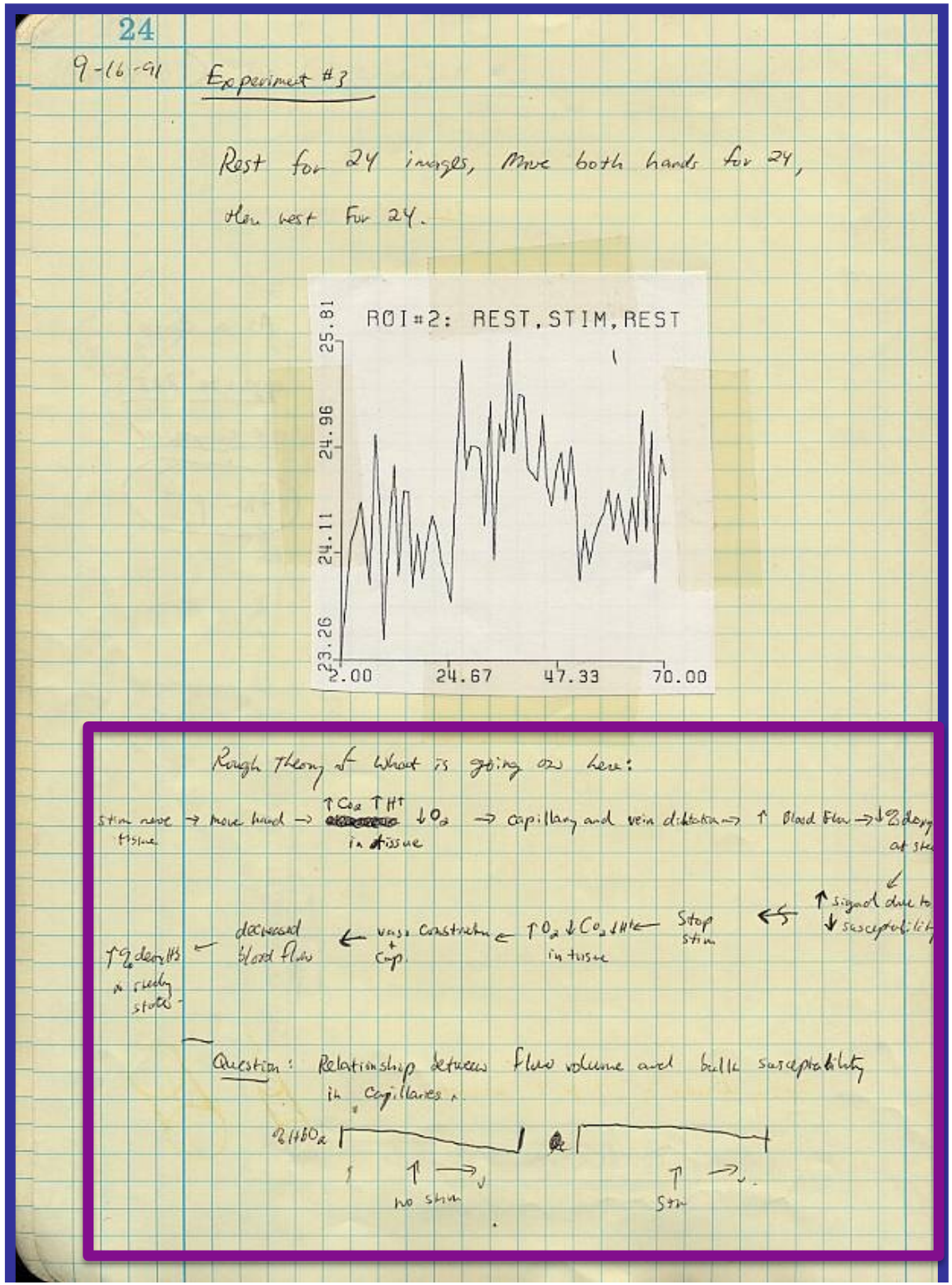

24

9-16-91

Experiment #3

Rest for 24 images, Move both hands for 24, then rest for 24.



Rough Theory of what is going on here:

Stim nerve tissue → move hand → ↑$CO_2$ ↑$H^+$ in tissue ↓$O_2$ → capillary and vein dilation → ↑ Blood flow → ↓% deoxy at site

↑ signal due to ↓ susceptibility

↑% deoxyHb in steady state ← decreased blood flow ← vasc. constriction + cap. ← ↑$O_2$ ↓$CO_2$ ↓$H^+$ in tissue ← Stop stim

Question: Relationship between flow volume and bulk susceptibility in capillaries.

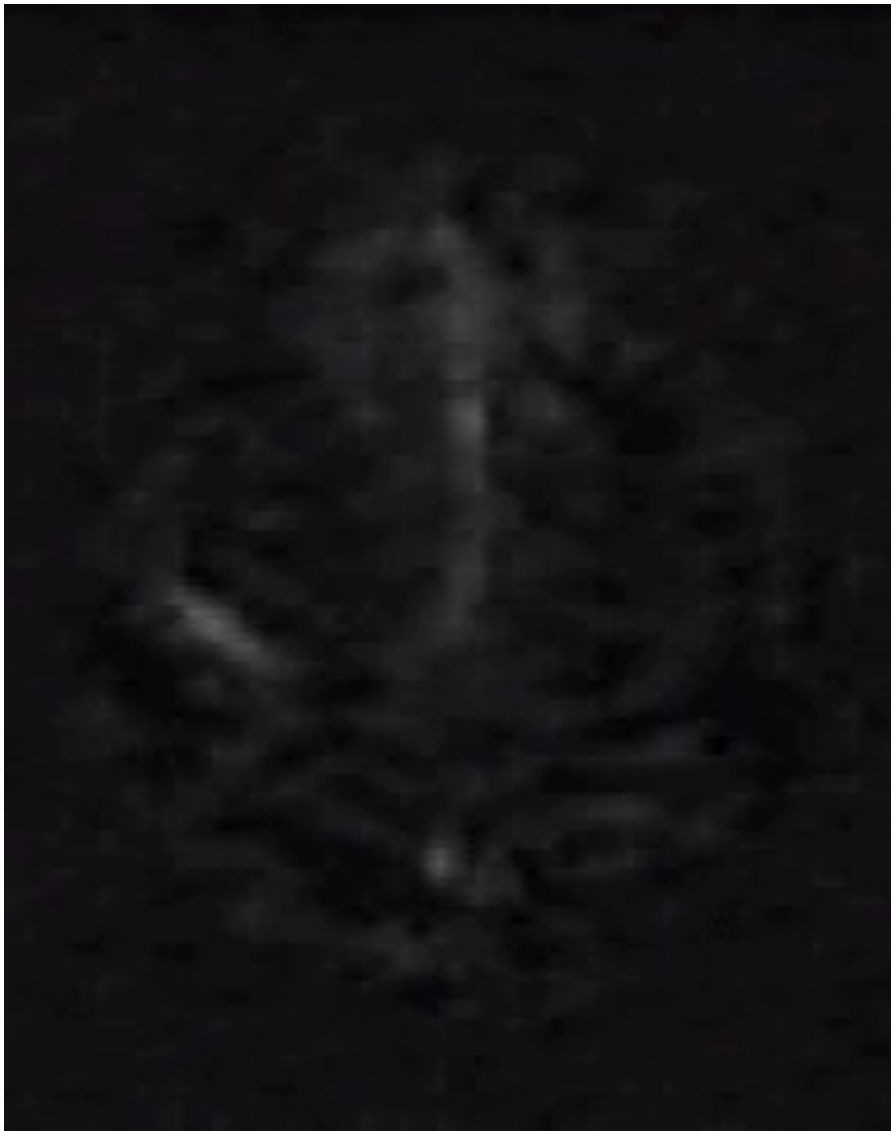

1991

The first event-related studies.

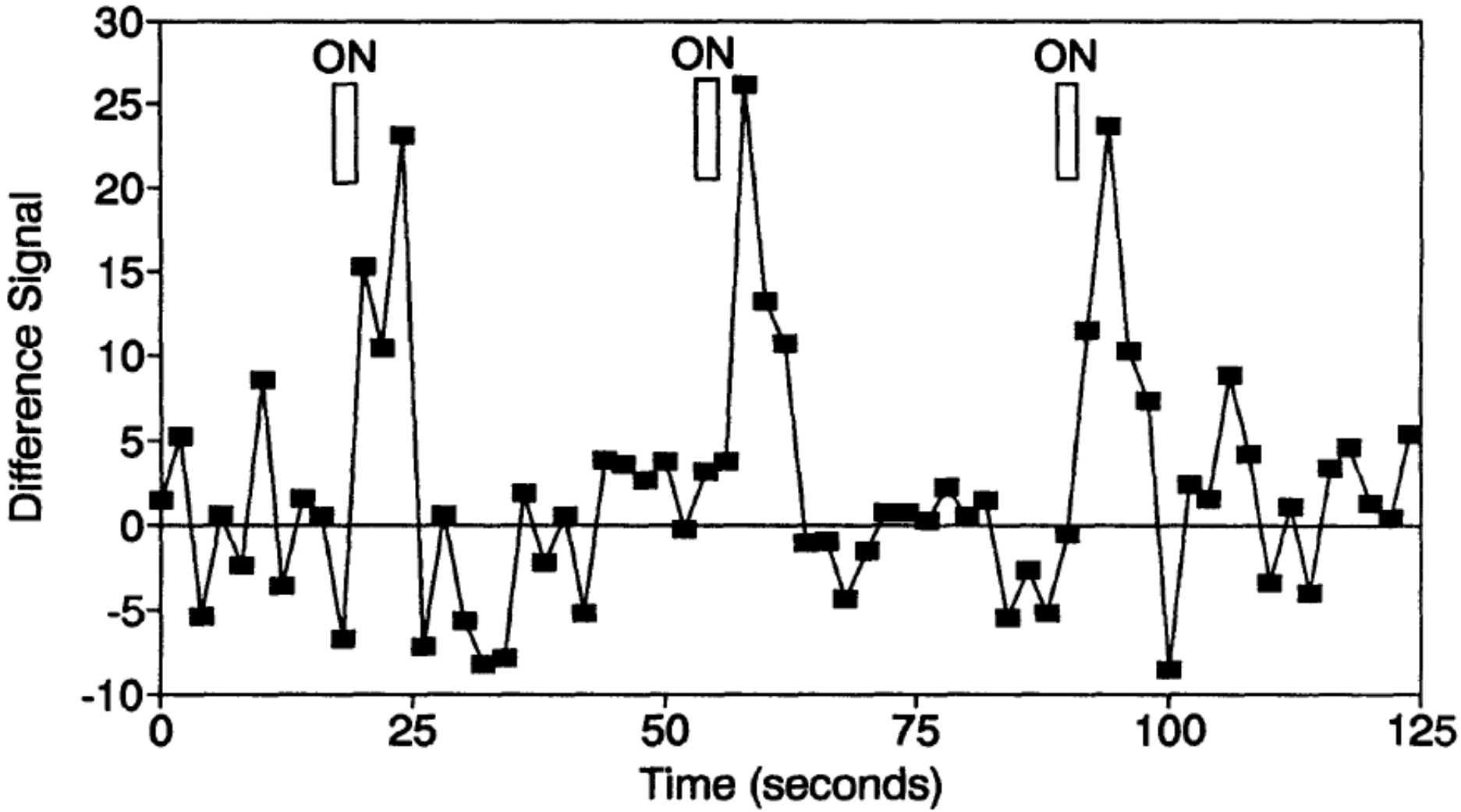


Blamire, A. M., et al. (1992). "Dynamic mapping of the human visual cortex by high-speed magnetic resonance imaging." Proc. Natl. Acad. Sci. USA 89: 11069-11073.

1992…Perfusion using Arterial Spin Labeling

MAGNETIC RESONANCE IN MEDICINE 23, 37–45 (1992)

# Perfusion Imaging

JOHN A. DETRE,*·† JOHN S. LEIGH,* DONALD S. WILLIAMS,‡ AND ALAN P. KORETSKY‡·§

* *Metabolic Magnetic Resonance Research Center and Department of Biochemistry and Biophysics, University of Pennsylvania School of Medicine, Philadelphia, Pennsylvania 19104; and ‡Pittsburgh NMR Center for Biomedical Research and §Department of Biological Sciences, Carnegie Mellon University, Pittsburgh, Pennsylvania 15213*

Received July 2, 1990; revised January 3, 1991

Measurement of tissue perfusion is important for the functional assessment of organs *in vivo*. Here we report the use of $^1$H NMR imaging to generate perfusion maps in the rat brain at 4.7 T. Blood water flowing to the brain is saturated in the neck region with a slice-selective saturation imaging sequence, creating an endogenous tracer in the form of proximally saturated spins. Because proton $T_1$ times are relatively long, particularly at high field strengths, saturated spins exchange with bulk water in the brain and a steady state is created where the regional concentration of saturated spins is determined by the regional blood flow and regional $T_1$. Distal saturation applied equidistantly outside the brain serves as a control for effects of the saturation pulses. Average cerebral blood flow in normocapnic rat brain under halothane anesthesia was determined to be $105 \pm 16$ cc · 100 g$^{-1}$ · min$^{-1}$ (mean ± SEM, $n = 3$), in good agreement with values reported in the literature, and was sensitive to increases in arterial $pCO_2$. This technique allows regional perfusion maps to be measured noninvasively, with the resolution of $^1$H MRI, and should be readily applicable to human studies. 

1992…Perfusion using Arterial Spin Labeling

*Proc. Natl. Acad. Sci. USA*
Vol. 89, pp. 212–216, January 1992
Biophysics

# Magnetic resonance imaging of perfusion using spin inversion of arterial water

**(cerebral blood flow/adiabatic fast passage/hypercarbia/rat brain/cold injury)**

DONALD S. WILLIAMS*, JOHN A. DETRE†‡, JOHN S. LEIGH†, AND ALAN P. KORETSKY*§

*Pittsburgh Nuclear Magnetic Resonance Center for Biomedical Research, and §Department of Biological Sciences, Carnegie Mellon University, Pittsburgh, PA 15213; and †Metabolic Magnetic Resonance Research Center, Department of Radiology, and ‡Department of Neurology, University of Pennsylvania School of Medicine, Philadelphia, PA 19104

*Communicated by Mildred Cohn, September 19, 1991*

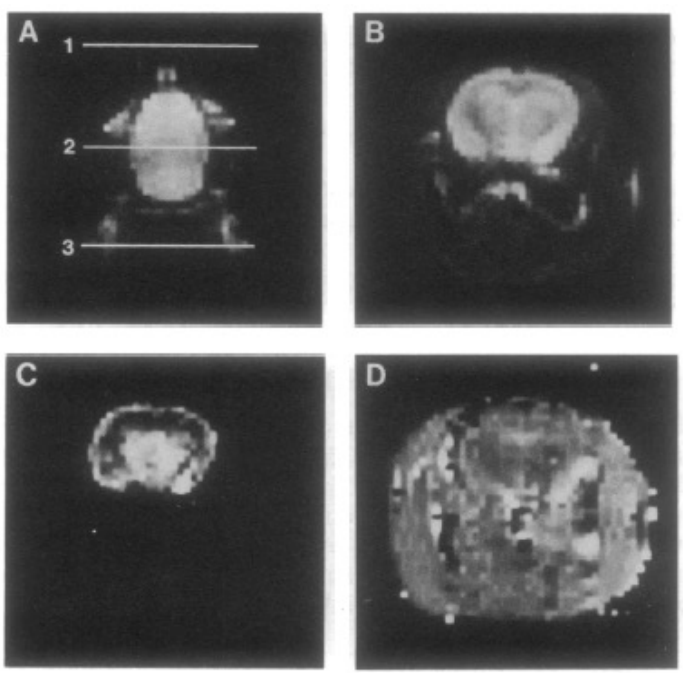


FIG. 2. (*A*) Coronal image of a rat head. The resonance planes for radiofrequency used for spin inversion by AFP for control and inversion images are indicated by 1 and 3, respectively, and plane 2 is the detection plane. (*B*) Control transverse image from the detection plane (plane 2 in *A*). (*C*) Difference image between control and inversion images. (*D*) $T_{1app}$ image.

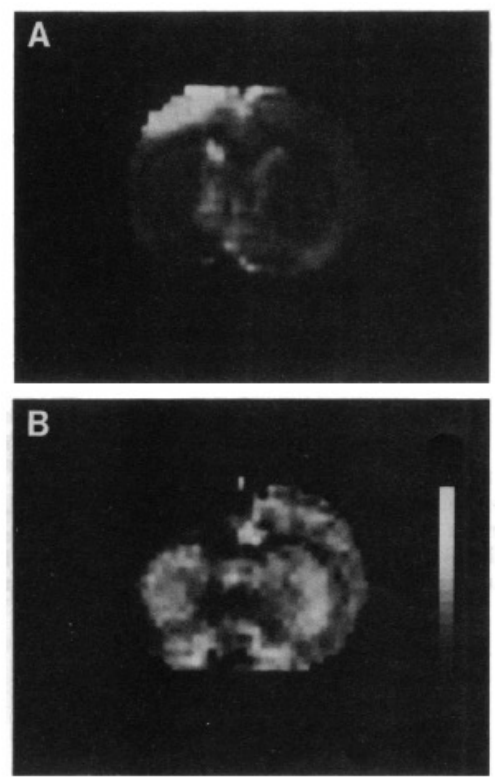


FIG. 5. Comparison of conventional MRI and perfusion imaging of a rat brain subjected to a regional cold injury. (*A*) Conventional $T_2$-weighted image (TE = 60 ms, TR = 2 s). The injured region shows up as hyperintensity due to a longer $T_2$. (*B*) Perfusion image of the same slice. The grey scale is from 0 to 6 $ml \cdot g^{-1} \cdot min^{-1}$. The injured region is dark due to low flow.

# Perfusion Contrast

EPISTAR

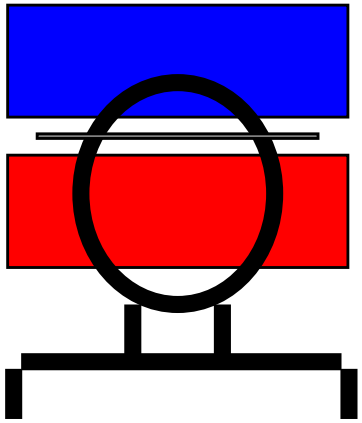

FAIR

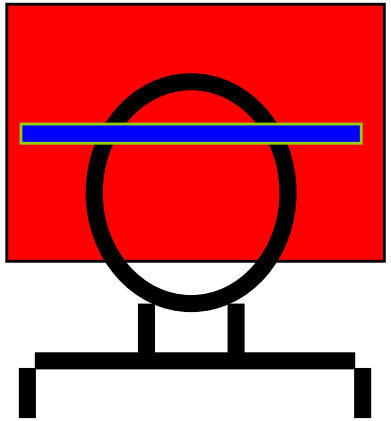

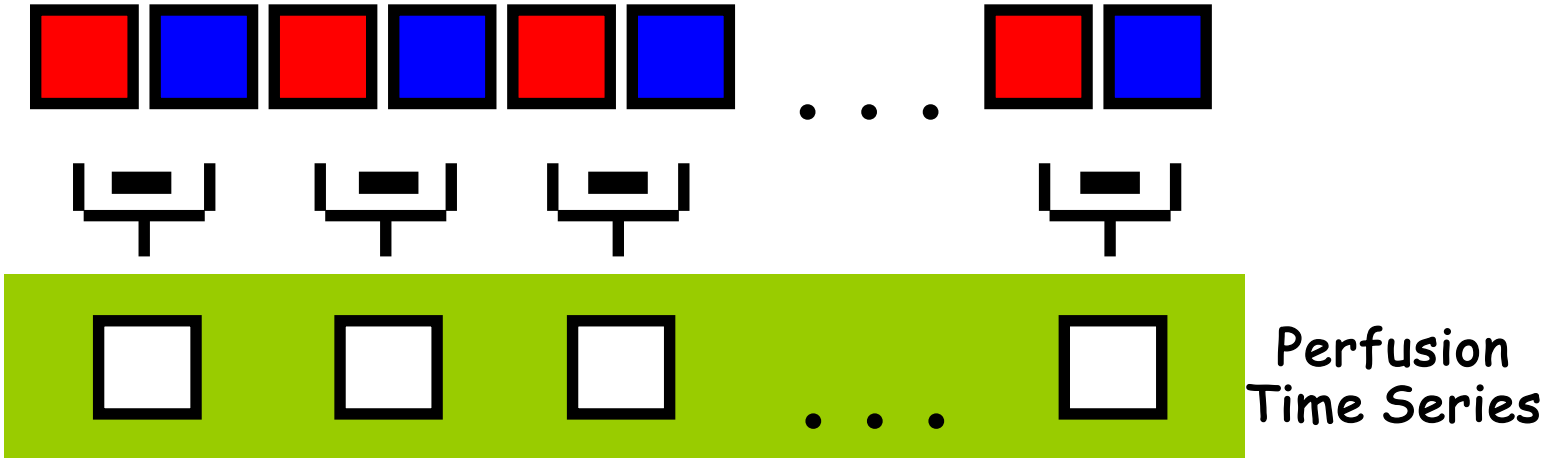

| TI (ms) | FAIR | EPISTAR |
|---|---|---|
| 200 | | |
| 400 | | |
| 600 | | |
| 800 | | |
| 1000 | | |
| 1200 | | |

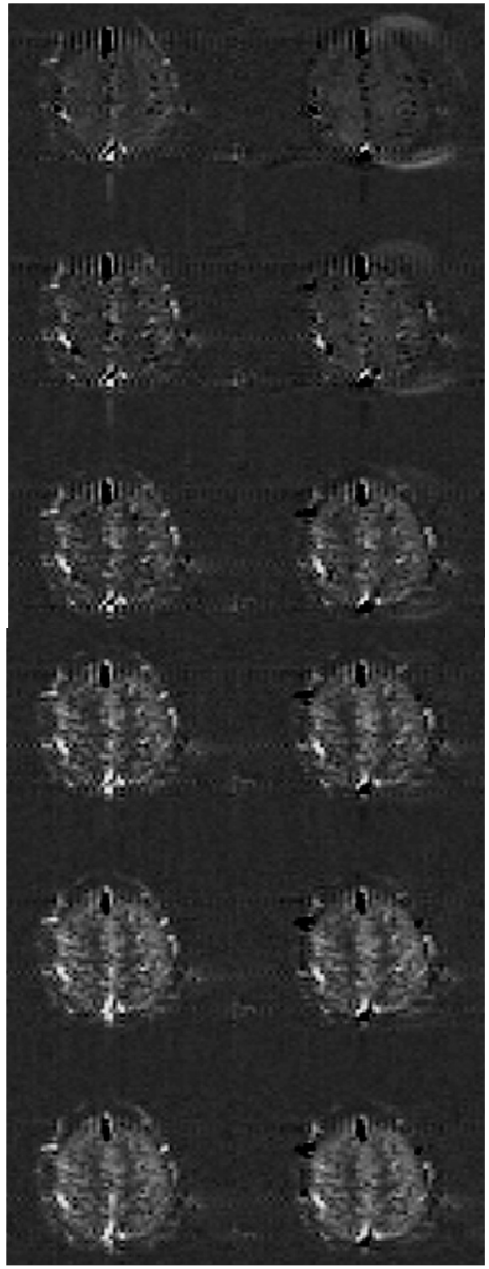

# Functional MRI of the Brain

A Report on the SMRM/SMRI Workshop held in Arlington, Virginia

June 17–19, 1993

MRM 30:405–408 (1993)

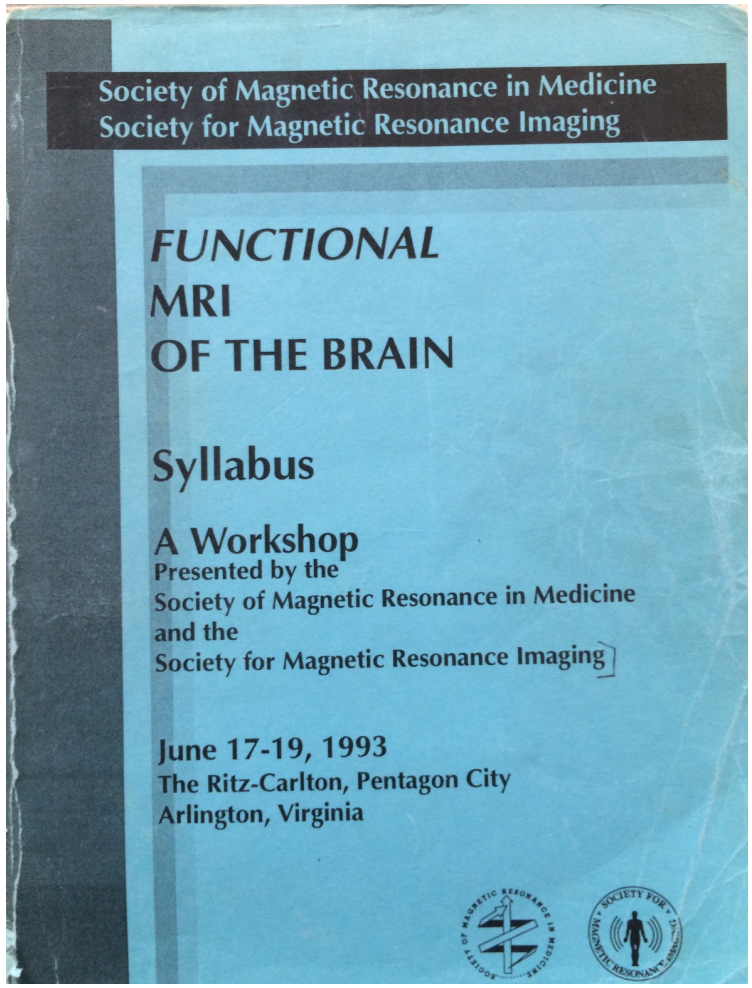


Denis Le Bihan
National Institutes of Health
Diagnostic Radiology Department
Building 10, Room 1C-660
Bethesda, Maryland 20892

Robert Turner
National Institutes of Health
Laboratory of Cardiac Energetics
Building 10, Room B1D-161
Bethesda, Maryland 20892

Michael E. Moseley
Department of Radiology
Stanford University
Stanford, California 94305-5488

James S. Hyde
Biophysics Research Institute
Medical College of Wisconsin
8701 Waterton Plank Road
Milwaukee, Wisconsin 53226

A proposed acronym...

# Functional Neuroimaging with EPI: Sequence Issues

Robert Turner, Peter Jezzard, #Lucie Hertz-Pannier, #Denis Le Bihan, *David Feinberg

Laboratory of Cardiac Energetics, National Heart, Lung, and Blood Institute, and #Diagnostic Radiology Department, Clinical Center, NIH, Bethesda, MD 20892
*Department of Radiology, NYU Medical Center, New York, NY

## ABSTRACT

Freedom from motion artifact, comparatively good SNR, rapid multi-slice capability, and excellent time resolution make Echo-Planar Imaging an excellent choice for BOLD contrast MR functional neuroimaging. However, when the gradient echo version of EPI is used for this purpose, problems arise regarding image quality and interpretation. Large draining veins distant from active neural regions are the major confusing factor. At high enough static magnetic fields, spin-echo EPI can be used to obtain images showing local changes of blood oxygenation related to brain activation, in which draining veins have less effect. The idea MRFN equence will combine gradient-recalled echo and spin echo features, and thus will be some variant of GRASE (GRAdient echo and Spin Echo).

A proposed acronym...

The earliest successful magnetic resonance functional neuroimaging (MRFN) studies with BOLD contrast were made using a gradient-echo version of echo-planar imaging (EPI). The EPI technique, proposed by Mansfield in 1977 (4), allows the capture of a complete MR image in under 100 ms. Thus most motions in the body are frozen and motion artifact rarely appears. EPI relies on a very rapidly switched magnetic field gradient of large amplitude, and a fast data capture rate. Since these features were not considered necessary by most manufacturers of commercial MR systems until recently, the technique has been available only in a few pioneering laboratories. The technique normally uses a full 90 degree rf pulse for spin excitation, and hence provides a comparatively high single-shot signal/noise ratio (SNR), considering the large receiver bandwidth required. For brain imaging, with equal voxel size, an EPI image with 40 ms acquisition time has been found to have the same SNR as a FLASH image with optimized bandwidth taking 2 seconds to acquire. Faster FLASH images will have a poorer SNR than EPI. Low flip-angle variants of EPI (5) can of course provide much higher values of SNR/unit time, though this sacrifices SNR in each

# Functional Mapping of the Human Visual Cortex at 4 and 1.5 Tesla Using Deoxygenation Contrast EPI

R. Turner, P. Jezzard, H. Wen, K. K. Kwong, D. Le Bihan, T. Zeffiro, R. S. Balaban

MRM 29:277–279 (1993)

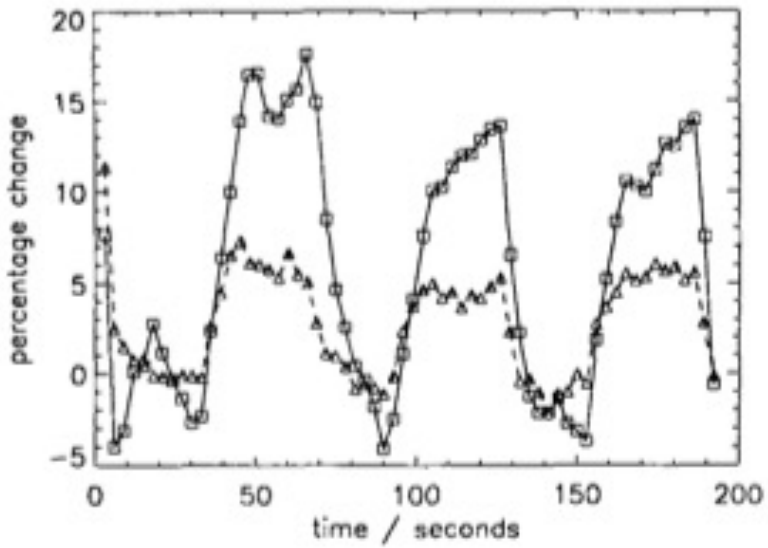


FIG. 2. Plot of fractional change in 4 T (squares) and 1.5 T (triangles) EPI image intensity versus time in the eight-voxel regions of interest in the visual cortex shown in Fig. 1, for a volunteer experiencing alternate 30-s periods of rest and photic stimulation. Details of acquisition for the 4 and 1.5 T data are described in the

# Local Gradient Coil

FIG. 1

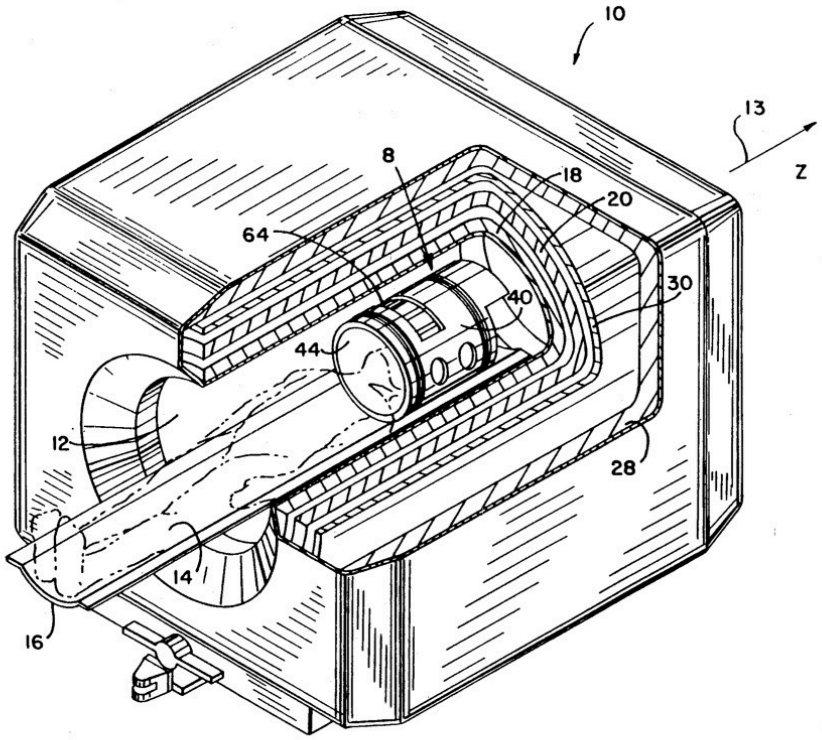


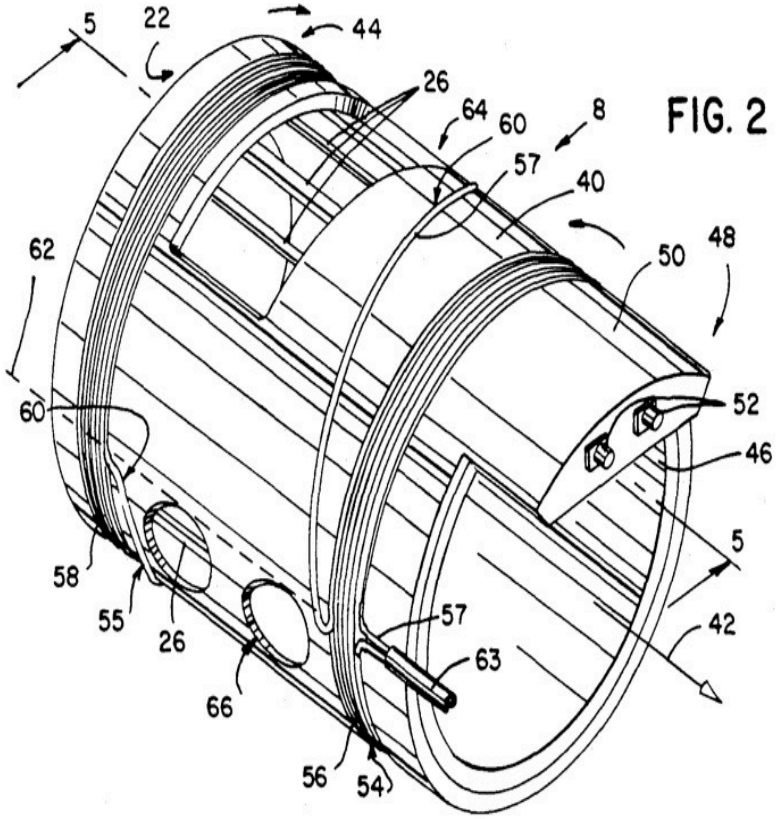


FIG. 2

# NIH 4T

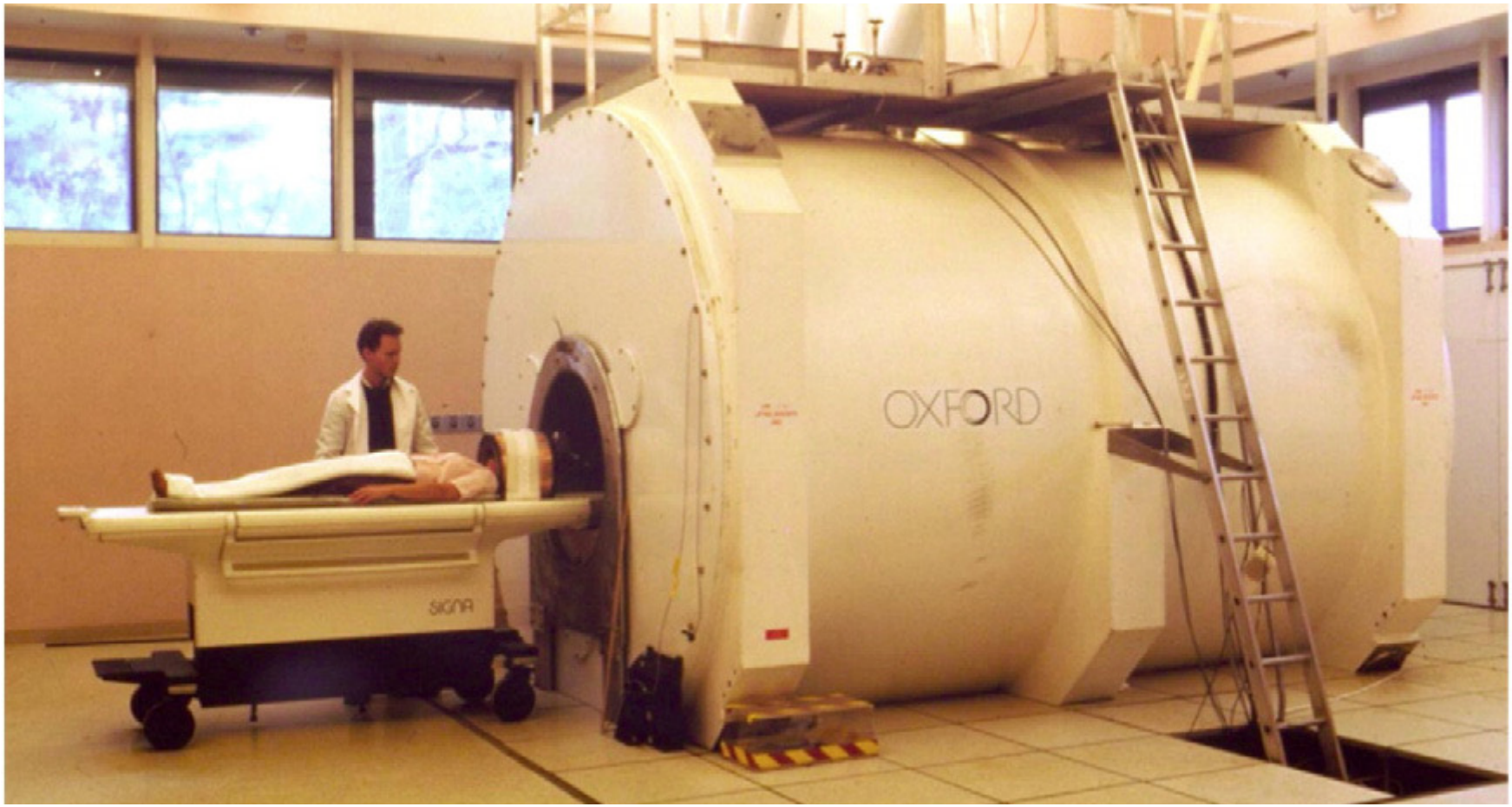

# Siemens' new 7T

# Five Key Factors For The Emergence of Functional MRI

1. Magnetic properties of red blood cells
2. Activation related hemodynamic changes
3. Spatial scale of brain activation
4. Echo Planar Imaging
5. Prevalence of MRI scanners

# Brain Function

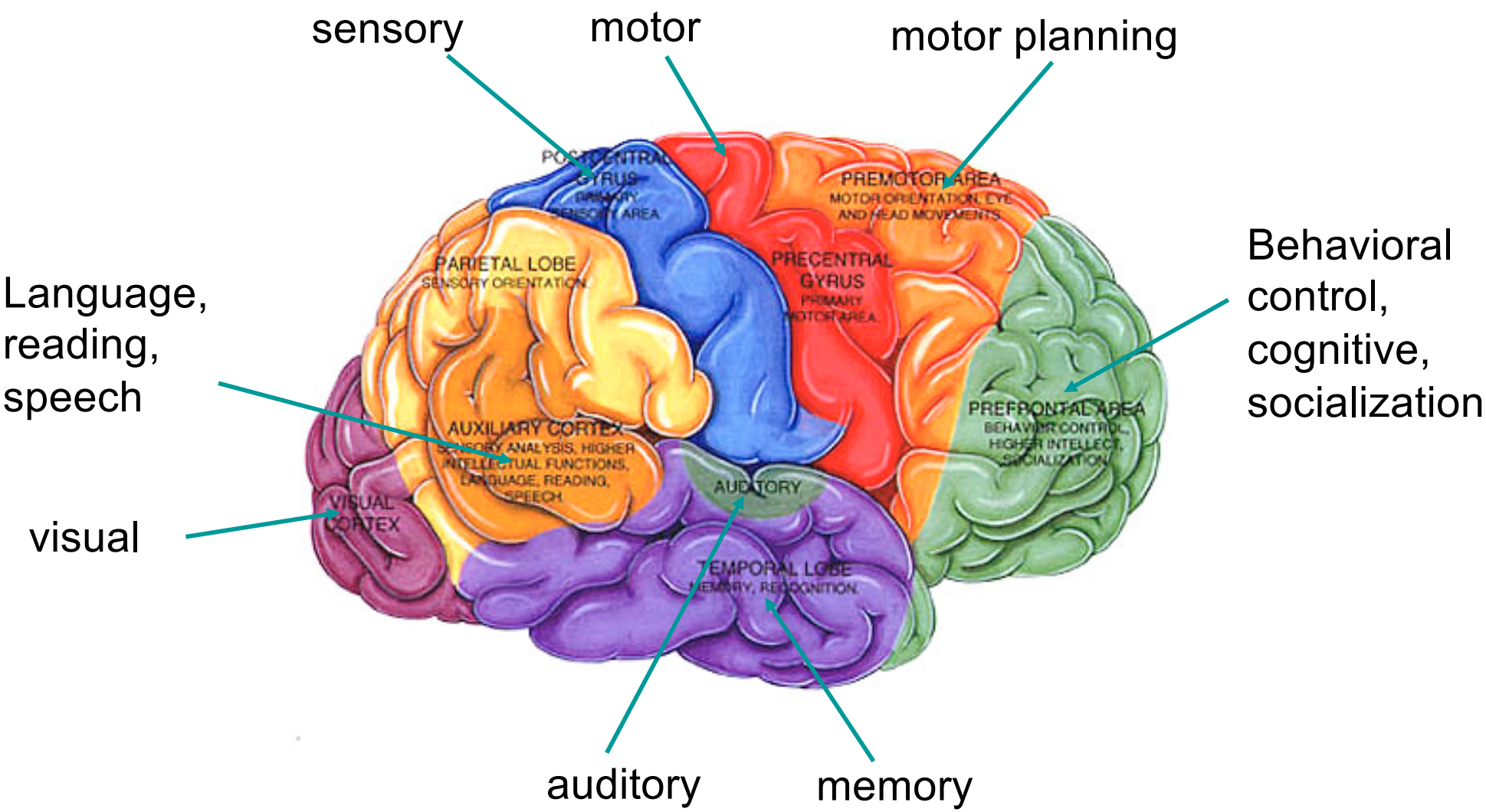

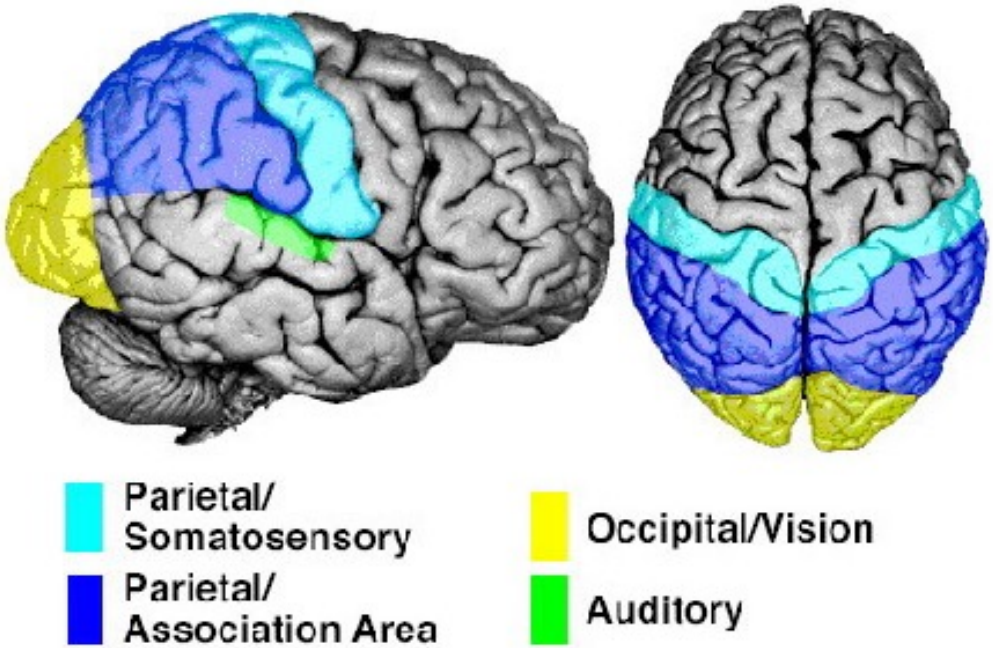
Parietal/
Somatosensory
Parietal/
Association Area
Occipital/Vision
Auditory

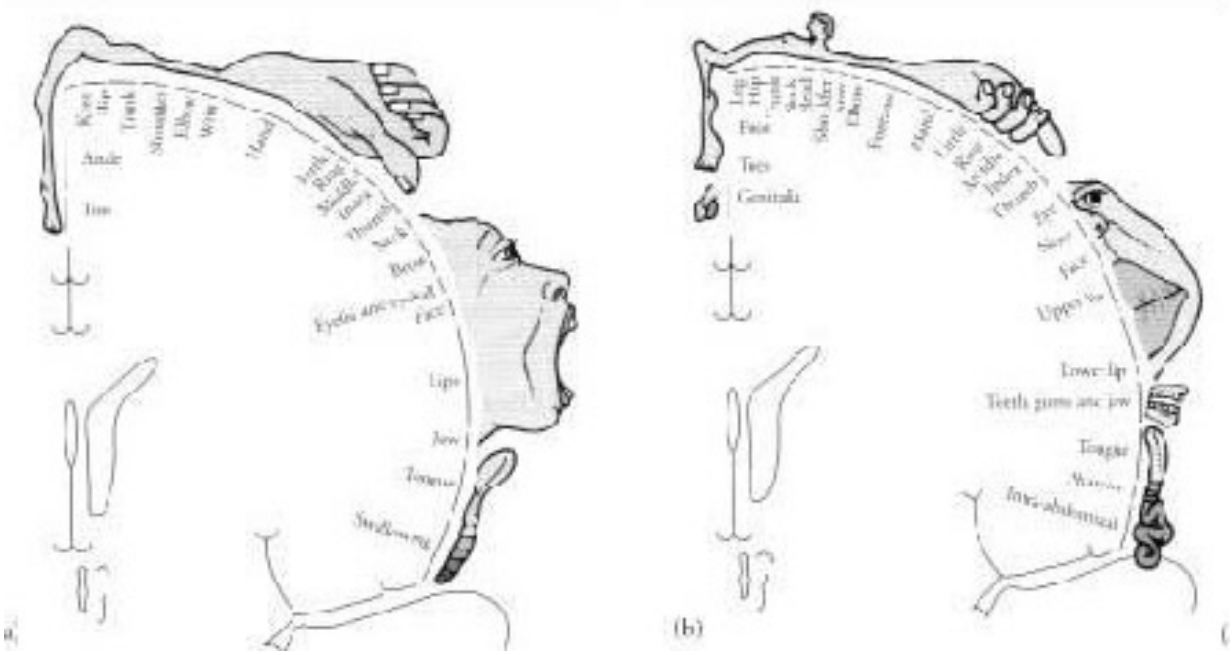
(b)

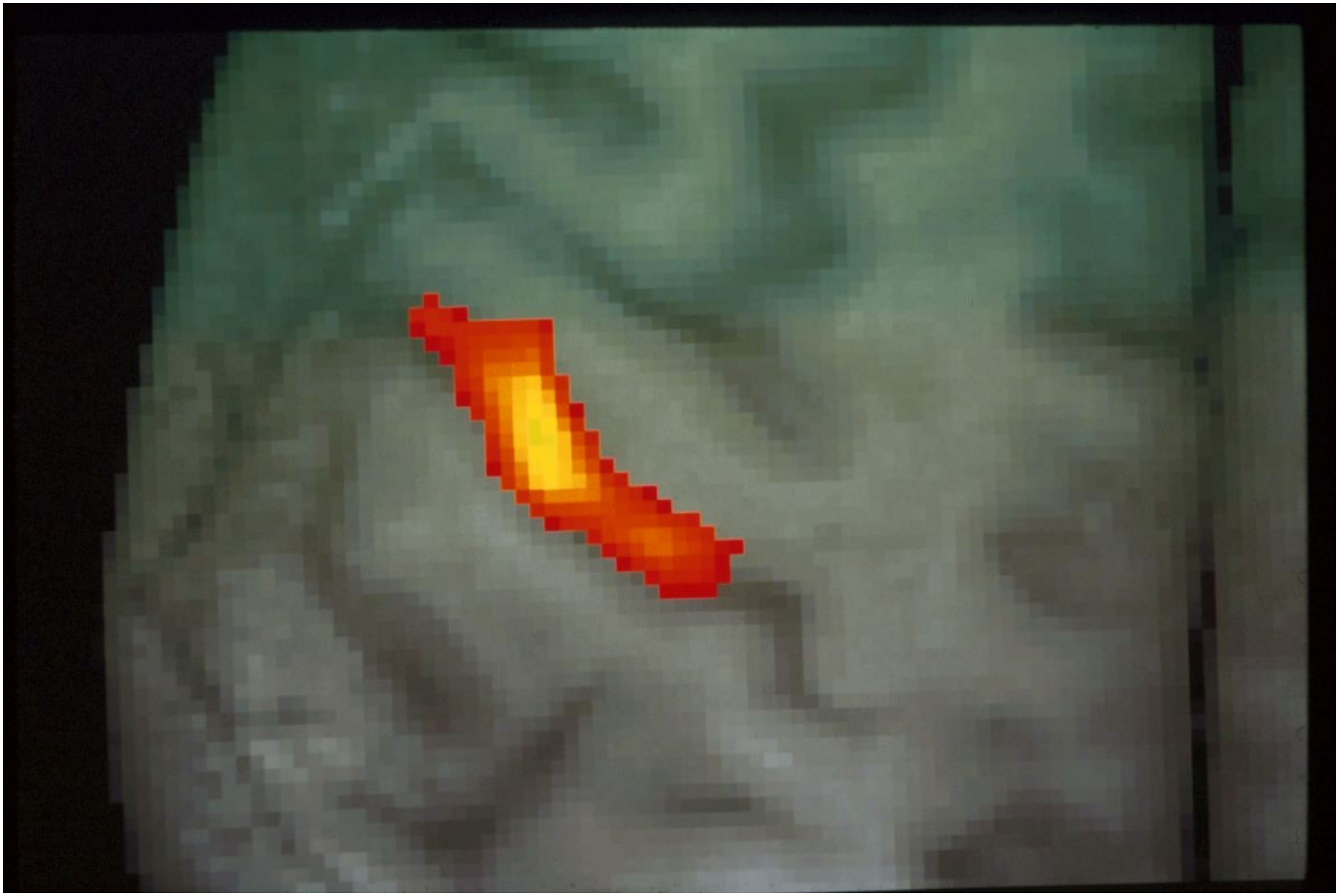

**Visual Cortex Organization**

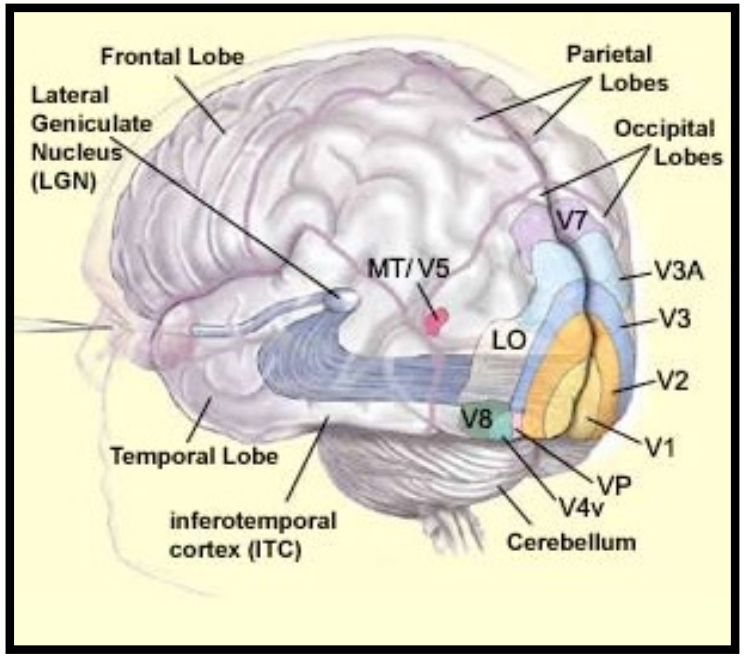


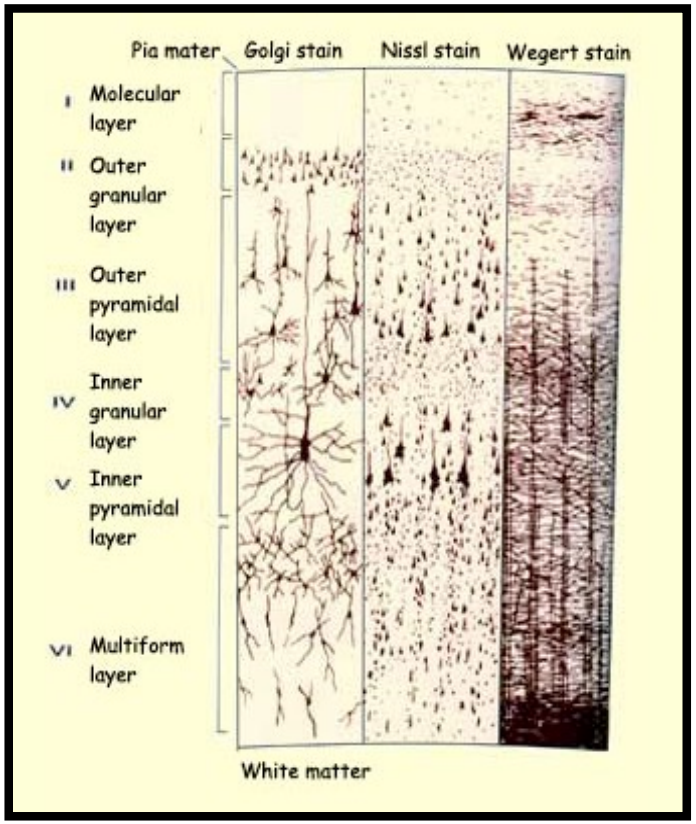


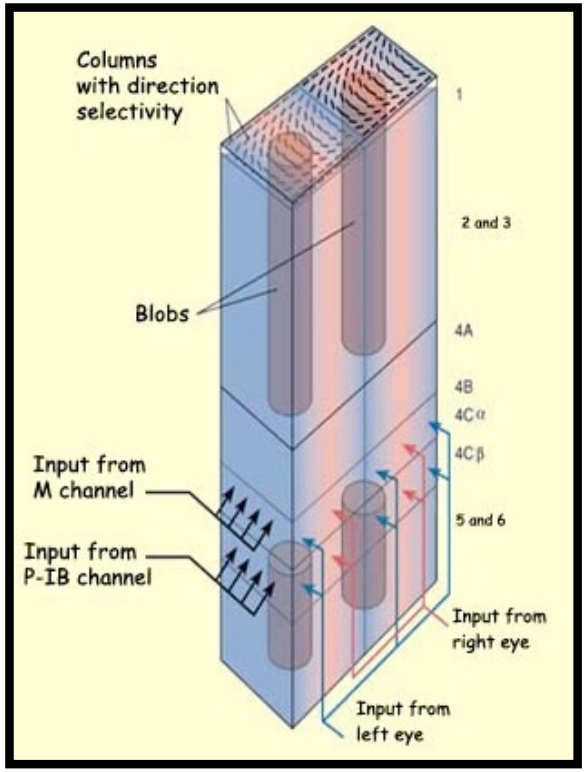


http://www.thebrain.mcgill.ca

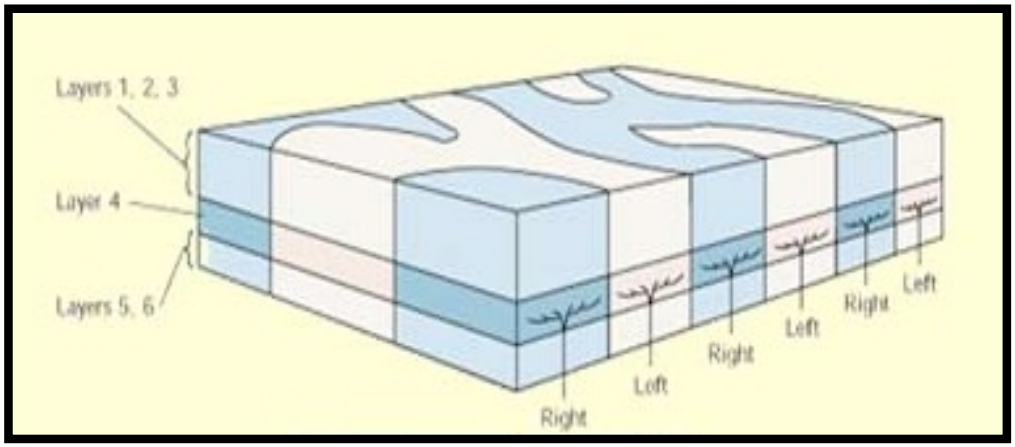

# Ocular Dominance Column Mapping

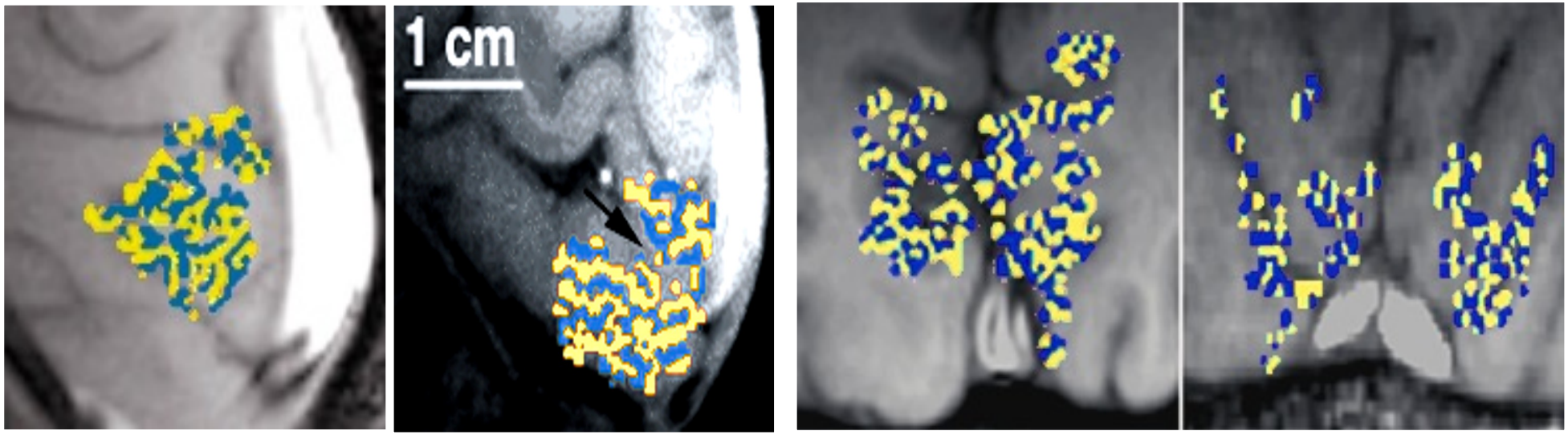


**Menon, R. S., S. Ogawa, et al. (1997). J Neurophysiol 77(5): 2780-7.**

0.54 x 0.54 in plane resolution

## Optical Imaging

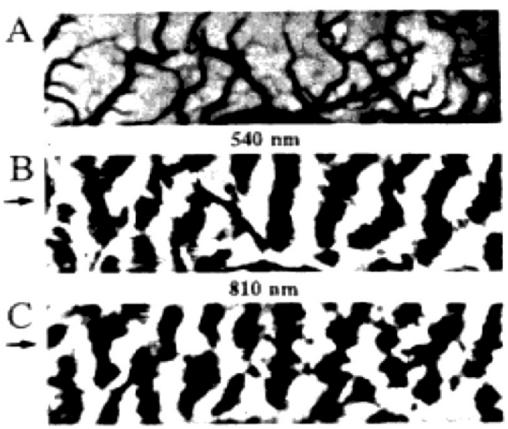


**R. D. Frostig et. al, PNAS 87: 6082-6086, (1990).**

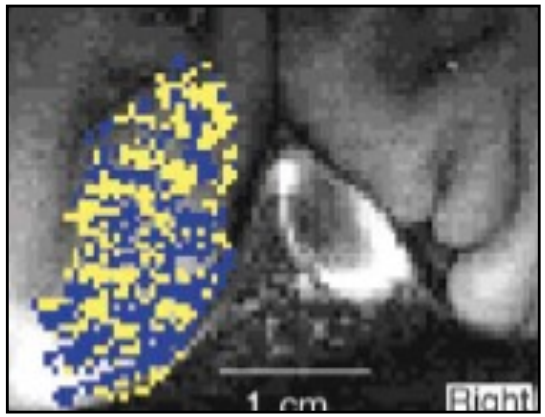


**Cheng, et al. (2001) Neuron,32:359-374**

0.47 x 0.47 in plane resolution

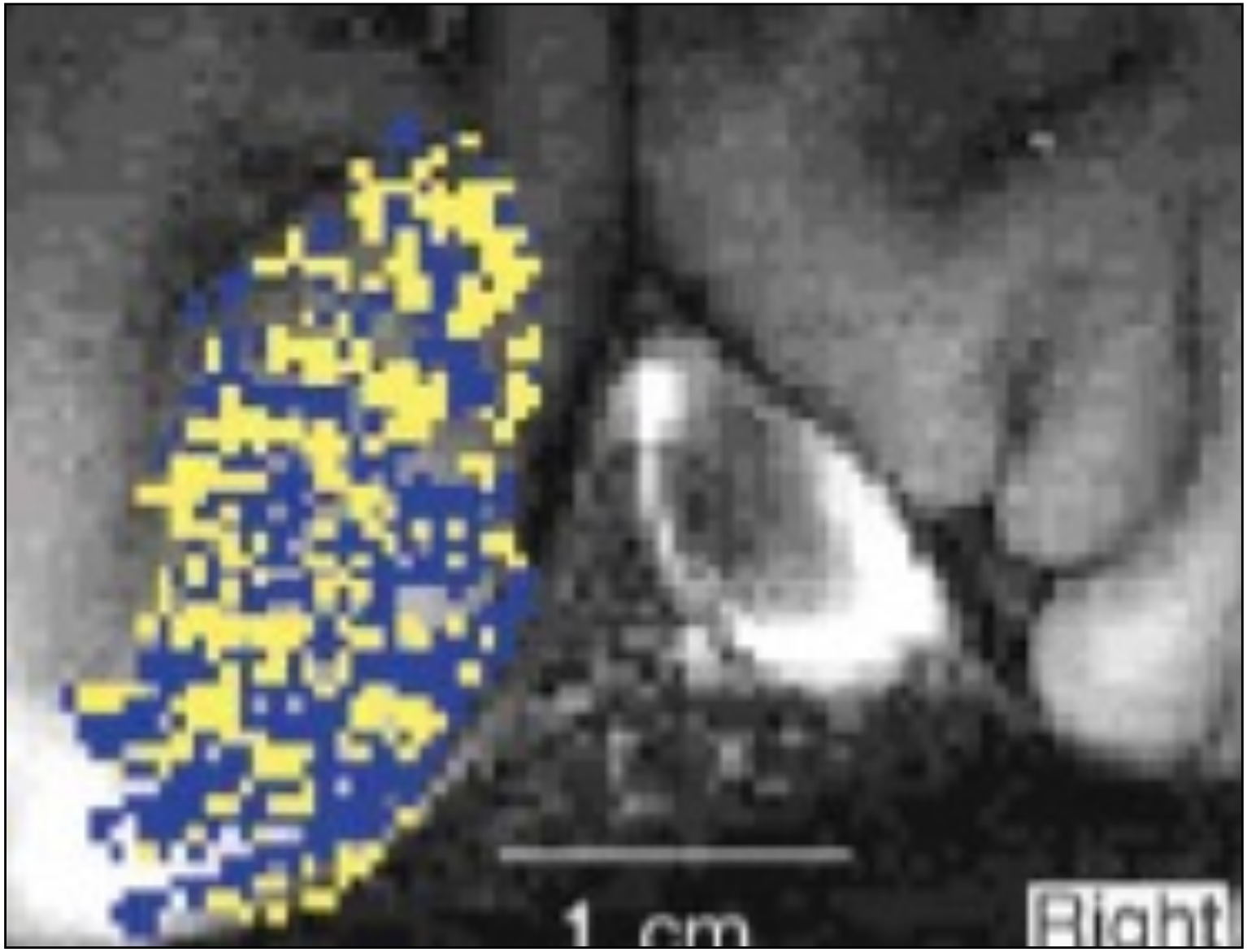


Cheng, et al. (2001) Neuron,32:359-374

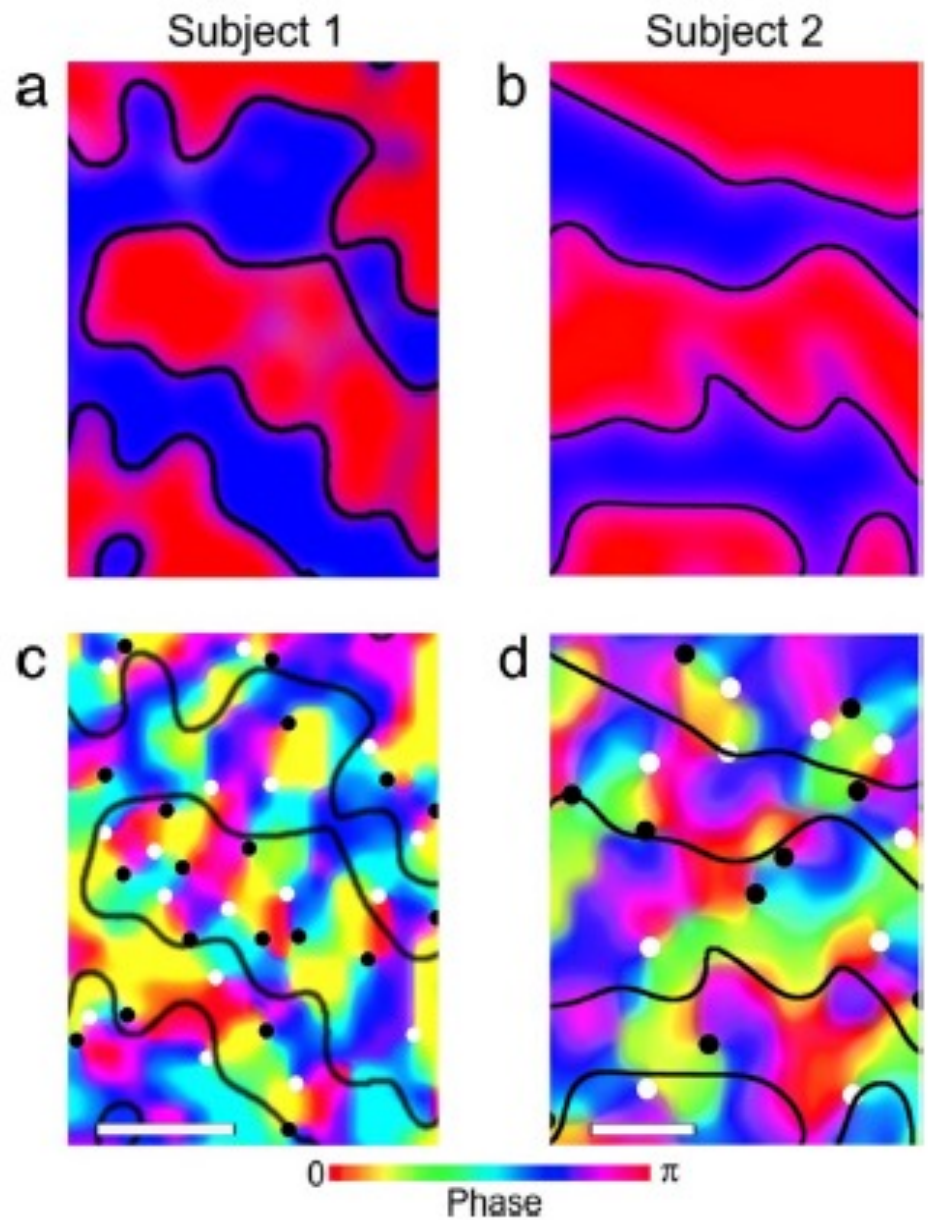


**Yacoub et al. PNAS 2008**

# Orientation Columns in Human V1 as Revealed by fMRI at 7T

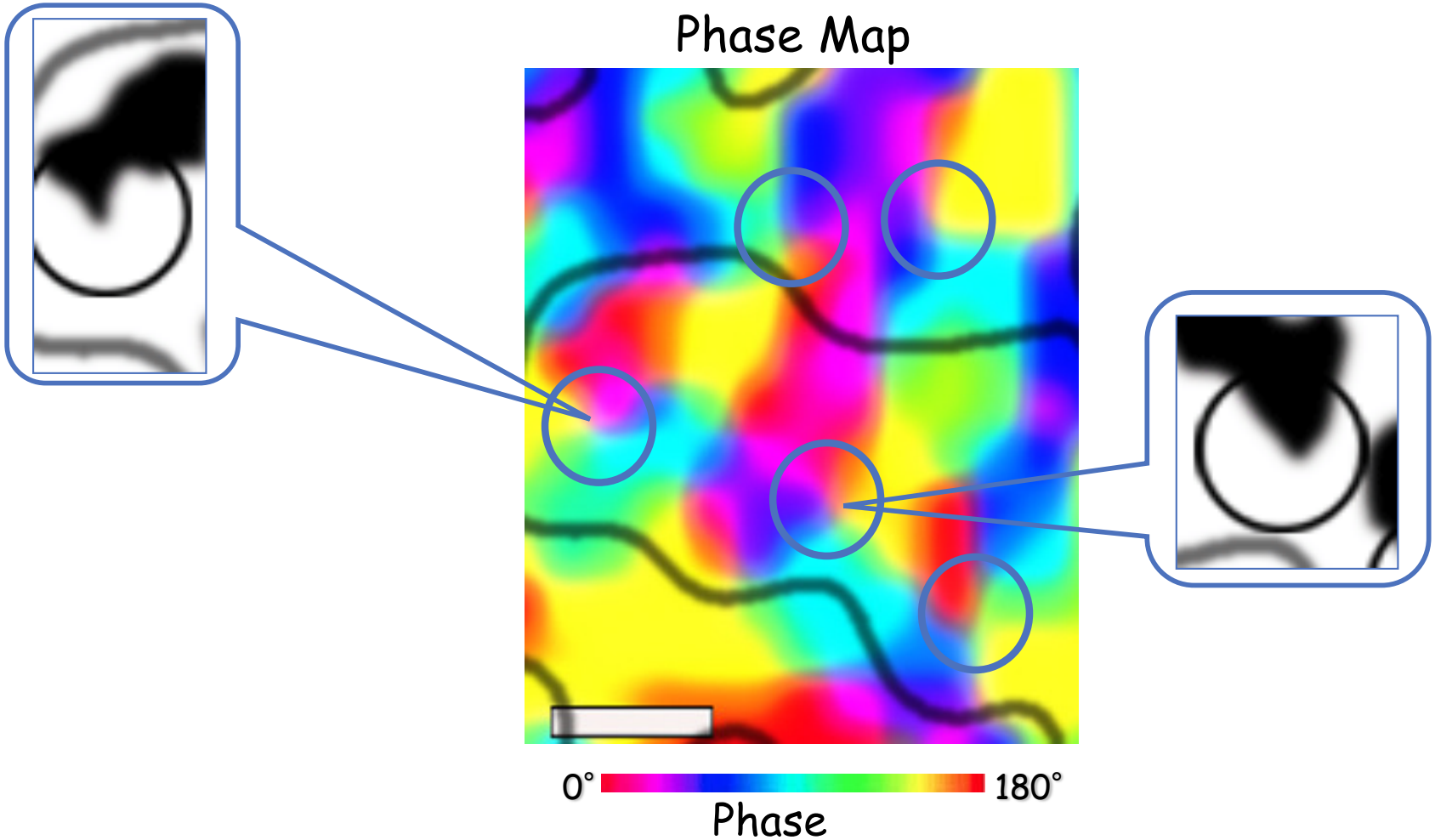


Scalebar = 0.5 mm

Yacoub et al. PNAS 2008

# Layer Dependent Activity

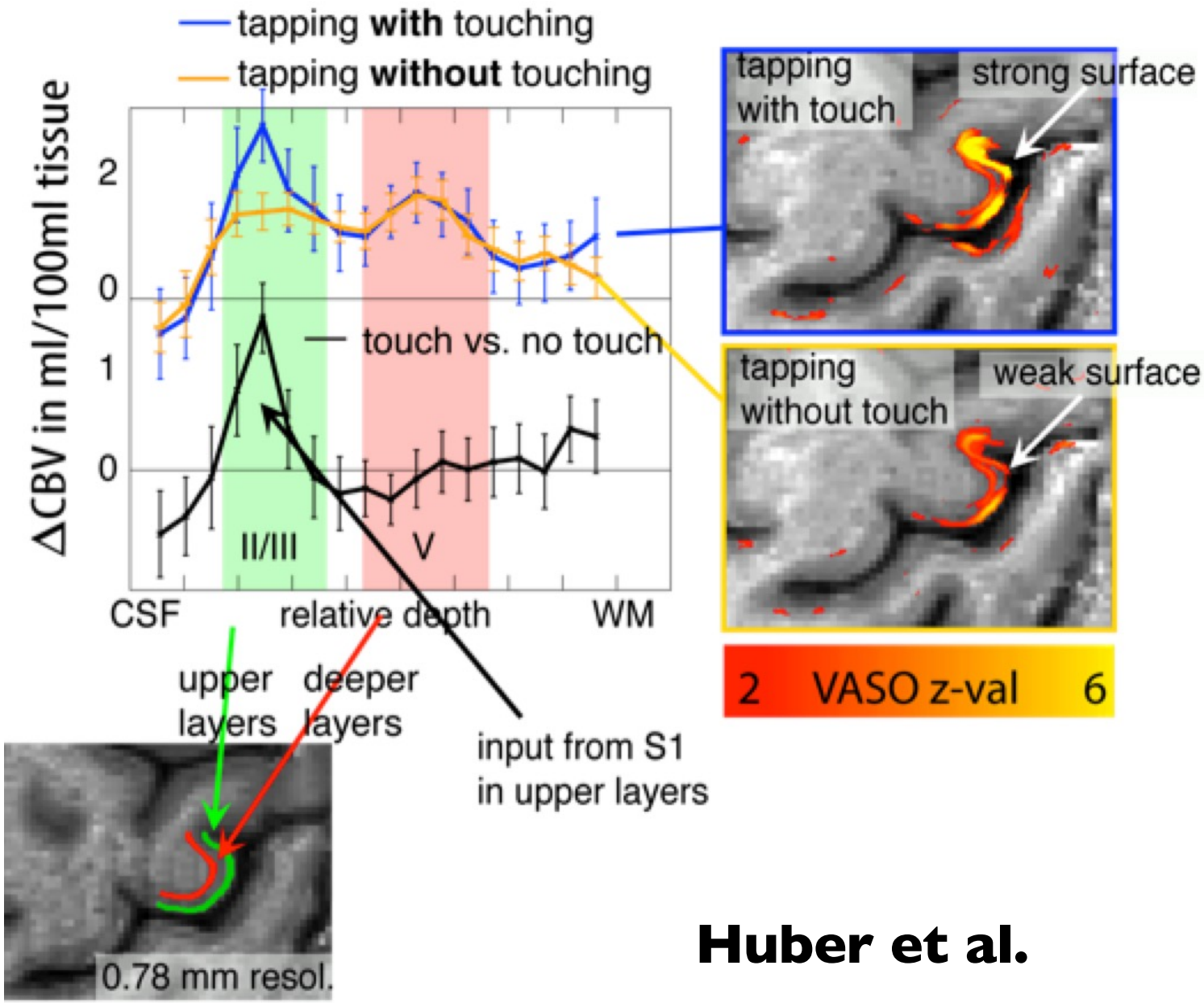


**Huber et al.**

# Multi-sensory integration

***M.S. Beauchamp et al.,***

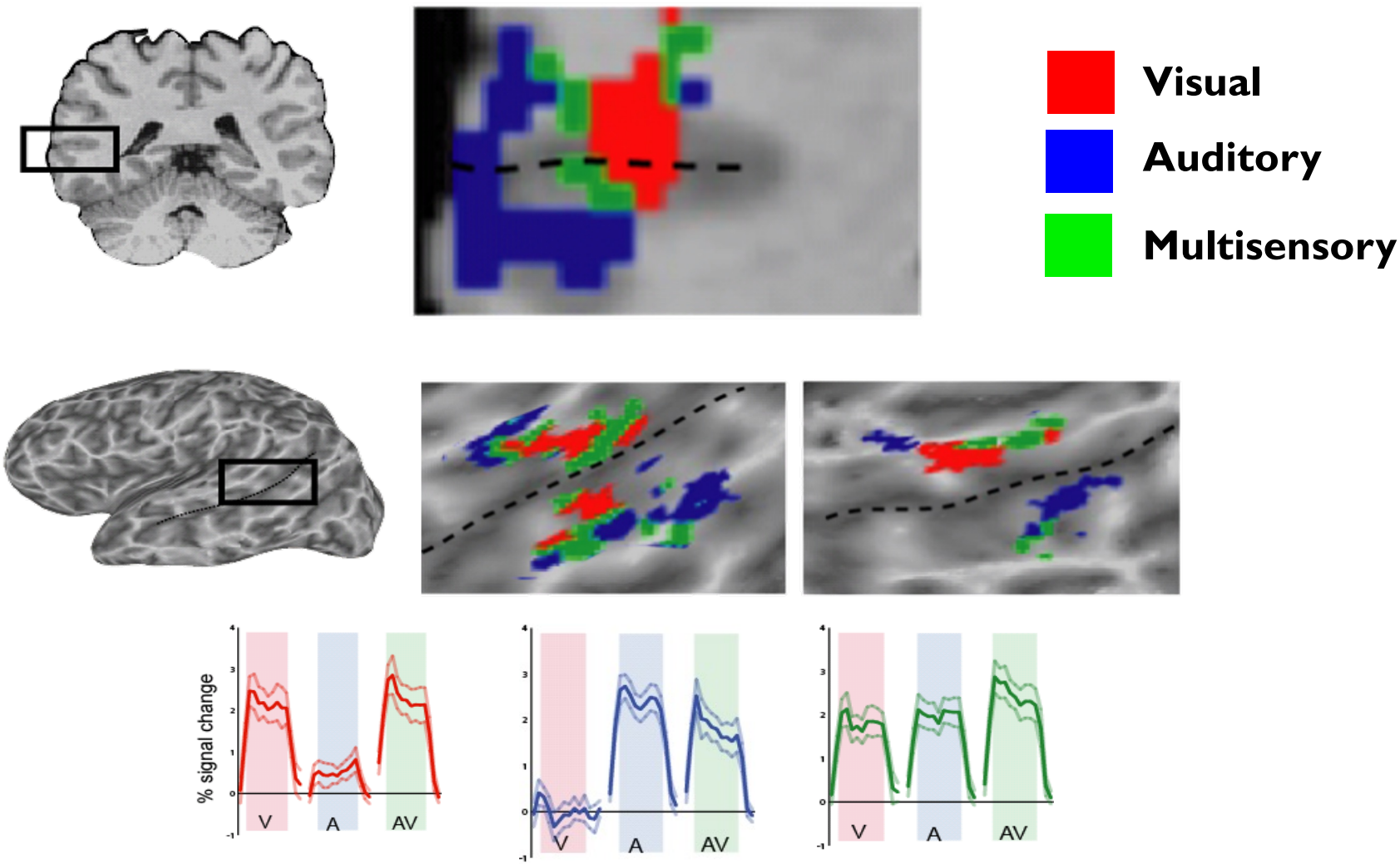

# Functional Neuroimaging Techniques

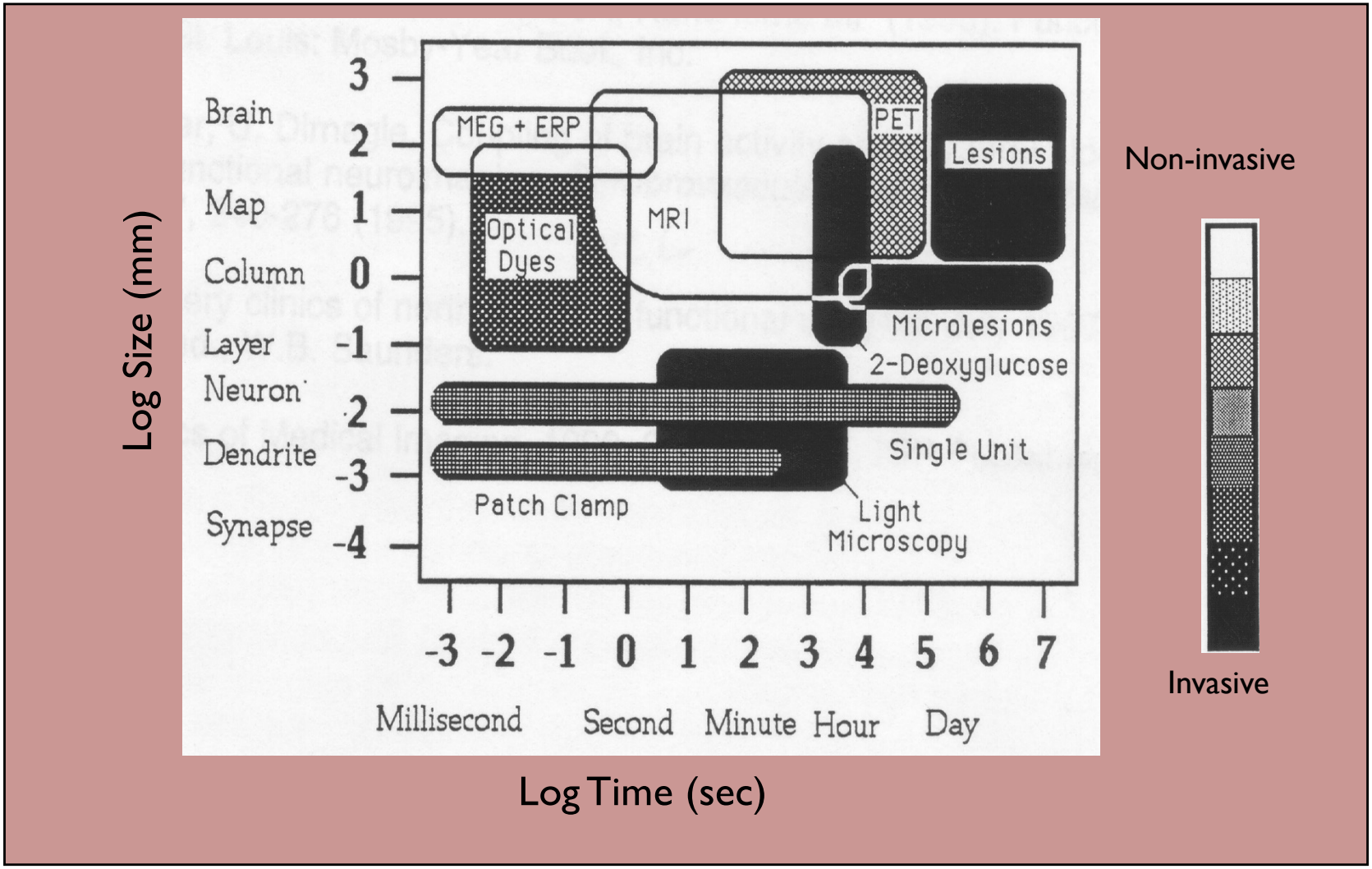


*after Churchland and Sejnowski, 1988*

# Five Key Factors For The Emergence of Functional MRI

1. Magnetic properties of red blood cells
2. Activation related hemodynamic changes
3. Spatial scale of brain activation
4. Echo Planar Imaging
5. Prevalence of MRI scanners

Single Shot Echo Planar Imaging (EPI)

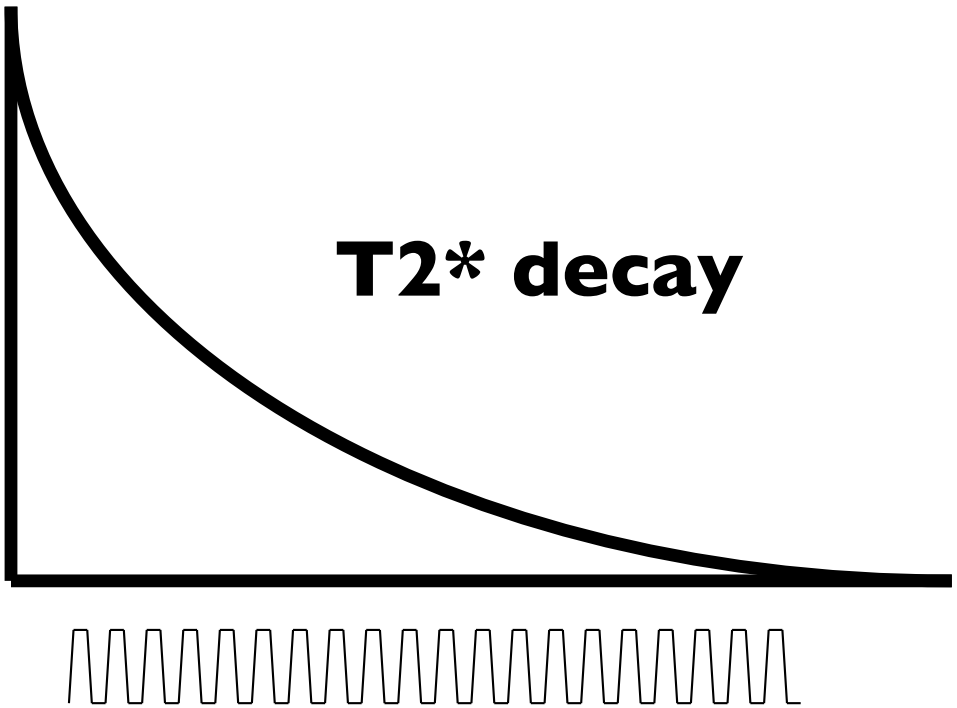


**EPI Readout Window**

**≈ 20 to 40 ms**

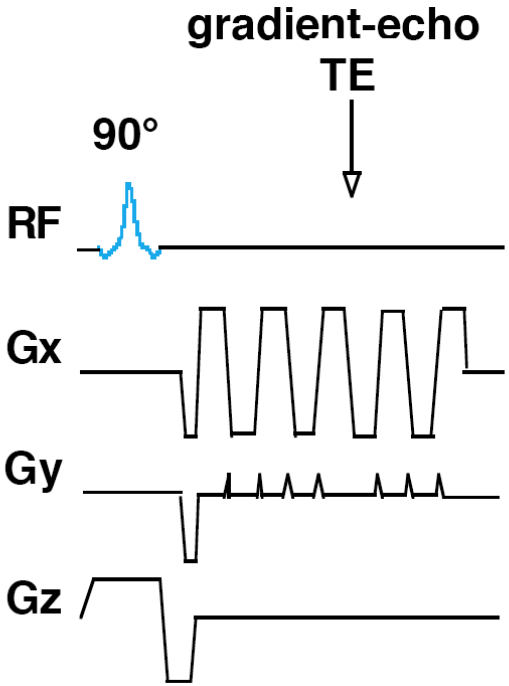


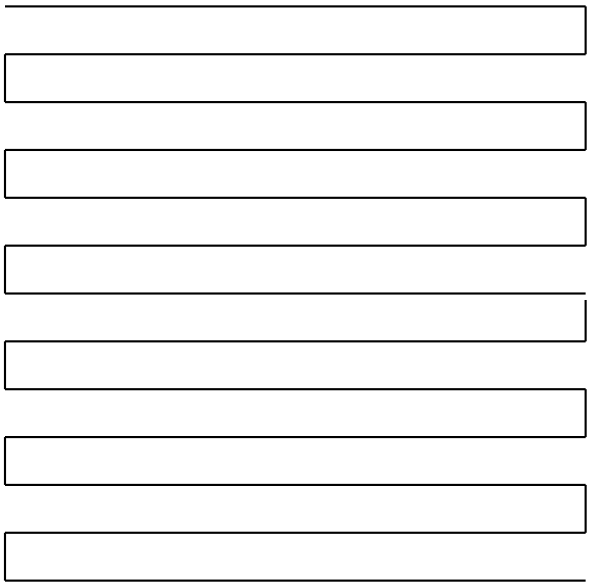

# MRI vs. fMRI

MRI

high resolution
(1 mm)

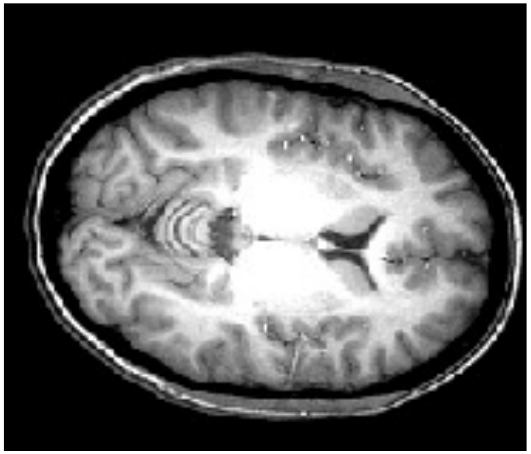

one image

fMRI

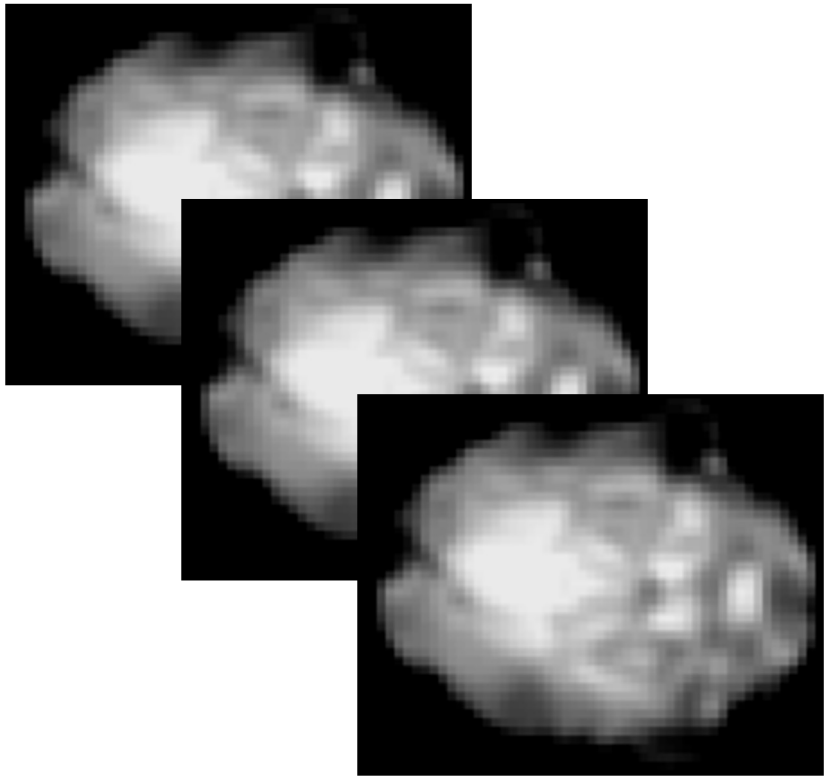

...

many images
(e.g., every 2 sec for 5 mins)

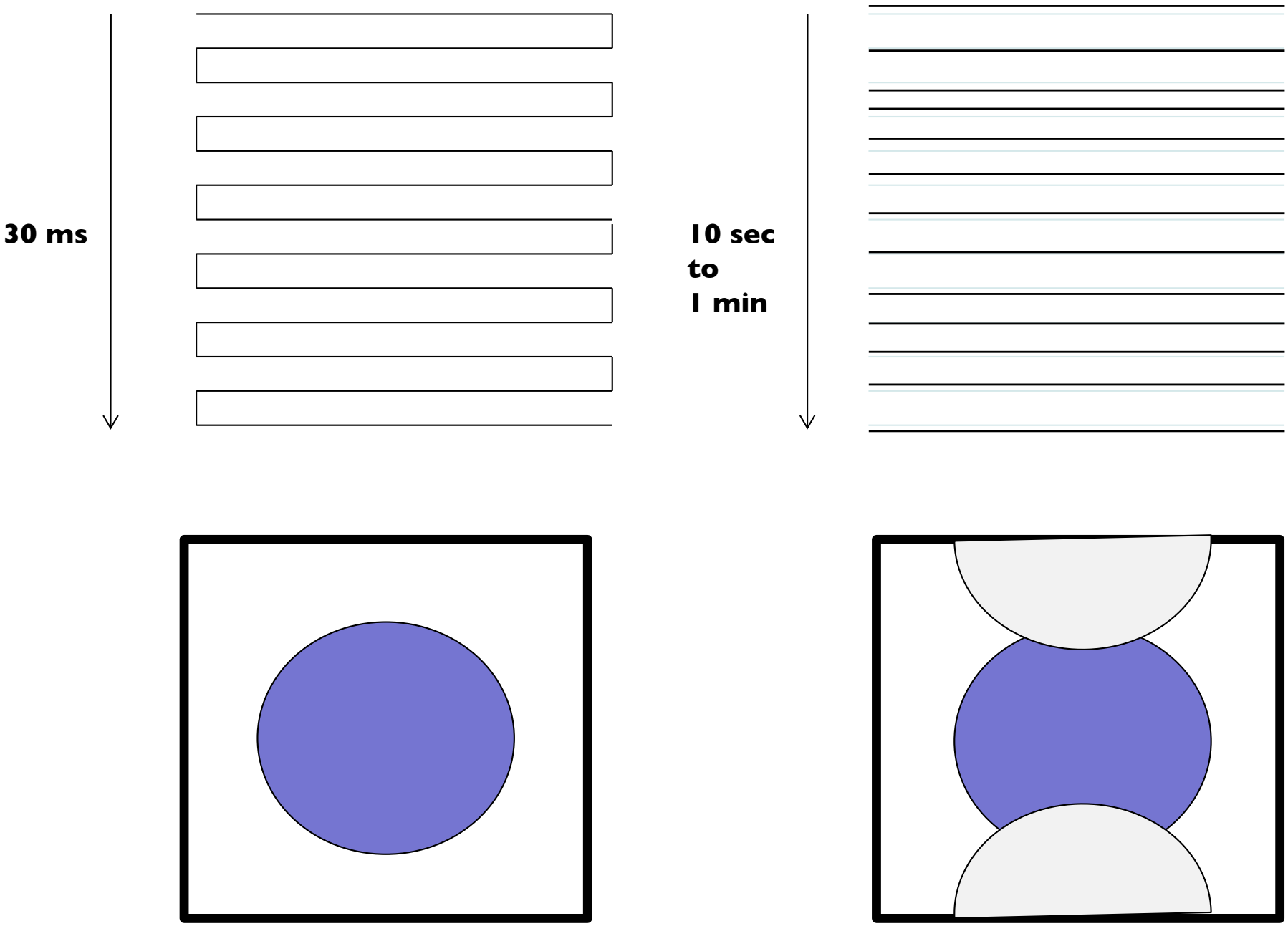
30 ms
10 sec
to
1 min

# Approximate EPI Timeline

**1976-84** P. Mansfield conceives of EPI
**1989** EPI of humans emerges on a handful of scanners
3 x 3 x 3-10 $mm^3$
**1989** ANMR retrofitted with GE scanners for EPI
**1991** Home built head gradient coils perform EPI
**1996** EPI is standard on clinical scanners
**2000** Gradient performance continues to increase
**2002** Parallel imaging allows for higher resolution EPI
**2006** 1.5 x 1.5 x 1.5 $mm^3$ single shot EPI possible
**2009** At 7T sub – mm single shot EPI for fMRI is possible

# Imaging System Components

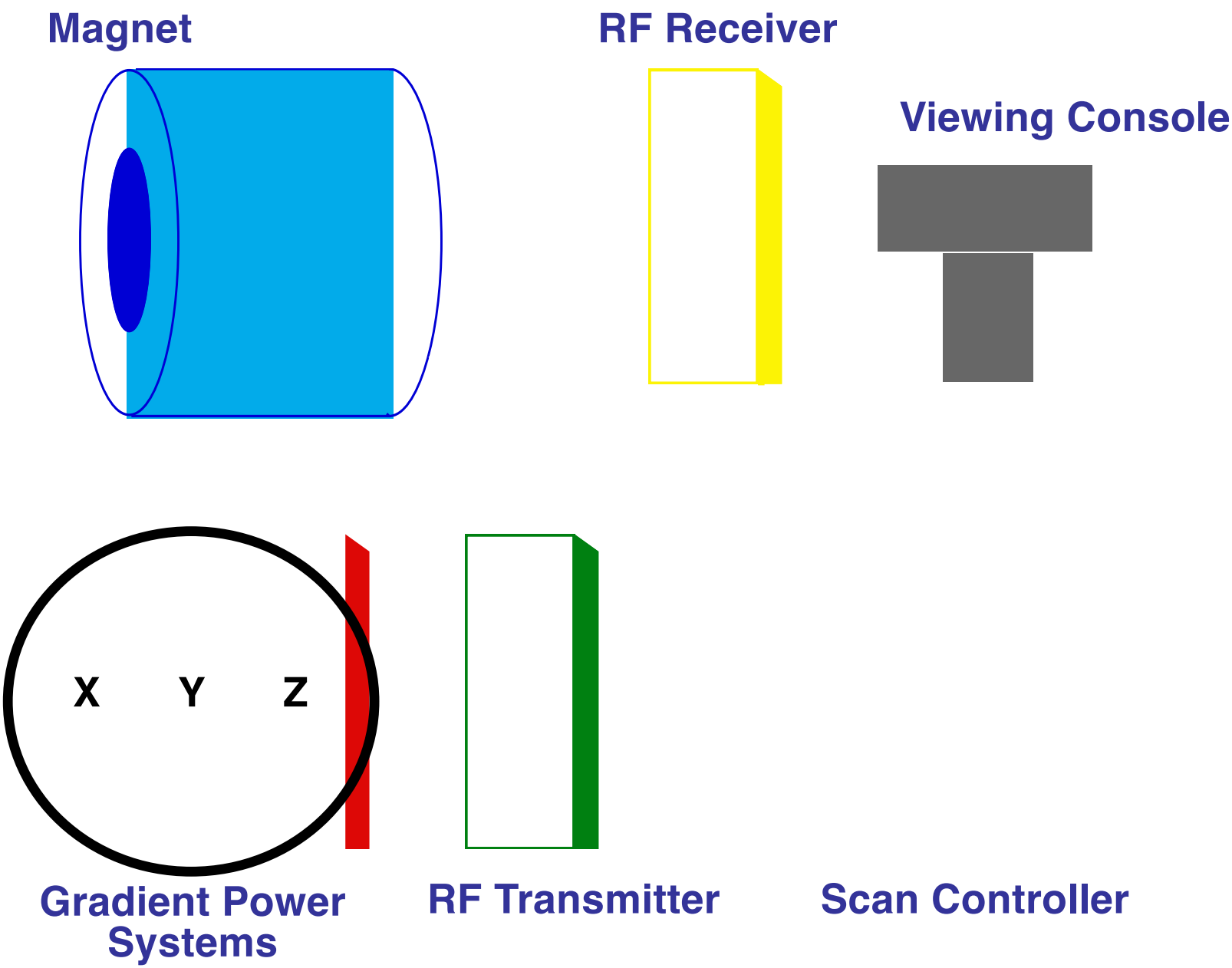

# Five Key Factors For The Emergence of Functional MRI

1. Magnetic properties of red blood cells
2. Activation related hemodynamic changes
3. Spatial scale of brain activation
4. Echo Planar Imaging
5. Prevalence of MRI scanners

# Scopus: Articles or Reviews Published per Year

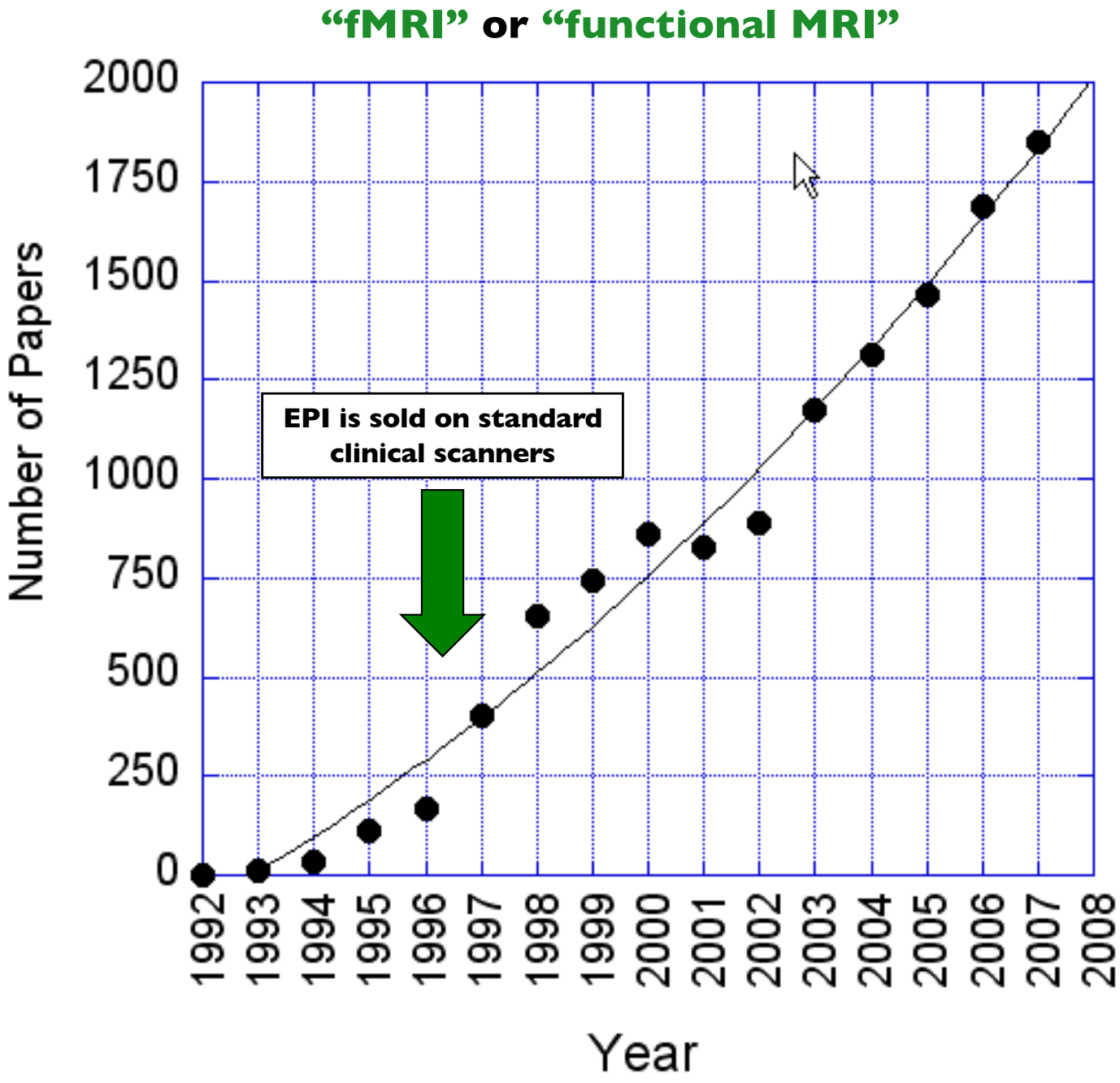

## *How it all came together…*

## Five Key Factors For The Emergence of Functional MRI

1. **Magnetic properties of red blood cells**
2. **Activation related hemodynamic changes**
3. **Spatial scale of brain activation**
4. **Echo Planar Imaging**
5. **Prevalence of MRI scanners**

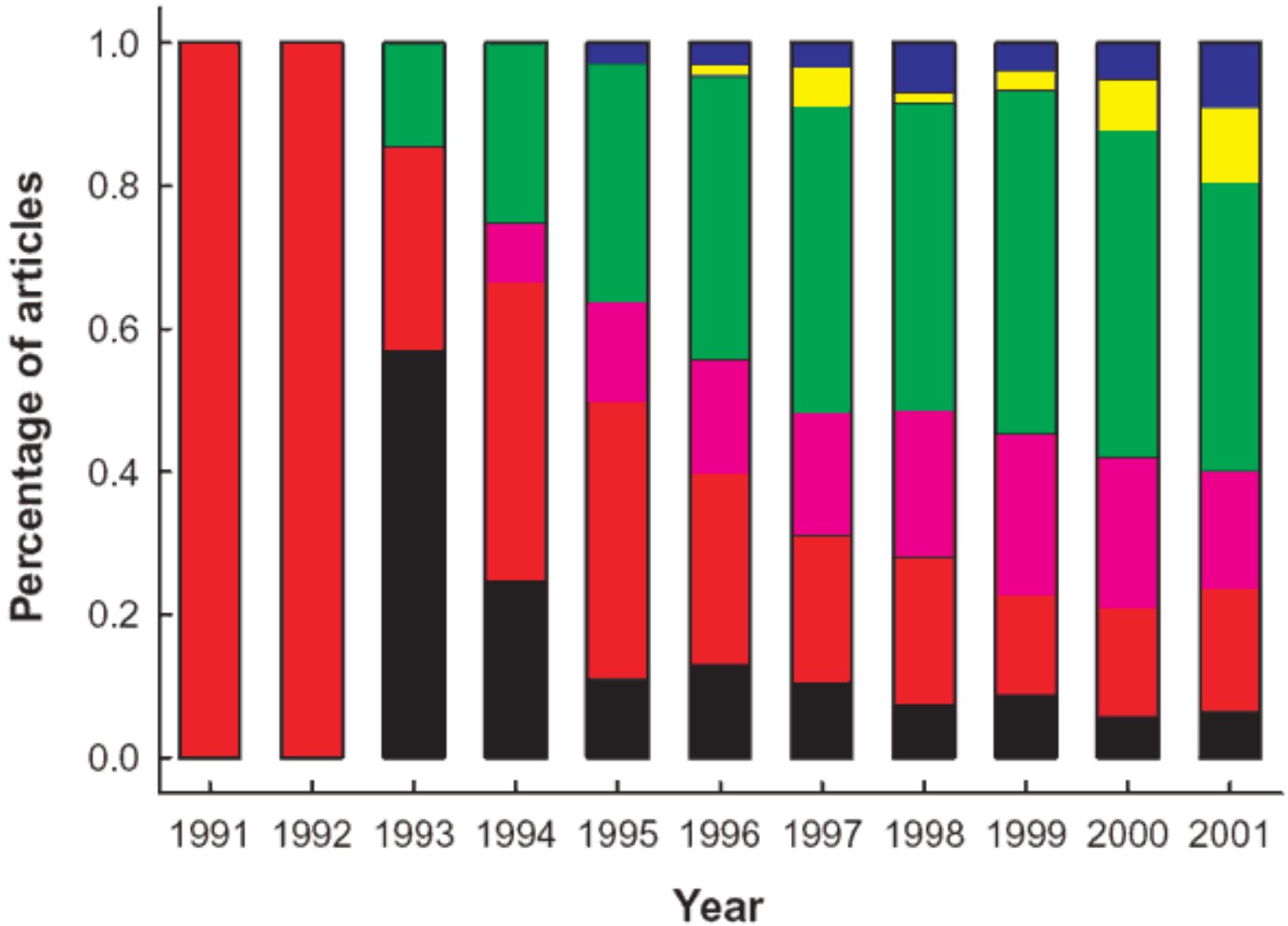


Motor (black)
Primary Sensory (red)
Integrative Sensory (violet)
Basic Cognition (green)
High-Order Cognition (yellow)
Emotion (blue)

J. Illes, M. P. Kirschen, J. D. E. Gabrielli,
Nature Neuroscience, 6 (3)m p.205

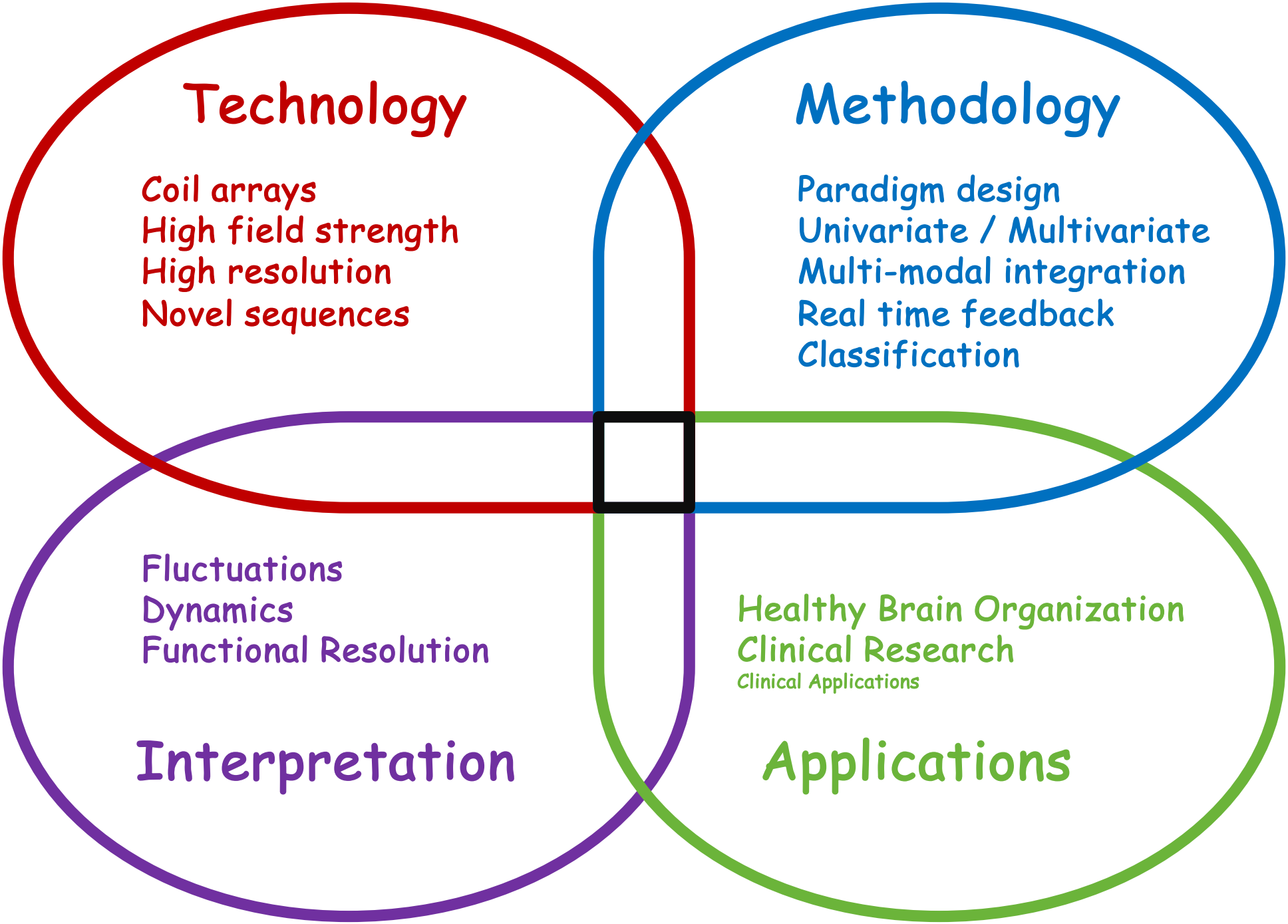
Technology
Coil arrays
High field strength
High resolution
Novel sequences
Methodology
Paradigm design
Univariate / Multivariate
Multi-modal integration
Real time feedback
Classification
Fluctuations
Dynamics
Functional Resolution
Interpretation
Healthy Brain Organization
Clinical Research
Clinical Applications
Applications

## Brief History of Brain Imaging

1. **Lesion-based Mapping.**
2. **Anatomic Imaging.**
3. **Hemodynamic and Metabolic Imaging.**
4. **Electrophysiologic Imaging**
5. **Functional MRI**

**Parametric manipulation of brain activation demonstrated that BOLD contrast approximately followed the level of brain activation: visual system (Kwong et al., 1992), auditory system (Binder et al., 1994), and motor system (Rao et al., 1996).**

**The use of continuous variation of visual stimuli parameters as a function of time was proven a powerful method for fMRI-based retinotopy: (Engel et al., 1994, Deyoe et al., 1994, Sereno et al., 1995).**

**Event-related fMRI was first demonstrated (Blamire et al., 1992).**

**Application of event-related fMRI to cognitive activation was shown (Buckner et al., 1996, McCarthy et al., 1997).**

**Development of mixed event-related and block designs was put forward: (Donaldson et al., 2002).**

**Paradigms were demonstrated in which the activation timing of multiple brain systems timing was orthogonal, allowing multiple conditions to be cleanly extracted from a single run (Courtney et al., 1997).**

**High resolution maps were created: For spatial resolution: ocular dominance columns (Menon et al., 1997, Cheng et al., 2001) and cortical layer activation maps were created (Logothetis et al., 2002).**

**Extraction of information at high spatial frequencies within regions of activation was demonstrated (Haxby et al., 2001).**

**For temporal resolution: Timings from ms to hundreds of ms were extracted (Ogawa et al., 2000, Menon et al., 1998, Henson et al., 2002, Bellgowan et al., 2003).**

**The development of "deconvolution" methods allowed for rapid presentation of stimuli (Dale and Buckner, 1997).**

**Early BOLD contrast models were put forward: (Ogawa et al., 1993, Buxton and Frank, 1997).**

**More sophisticated models were published that more fully integrated the latest data on hemodynamic and metabolic changes (Buxton et al., 2004).**

**The development of "clustered volume" acquisition was put forth as a method to avoid scanner noise artifacts: (Edmister et al., 1999).**

**The findings of functionally related resting state correlations: (Biswal et al., 1995) and regions that consistently show deactivation (Binder et al., 1999, Raichle et al., 2001) were described.**

**Observation of the pre-undershoot in fMRI (Hennig et al., 1997, Menon et al., 1995, Hu et al., 1997) and correlation with optical imaging was reported (Malonek and Grinvald, 1996).**

**Simultaneous use of fMRI and direct electrophysiological recording in non-human primate brain during visual stimulation elucidated the relationship between fMRI and BOLD contrast. (Logothetis et al., 2001). Simultaneous electrophysiological recordings in animal models revealed a correlation between negative signal changes and decreased neuronal activity (Shmuel et al., 2002). Simultaneous electrophysiological recordings in animal models provided evidence that inhibitory input could cause an increase in cerebral blood flow (Matheiesen et al., 1998).**